การควบคุมแบบโมเดลพรีดิกทีฟสำหรับเครื่องปฏิกรณ์แบบทริกเคิลเบด

นายอมรชัย อาภรณ์วิชานพ
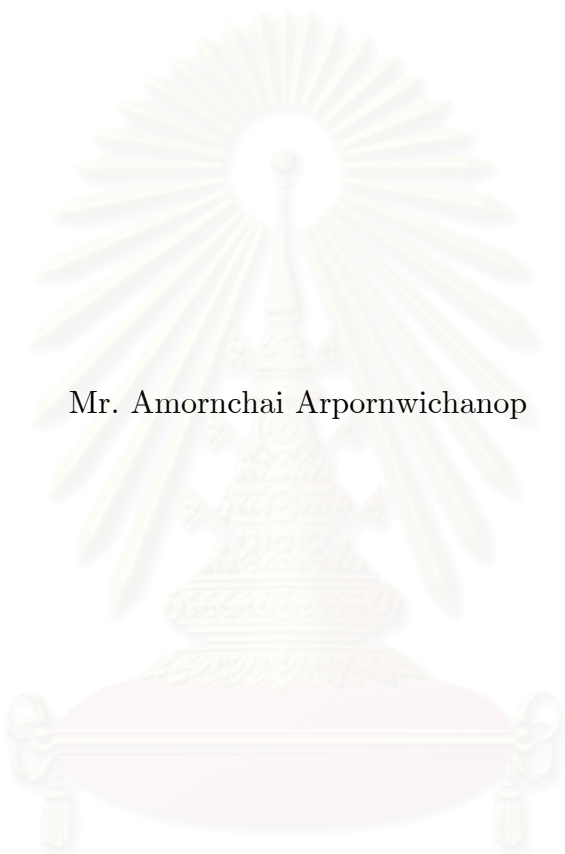
A MODEL PREDICTIVE CONTROL FOR A TRICKLE BED REACTOR

Mr. Amornchai Arpornwichanop

Thesis Title	A MODEL PREDICTIVE CONTROL FOR A TRICKLE BED REACTOR
By	Mr. Amornchai Arpornwichanop
Field of Study	Chemical Engineering
Thesis Advisor	Associate Professor Paisan Kittisupakorn, Ph.D.
Thesis Co-advisor	Assistant Professor Wirat Vanichsriratana, Ph.D.

Accepted by the Faculty of Engineering, Chulalongkorn University in Partial Fulfillment of the Requirements for the Doctor's Degree

………………………………………… Dean of Faculty of Engineering

(Professor Somsak Panyakeow, D.Eng.)

THESIS COMMITTEE

…………………………………….. Chairman

(Professor Piyasan Praserthdam, Dr.Ing.)

……………………………….…… Thesis Advisor

(Associate Professor Paisan Kittisupakorn, Ph.D.)

……………………………………. Thesis Co-advisor

(Assistant Professor Wirat Vanichsriratana, Ph.D.)

…………………………………….. Member

(Montree Wongsri, D.Sc.)

………………………………….….... Member

(Suphot Phatanasri, D.Eng.)

งานวิจัยนี้เสนอการควบคุมแบบโมเดลพรีดิกทีฟเพื่อควบคุมเครื่องปฏิกรณ์แบบทริกเคิลเบด ซึ่ง
เกิดปฏิกิริยาไฮโดรจีเนชั่นแบบมีตัวเร่งปฏิกิริยาของไพโรไลซีสแก๊สโซลีน เนื่องจากความสำเร็จของการ
ประยุกต์ใช้การควบคุมแบบโมเดลพรีดิกทีฟขึ้นกับแบบจำลองของระบบที่ถูกควบคุม แบบจำลองพลวัต
แบบดิสทริบิวท์ของกระบวนการซึ่งประกอบด้วยสมการจลน์ศาสตร์ของปฏิกิริยาไฮโดรจีเนชันของแก๊สโซลีน
และสมการดุลมวลสารและดุลพลังงานสำหรับเครื่องปฏิกรณ์จึงได้พัฒนาขึ้น ปัญหาออปติไมซ์เซชั่นได้สร้างขึ้น
เพื่อใช้กำหนดค่าพารามิเตอร์ ซึ่งทำให้ความคลาดเคลื่อนระหว่างค่าที่ทำนายจากแบบจำลองและค่าที่ได้จากข้อมูล
จากโรงงานมีค่าต่ำที่สุด แบบจำลองของกระบวนการที่พัฒนาขึ้นได้นำไปใช้ในการสร้างตัวควบคุมแบบโมเดลพรี
ดิกทีฟเพื่อควบคุมอุณหภูมิของเครื่องปฏิกรณ์แบบทริกเคิลเบด สมรรถนะของการควบคุมแบบโมเดลพรีดิกทีฟได้
แสดงให้เห็นในกรณีของการควบคุมระบบที่ค่าเซ็ตพอยท์และการขจัดผลการรบกวนที่มีต่อระบบ ผลการจำลอง
แสดงให้เห็นว่าการควบคุมแบบโมเดลพรีดิกทีฟให้สมรรถนะการควบคุมที่ดีกว่าเมื่อเปรียบเทียบกับตัวควบคุม
แบบพีไอดี

นอกจากการประยุกต์ใช้เทคนิคการควบคุมแบบโมเดลพรีดิกทีฟกับเครื่องปฏิกรณ์แบบทริกเคิล
เบดแล้ว งานวิจัยนี้ยังศึกษาสมรรถนะของการควบคุมแบบโมเดลพรีดิกทีฟในการควบคุมเครื่องปฏิกรณ์เคมีแบบ
กะและแบบต่อเนื่อง ในกรณีของเครื่องปฏิกรณ์แบบกะ การควบคุมแบบโมเดลพรีดิกทีฟได้นำไปใช้เพื่อปรับปรุง
การดำเนินการโดยการปรับค่าเซ็ตพอยท์ของอุณหภูมิที่เหมาะสมแบบออนไลน์ ในกรณีเครื่องปฏิกรณ์
แบบต่อเนื่อง การควบคุมแบบโมเดลพรีดิกทีฟได้นำไปใช้ในการควบคุมความเข้มข้นของผลิตภัณฑ์ ผลการ
จำลองแสดงให้เห็นว่าการควบคุมแบบโมเดลพรีดิกทีฟสามารถนำไปใช้ในการควบคุมและปรับปรุงประสิทธิภาพ
ของเครื่องปฏิกรณ์ทั้งสองแบบได้ดี

ภาควิชา	วิศวกรรมเคมี	ลายมือชื่อนิสิต ....
สาขาวิชา	วิศวกรรมเคมี	ลายมือชื่ออาจารย์ที่ปรึกษา ....
ปีการศึกษา	2545	ลายมือชื่ออาจารย์ที่ปรึกษาร่วม ....….....…

This research presents the implementation of a model predictive control (MPC) strategy to control a trickle bed reactor (TBR) in which catalytic hydrogenations of pyrolysis gasoline take place. As the success of MPC applications relies on the availability of models of the system to be controlled, dynamic distributed process models consisting of kinetic expressions for the gasoline hydrogenation, and mass and energy balances for the reactor have been developed. An optimization problem is formulated to determine the kinetic parameters minimizing an error between model prediction and plant data. The process models developed are used in the formulation of the MPC controller for controlling the temperature of the trickle bed reactor. The performance of the MPC scheme is demonstrated in cases of set point tracking and disturbance rejection. The simulation results have shown that the MPC provides a better control performance compared with a conventional PID controller.

In addition to applying the MPC technique to the trickle bed reactor, this research investigates the performance of the MPC in controlling batch and continuous chemical reactors. In the case of the batch reactor, the MPC is applied to improve an operation by on-line modifying an optimal temperature set point profile. In the case of the continuous reactor, the MPC is utilized to control a product concentration. Simulation results have demonstrated that the MPC control strategy is applicable to control as well as improve the efficiency of both reactors with great success.

Deparment	Chemical Engineering	Student's signature………………….…………………
Field of study	Chemical Engineering	Advisor's signature………………….…………………
Academic year	2002	Co-advisor's signature.......…..............………….....

Acknowledgements

Contents

List of Tables

List of Figures

Nomenclature

Control Algorithm

A	weighting matrix for first derivative term
h_k	length of element k
K_1, K_2	GMC controller parameters
$ncol$	a number of collocation points in each element
NE	a number of finite element
p	model parameters
P	covariance matrix of prediction
Q	covariance matrix of process noise
R	covariance matrix of measurement noise
T_p	prediction time horizon
u	control variables
w	weighting factor for integral term
x	state variables
y	output variables

Trickle Bed Reactor

A	reactor cross sectional area $[m^2]$
a_i	catalyst surface area/volume ratio $[m^2/m^3]$
C_i	concentration of component i $[kmol/m^3]$
C_p	specific heat capacity $[J/(kg.K)]$
D	diffusivity $[m^2/s]$
d_p	catalyst diameter $[m]$
E_a	apparent activity energy $[J/mol]$
g	gravitational constant $[m/s^2]$
G	mass velocity $[kg/(hr.m^2)]$
H	Henry constant

ΔH	heat of reaction $[J/kmol]$
k_0	apparent pre-exponential factor
k_1, k_2	specific reaction rate constant
k_{ad}	adsorption constant
$k_g a_i$	gas phase mass transfer coefficient $[1/s]$
$k_l a_i$	liquid phase mass transfer coefficient $[1/s]$
Q	flow rate $[m^3/hr]$
r_1, r_2	rate of reaction $[kmol/(m^3.hr)]$
T	reactor temperature $[K]$
u	superficial velocity $[m/hr]$
Z	reactor length $[m]$

Greek Symbols

ϵ	void fraction
ϵ_g	gas holdup
ϵ_l	liquid holdup
ρ	density $[kg/m^3]$
μ	vicosity $[kg/(m.hr)]$

Subscripts

di	diolefins
f	feed stream
g	gas phase
HC	lumped hydrocarbon components
H_2	hydrogen
i	reaction index
l	liquid phase
ole	olefins
$para$	paraffins
q	quench stream

Batch Reactor

A	heat transfer area $[m^2]$
Cp	mass heat capacity $[kJ/(kg.^oC)]$
Cp_i	molar heat capacity of component i $[kJ/(kmol.^oC)]$
F	flowrate $[m^3/min]$
ΔH_i	heat of reaction of reaction i $[kJ/kmol]$
k_i	rate constant for reaction i $[1/(kmol.s)]$
k_i^1	rate constant 1 for reaction i
k_i^2	rate constant 2 for reaction i
M_i	a amount of moles of component i $[kmol]$
MW_i	molecular weight of component i $[kg/kmol]$
Q_r	heat released from reactions $[kJ/min]$
r	radius of reactor $[m]$
R_i	rate of reaction i $[kmol/min]$
t	time $[min]$
Δt	sampling time $[min]$
T	reactor temperature $[^oC]$
U	heat transfer coefficient
V	reactor volume $[m^3]$
W	reactor content $[kg]$

Superscripts

sp	setpoint

Subscripts

f	filter
j	jacket
r	reactor

Continuous Reactor

C_A	concentration of component A $[mol/m^3]$
C_B	concentration of component B $[mol/m^3]$

C_p heat capacity $[J/(kg.K)]$

E activity energy $[J/mol]$

ΔH heat of reaction $[J/mol]$

k_0 Arrhenius pre-exponential constant

q dimensionless feed flowrate

T reactor temperature $[K]$

u dimensionless manipulated variable

U heat transfer coefficient $[J/(s.K.m^2]$

v dimensionless feed temperature disturbance

V reactor volume $[m^3]$

x_1 dimensionless concentration of component A

x_2 dimensionless concentration of component B

x_3 dimensionless reactor temperature

Greek symbols

ρ density $[kg/m^3]$

β dimensionless heat of reaction

δ dimensionless heat transfer coefficient

γ dimensionless activation energy

ϕ dimensionless rate constant (Damkohler)

τ dimensionless time

Superscripts

sp setpoint

Subscripts

c coolant

f feed condition

Chapter 1

Introduction

It is well known that many chemical processes, for example, chemical reactors, distillation columns and bioprocesses exhibit inherently complex and nonlinear dynamic behavior. The presence of complexity and nonlinearity in such processes posts a challenging control problem that is difficult to handle with linear control techniques; linear controllers usually perform poorly when applied to highly nonlinear systems.

Due to the limitation of linear controllers to achieve satisfactory control performance, many nonlinear control algorithms have been devised and studied over the past years. An excellent review on advanced control strategies based on a nonlinear representation of the process is provided by Bequette (1991). Among of them, a model predictive control (MPC), also refer to as receding horizon control or moving horizon control, has emerged as a powerful practical control technique. MPC is known as an optimal control based method for computing control inputs minimizing an objective function. It has been broadly adopted in a wide variety of control applications (Qin and Badgwell, 1997). A key feature contributing to the success of MPC is its ability to deal with multivariable systems naturally since explicit pairing of input and output variables is not required. Moreover, various process constraints can be incorporated directly into the associated open loop optimal control problem (Henson, 1998). A comprehensive review of MPC is provided by several authors (Meadows and Rawlings (1997); Morari and Lee (1999); Rawlings, J. B. (2000); Mayne et al. (2000)).

1.1 Model Predictive Control

Model predictive control (MPC) refers to a class of control algorithms that compute a sequence of manipulated variables in order to optimize the future behavior of a

plant. The name MPC originates from the idea of employing an explicit model of the plant to be controlled to predict the future output behavior. The prediction is used to determine optimal control moves that will bring the plant to a desired condition. The current control action is obtained by solving an on-line finite horizon open loop optimal control problem, using the current state of the plant as the initial state. The optimizaton problem is solved subject to constraints imposed by the model equations as well as input and output constraints, and yields an optimal control sequence. However, only the first control in this sequence is applied to the plant. Once some feedback information is available, the optimization is then repeated for the next sampling time interval. Figure 1.1 illustrates the basic idea of MPC.

Since MPC is formulated as solving an optimization problem, the desired control performance can be designed by choosing appropriate specific forms of an objective function. However, the common used objective function is an integral square error between the prediction of controlled variables and their desired references.

In the MPC algorithm, both linear and nonlinear dynamic models of the plant can be used. These models may be based on either a fundamental model which is derived from basic conservation laws or a empirical model which is developed from the relation of input and output plant data. In the early version of MPC applications, step or impluse response models are always employed. This is due to the ease of understanding provided by these model forms. Nevertheless, the possibility of improved control performance motivates the use of nonliner models in the MPC algorithm.
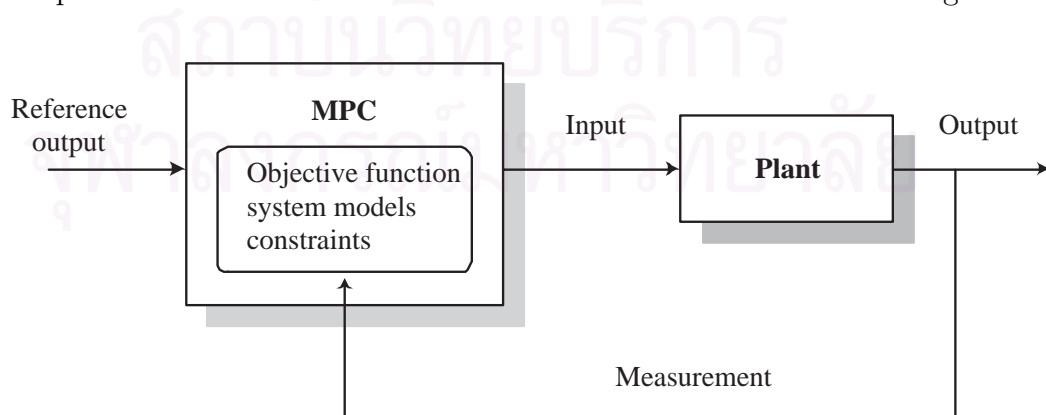
Figure 1.1: Structure of model predictive control strategy

1.2   Trickle Bed Reactor

Multiphase reactors involving gas, liquid, and solid are often encountered in chemical process industries. The most common use of the multiphase reactors is in hydroprocessing such as hydrogenation and hydrodesulfurization processes. In general, the type of gas-liquid-solid reactors used in industries can be mainly divided into two categories: one where the solids are fixed and the others where the solids are in a suspended state (Shah, 1979).

Trickle bed reactor, one of the widely used three-phase reactors, is a fixed bed of catalyst particle through which gas and liquid are allowed to flow. Although three ways of the reactor operation i.e. cocurrent downflow of both gas and liquid, cocurrent upflow of both gas and liquid, and countercurrent flow of gas and liquid, are possible, typically the gas and liquid flow cocurrently downward through the reactor as illustrated in Figure 1.2. A comparison among various modes in operating the trickle bed reactor including their advantages and disadvantages is discussed in Ramachandran and Chaudhari (1983).

Many applications of trickle bed reactors can be found primarily both in petroleum industry for hydrocraking, hydrodesulfurization and hydrodenitrogenation, and in petrochemical industry for hydrogenation and oxidation (Gianetto and Specchia, 1992).

1.3   Motivation

As seen from the literature, a large number of MPC applications focus on the processes that their dynamic behaviors can be described by relatively simple models usually consisting of ordinary differential and/or algebraic equations. The implementation of nonlinear MPC in more complex systems like a distributed parameter system which is naturally modeled by a system of nonlinear partial differential equations (PDEs) has been rarely appeared. It is accepted that controlling a PDE system provides a challenging task. This is attributable to inherent difficulties involved with high nonlinearity as well as the presence of spatial variations. Such difficulties stir the need for an effective control algorithm of the PDEs system.
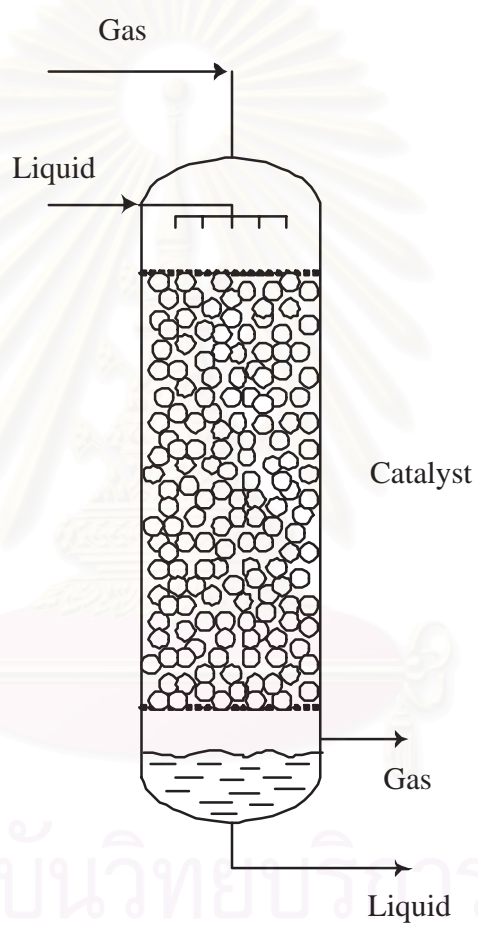
Figure 1.2: Schematic diagram of a trickle bed reactor

The work presented in this dissertation is focused on the implementation of a model predictive control (MPC) algorithm to control a distributed parameter system. A trickle bed reactor where hydrogenation of raw gasoline takes place is chosen to represent such a system. Since the success of MPC is largely depend on the availability of models of the process to be controlled, this research concentrates on the development of a mathematical model for describing the dynamics of the trickle bed reactor. The developed model, based on industrial plant data, is then used to design the MPC.

Since other chemical reactors like batch and continuous reactors have been widely used in chemical processes, this research studies the performance of MPC in the control of such reactors as well. For a batch reactor, the MPC is proposed in order to improve the batch reactor operation while for a continuous reactor, the MPC is utilized to control a product concentration.

1.4   Dissertation Overview

This dissertation is organized as follows. Chapter 2 reviews the literature for work related to model predictive control (MPC) strategy, control of distributed parameter systems, and modeling of trickle bed reactors.

Chapter 3 discusses the basic formulation of MPC problem. Since MPC determines a sequence of control input at each sampling time by solving an open loop optimal control problem, the numerical solution methods of such a problem are provided in this chapter. Two direct optimization strategies: sequential and simultaneous model solution and optimization are described.

Chapter 4 begins with an introduction to the catalytic hydrogenation of pyrolysis gasoline and the process description of the first stage hydrogenation studied in this work. The mathematical model of trickle bed reactor (TBR) derived from mass and energy balances is developed. An optimization problem is presented in order to estimate kinetic parameters based on industrial plant data.

Chapter 5 provides some applications of MPC to batch and continuous reactors as illustrative case studies. In the batch reactor, we demonstrate the implementation of

MPC as a high level controller to determine on-line optimal temperature profile, which is sent to a local controller as a set point, for operating the batch reactor. For the continuous reactor, the use of MPC to control a product concentration in the reactor is discussed. The study of dual mode MPC, an extended version of MPC, on the continuous reactor is given as well.

Chapter 6 describes the implementation of MPC to control a trickle bed reactor. The reactor model developed in Chapter 4 is used here to design the MPC controller. To evaluate the performance of the MPC, results are compared with a traditional PID controller. Simulation studies of the MPC and PID controllers are demonstrated and discussed.

Chapter 7 gives a conclusion of this dissertation.

Chapter 2

Literature Reviews

2.1 Model Predictive Control

Model predictive control (MPC), also known as moving horizon control or receding horizon control, refers to a class of control strategies in which control inputs are computed, based on an optimization criteria that is formulated over a prediction horizon, using an explicit model to predict the effect of future inputs on system states or outputs. MPC incorporates feedback by dynamically updating the optimization problem to include the effects of process measurements.

MPC approach has found to be successful in industrial applications as given in the review by Richalet (1993). This is due to the outstanding characteristics of the MPC for coping with *i)* inherent nonlinear processes, *ii)* multivariable systems, and *iii)* constraints on processes. A more complete overview on industrial MPC techniques with details and comparisons can be seen in Qin and Badgwell (1997), where more than 2200 applications in a wide range from chemical to aerospace industries are also summarized.

In general, model predictive control can be divided into two classes: linear model predictive control and nonlinear model predictive control. Linear MPC refers to a family of MPC schemes in which linear models are used to predict the system dynamics even though the dynamics of the system is nonlinear, while nonlinear MPC refers to the general cases in which the dynamic system models, performance objective, and constraints may be in nonlinear function of state, input and output variables.

Two well-known linear MPC algorithms are dynamic matrix control (DMC) and model algorithmic control (MAC) (Garcia et al., 1989). In principle, both control

techniques use linear models of the system to predict the system response resulting from the calculated profile of manipulated variables. However, the linear models used in DMC is obtained from step response test whereas that used in MAC is obtained from impulse response test. These control strategies have been widely used with success in industrial applications due to the ease in developing linear process models.

However, it has been known that most chemical engineering processes exhibit highly nonlinear dynamic. In addition, higher product quality specifications and increasing productivity demands, tighter environmental regulations and demanding economical consideration in the process industry require systems to be increasingly complex and to be operated closer to the boundary of the admissible operating region and occasionally in a wide range of operation. In such cases, linear models are not adequate to describe the process dynamics and therefore, nonlinear models need to be used (Chen and Allgower, 1998c).

Even though, a construction of nonlinear process models is sometimes very difficult and time-consuming task, they can be used to describe the system in a wide range of operating condition. Moreover, due to advanced numerical techniques for optimization and powerful computer, it is possible to solve the nonlinear programming problem resulting from the formulation of nonlinear MPC.

2.1.1   Basic Principle of Nonlinear MPC

In general, a nonlinear model predictive control (MPC) problem is formulated as solving on-line a finite horizon open loop optimal control problem at each sampling time (Δt) subject to nonlinear system models and constraints on state and control variables.

Figure 2.1 shows the basic principle of model predictive control. Based on available measurement at time t and a model of the system to be controlled, the MPC controller predicts the future dynamic behavior of the system over a prediction horizon (T_p) and determines a set of future control input minimizing a predetermined objective function (performance index). It has been known that if there were no disturbance and no plant-model mismatch, and if the optimization problem could be solved for infinite
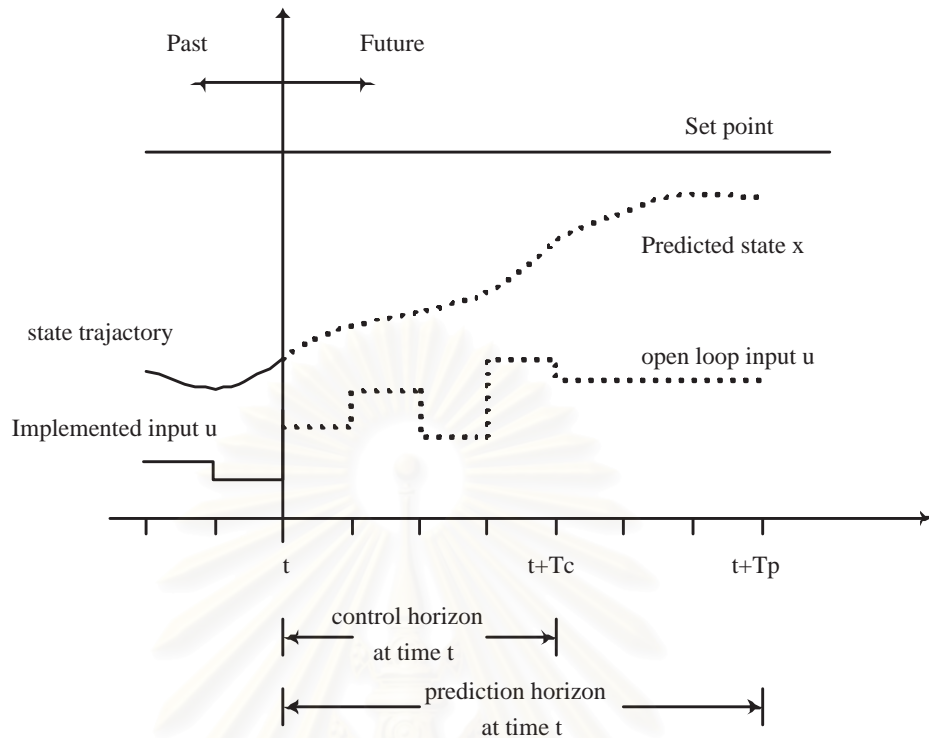
Figure 2.1: Basic concept of model predictive control

horizons, one could apply the sequence of the control input profile calculated at time t to the system. However, in the presence of unknown disturbance and/or plant-model mismatch, the dynamic system behavior is different from the predicted behavior. To make use some feedback information e.g. measurement and estimation, only the initial value of the control profile computed is applied to the system and then, after obtaining new information at the next sampling time, the optimization procedure is repeated to find a new control input with the control and prediction horizons shifting ahead one sampling time step. This results in a feedback control law; closed loop inputs are computed by solving on-line the optimization problem at each sampling time based on new feedback information from the system.

It is noted that as the MPC determines the manipulated variables by solving the optimization problem, it can naturally take into account constraints on state and control variables in the MPC formulation. This makes the MPC controller very attractive for real industrial application.

2.1.2   Stability Issue of Nonlinear MPC

To implement model predictive control, one important aspect needed to be addressed is a closed loop stability property. The minimum requirement of a model-based feedback controller is that it provides a stable closed-loop system if a perfect model of the system is available. This is known as a nominal closed-loop stability (Henson, 1998).

As mentioned above, the open loop optimal control that has to be solved on-line is often formulated in a finite horizon and the control input is usually parameterized finitely, in order to allow a numerical solution of the nonlinear open loop optimal control problem. From a computational point of view, to implement MPC strategy, the shorter finite horizon requires less computation in solving the on-line optimization problem. However, it has been found that if a finite prediction horizon is used, the actual closed loop input and state trajectories quite differ form the predicted open loop trajectories, especially when a short horizon is chosen. In addition, the closed loop stability is not guaranteed for a generic finite horizon cost function (Bitmead et al., 1990).

An intuitive way to achieve guaranteed stability is to use an infinite time horizon in the MPC formulation ($T_p \rightarrow \infty$). This results in an infinite dimensional optimization problem. For linear cases, the closed loop stability can be proved by Rawlings and Muske (1993) and Scokaert and Rawlings (1996). They introduced an terminal penalty term, which is equal to the infinite horizon cost, to transform the infinite horizon optimization problem into an finite optimization problem. The prediction is exactly considered over an infinite horizon but the control input is considered over a finite horizon. For nonlinear systems, solving such an optimization problem is very difficult and may be impossible.

To avoid such difficulties, many researchers have approached to the stability properties of the model predictive control using a finite horizon instead of an infinite horizon. Most of these methods modify the MPC formulation such that stability of the closed loop can be guaranteed independently of the plant and performance specifications. This is usually achieved by adding suitable equality or inequality constraints and suitable additional penalty term to the objective function.

The simplest and straightforward way to ensure the stability of the closed loop system is to include a terminal equality constraint:

$$x(t + T_p) = 0 \tag{2.1}$$

into the MPC formulation. That is, with this additional requirement, the controlled system is forced to move from any initial condition to a desired condition at the terminal time. Chen and Shaw (1982), Keerthi and Gilbert (1988), and Mayne and Michalska (1990) showed for discrete and continuous systems that the MPC with terminal equality constraint guarantees closed loop stability. However, one obstacle of this approach is that the terminal zero constraint may cause an infinite number of iterations in the exact solution of constrained optimal control problem. Furthermore, it can lead to an infeasible solution problem in case where a short prediction horizon is used (Chen and Allgower, 1998c). Motivated by this, Michalska and Mayne (1993) proposed a relaxed terminal inequality constraint in the MPC formulation, as shown in the form below (Equation (2.2)), such that the states are on the boundary of a terminal region at the end of the prediction horizon. The terminal region is a region of attraction for the nonlinear system controlled by a local linear state feedback law. This brings to the so-called dual mode nonlinear MPC scheme.

$$x(t + T_p) \in E \tag{2.2}$$

where E is some region in a neighborhood of a desired operating condition. The use of terminal region constraint would give the dual mode nonliner MPC computational advantage.

Another way to achieve closed loop stability of MPC is given by Chen and Allgower (1998b). This method is known as a quasi-infinite horizon MPC in which a terminal region constraint and a terminal penalty term are included in the control formulation. The terminal penalty term is determined off-line such that the objective function with the terminal penalty term gives an upper approximation of the infinite horizon objective function.

2.1.3 Robustness of Nonlinear MPC

Another important issue to be considered in implementing MPC is its robustness to model uncertainties. The basic MPC algorithm described earlier requires that the system to be controlled and the model used for prediction and optimization are identical; that is, there are no plant/model mismatches or no unmeasured disturbances. Nevertheless, this requirement is quite impractical in reality. Hence, the development of MPC framework to address robustness issue is also significant.

In principle, there are two approaches to consider the robustness of MPC. First, one analyses the robustness property of MPC designed for a nominal model without taking the uncertainty into account. Secondly, one examines the MPC algorithm constructed by directly taking into account the uncertainty. Even though the analysis of robustness property in MPC is still a subject of researches, there are few preliminary results available in the literature. For example, Genceli and Nikolaou (1993) gave sufficient conditions for robust closed loop stability and investigated the robustness performance of MPC with hard input and soft output constraints. They derived a robustness test in terms of simple inequalities to be satisfied. Primbs and Nevistic (1998) provided an off-line robustness analyst test of constrained finite receding horizon control which is required the solution of a set of linear matrix inequlities.

Further discussion on the robustness of model predictive control can be seen in Zheng and Morari (1993), Nicolao, Magni and Scattolini (1996), and Mayne et al. (2000).

2.1.4 Application of Nonlinear MPC

Nonlinear model predictive control has been applied to a wide variety of process systems. For instance, Chen and Allgower (1998a) applied a quasi-infinite horizon nonlinear MPC strategy to control a realistic continuous stirred tank reactor (CSTR) with cooling jacket for the production of cyclopentenol from cyclopentadiene. They compared the performance of the proposed nonlinear MPC with that of other MPC schemes. It was found that the developed quasi-infinite horizon MPC requires less

on-line computation than other nonlinear MPC techniques.

Norquay et al. (1999) used a nonlinear Wiener MPC to control overhead composition of a C2 splitter. Simulation studies, using the Wiener model for the plant representation, have shown the Wiener MPC based scheme to be successful in rejecting major disturbances and comparisons with linear IMC and IMC using a logarithmic transformation on the output showed the Wiener based version to be superior, as expected for a nonlinear process.

Ju et al. (2000) proposed a nonlinear MPC to control a fabric filtration process. The control algorithm formulated in a multiple-objective optimization framework takes an economic factor into consideration. The global optimization technique is used to compute a manipulated input profile. Simulation results showed that the proposed MPC is especially suitable to the filtration process where the set point change and process disturbance occur frequently.

Seki et al. (2002) formulated the nonlinear MPC based on a successively linearized nonlinear model and applied it to an industrial polypropylene semi batch reactor process as well as to a high density polyethylene (HDPE) continuous stirred tank reactor process. For the semi batch reactor, the nonlinear MPC successfully prevented thermal runaway of the reactor temperature control. For the continuous reactor, the nonlinear MPC improved the closed loop performance during the grade changeover operation, compared with the conventional linear MPC.

Another application of nonlinear MPC is presented by Ahn et al. (1999). The control algorithm combined with an extended Kalman filter was implemented experimentally to control the conversion and the weight-average molecular weight of a polymer product in a continuous methyl methacrylate (MMA) polymerization reactor using jacket inlet temperature and feed flow rate as manipulated variables. The experiment results indicated that the nonlinear MPC performs better than the linear MPC or the PID controller in the sense of better regulation and less oscillation.

Table 2.1 lists a summary of some applications of nonlinear MPC in the literature. It contains the processes considered and the type of model used in controller design. Further nonliner MPC applications in industries are provided by Qin and Badgwell

Table 2.1: Applications of nonlinear MPC

Reference	Process	Model used
Afonso et al. (1996)	Continuous reactor	ODEs
Ali and Elnashaie (1997)	Fluid catalytic cracking	ODEs
Ahn et al. (1999)	Polymerization reactor	ODEs
Chen and Allgower (1998a)	Continuous reactor	ODEs
Eaton and Rawlings (1990)	Batch chemical reactor	ODEs
	Batch crystallizer	PDEs
Ju et al. (2000)	Filtration process	ODEs
Maner et al. (1996)	Polymerization reactor	Volterra
Meadows and Rawlings (1997)	Fluidized bed reactor	ODEs
Norquay et al. (1999)	Splitter	Wiener
Patwardhan et al. (1992)	Packed distillation column	PDEs
	Fixed bed reactor	PDEs
Qin et al. (1997)	Wastewater treatment reactor	ODEs
Seki et al. (2002)	Semi-batch reactor	ODEs
	Continuous reactor	ODEs
Sistu and Bequette (1991)	Continuous reactor	ODEs
Zhan and Ishida (1997)	Continuous reactor	Neural network

(2000). As seen in Table 2.1, the majority of application studies is restricted to the systems that their dynamics are described by ordinary differential equations (ODEs). The implementation of nonlinear MPC in more complex systems like a distributed parameter system of which the model form is partial differential equations is rare. Only few works (i.e. Patwardhan et al. (1992) and Eaton and Rawlings (1990)) have been reported. Therefore, control studies on this type of systems, which is difficult and challenging, are still the subject of interest.

2.2 Control of Distributed Parameter System

Many chemical processes such as a fixed-bed reactor and a tubular reactor are characterized by a nonlinear distributed parameter system in which state variables e.g. concentration and temperature depend on spatial position as well as time. As a consequence, these processes are generally modeled by a set of partial differential equations (PDEs). The controller design for such a PDE system may be considerably complicated due to several characteristics (Hua and Jutan, 2000): *i)* high nonlinearity, *ii)* the presence of spatial variations, *iii)* the stiff character of the system models resulting from different time scales of the internal physical and chemical processes and *iv)* limited on-line measurement information. These difficulties motivate the need for effective control algorithms of the PDEs system. Traditionally, the approaches to control the PDEs system is mainly based on various lumping techniques. It can be classified into two different methodologies: early lumping and late lumping of system models (Ray, 1981).

2.2.1 Early Lumping Approach

The early lumping method is a straightforward approach and widely used in chemical engineering. The idea behind the approach is that a distributed parameter system is first converted into an approximate model (lumping), with the use of discretization techniques, usually consisting of a set of ordinary differential equations (ODEs). Then, traditional control algorithms based on the resulting approximate model (ODEs) of the system are applied directly to design a control system. The lumping techniques are often realized by numerical techniques such as finite differences, orthogonal collocation or finite elements.

The early lumping approach can be regarded as a classical PDE control approach, as similar as an approximate and then design method for the PDE system. The advantage of this method is attributable to the fact that it can gain benefit of using well-developed and advanced control methodologies designed for a finite dimensional ODEs system. Thus, the method possibly conforms to the practical implementation

(Wu and Liou, 2001). However, one limitation of this approach is that it is difficult to know the connection between the original distributed parameter model and its approximate discretized version, so that the dynamic properties of both models may be difficult to carry out the evaluation of the designed control strategies in correct and rigorous way (Dochain et al., 1997).

Based on the early lumping technique, several control approaches for nonlinear partial differential equation systems have been proposed. Patwardha et al. (1992) developed a nonlinear model predictive control strategy for controlling two distributed parameter systems: a packed distillation column and a fixed-bed catalytic reactor. An orthogonal collocation on finite elements was the method of choice to be used to discretize a spatial term of the PDE models. To improve the robustness of the model predictive control scheme, the feedback mechanism was incorporated into the controller.

Hanczyc and Palazoglu (1995) studied the extension of a sliding mode control scheme to regulate nonlinear distributed parameter chemical processes. The characteristic method was used to transform the PDE systems into a finite set of ODE models and then the sliding mode control was applied to the finite dimensional ODE models.

Research by Christofieds (2001) addressed the use of a combination of Galerkin's method with a procedure for the construction of approximate ODE systems. These ODE systems were then applied to synthesis of output feedback controllers for non-isothermal tubular reactors that guarantee stability and enforce the output of the closed loop system to follow a desired response.

Boskovic and Krstic (2002) applied a globally stabilizing boundary feedback control to a nonlinear PDE model of a chemical tubular reactor. The control objective was to stabilize an unstable steady state using the boundary control of temperature and concentration on the inlet side of the reactor. To achieve that, the original PDE model was discretized using a finite difference method giving a system of nonlinear ODEs. Then, a backstepping method was used to design the reactor controller.

Hua and Jutan (2000) presented a nonlinear inferential cascade control strategy for a fixed-bed reactor with highly exothermic reaction. The cascade control structure

was developed by lumping a PDE system and partitioning it into subsystems. Then, the direct synthesis approach for nonlinear control systems was used to design the controllers in each subsystem separately.

2.2.2 Late Lumping Approach

In contrast to the early lumping technique, an alternative late lumping approach first applies a distributed parameter control theory to full PDE models for designing a control system. After the controller design has been completed, the resulting control equations are then solved by lumping approximate techniques.

This approach has the advantage of designing a control algorithm which can remain closer to the original control problem. In another word, the PDE systems directly account for their distributed nature in the synthesis of the control algorithm. However, this approach requires a greater knowledge of the distributed system control theory

Various approaches have been considered to directly use PDE models in controller designs. Examples include the control algorithm proposed by Dochain et al. (1997) for controlling a fixed-bed reactor which is based on nonlinear distributed parameter models of the reactor. The control algorithm extends the application of adaptive linearizing control schemes to control the substrate concentration at the reactor output in the anaerobic digestion wastewater treatment process.

Another approach to design a control strategy using directly a PDE model was investigated by Renou et al. (2001). The proposed strategy composed of two control loops: the inner loop and the outer loop. The former contains an adaptive controller designed by considering the Lyapunov theory. The latter combines feedforward and feedback control. The performance of the controller was illustrated for the concentration control of a bleaching reactor. Simulation results showed that the designed controller based on the late lumping approach give good control performances in case of set point tracking and disturbance rejection.

Christofides and Daoutidis (1996) applied an extension of the geometric control method to hyperbolic PDE systems which quasi-linear hyperbolic PDE systems can

Table 2.2: Control studies of distributed parameter systems

Reference	Process	Lumping	Control technique
Armaou and Christofides (2002)	Tubular reactor	Early	Optimal control
Asteasuain et al. (2001)	Polymerization reactor	Early	Optimal control
Boskovic and Krstic (2002)	Tubular reactor	Early	Globally stabilization
Christofides (2001)	Tubular reactor	Early	Feedback control
Christofides and Daoutidis (1996)	Tubular reactor	Late	Geometric control
Christofides and Daoutidis (1998)	Fixed bed reactor	Late	Lyapunov method
Dochain et al. (1997)	Bioreactor	Late	Adaptive control
Hanczyc and Palazoglu (1995)	Heat exchanger	Early	Sliding mode control
Hua and Jutan (2000)	Fixed bed reactor	Early	Nonlinear cascade control
Lee et al. (1999)	Activated sludge process	Early	Generic model control
Renou et al. (2001)	Tubular reactor	Late	Adaptive control
Wu and Lion (2001)	Tubular reactor	Late	Feedback linearization

be input and output linearized and distributed in space. The concept of characteristic index was introduced and used for the synthesis of distributed state feedback laws that guarantee output tracking in the closed loop system.

Wu and Liou (2001) addressed the output regulation problem for a nonisothermal plug flow reactor (PFR) system. The input/output linearization technique was employed to synthesis the distributed nonlinear controller. It have been shown that the control methodology can prevent the appearance of the undesired state distribution (e.g. hot spot) inside the reactor.

Table 2.2 shows a summary of control algorithms which have been studied and applied to distributed parameter systems.

2.3 Trickle Bed Reactor

A trickle bed reactor (TBR) is one of several types of multiphase reactors which have been widely used in industrial chemical processes for many years. Many applications of trickle bed reactors can be found primarily in petroleum industry for hydrocrak-

ing, hydrodesulfurization, and hydrodenitrogenation. In addition, trickle bed reactors are also employed in the petrochemical industry, involving mainly hydrogenation and oxidation of hydrocarbon compounds (Gianetto and Specchia, 1992).

In a trickle bed reactor, the liquid phase flows down over a fixed bed of catalyst in the form of a thin liquid film while the continuous gas phase flows through the catalyst bed either cocurrently or countercurrently. However, in most common mode of operation in industrial practice, gas and liquid phases flow cocurrently downward because of the absence of flooding and its relatively lower pressure drop, compared with other modes of operation (i.e. cocurrent upflow or countercurrent flow) (Satterfield, 1975). The commercial trickle bed reactors are operated under plug flow conditions. The catalysts are effectively wetted. These result in high conversion to be achieved in the reactor. In addition, the low pressure drop allows for a uniform partial pressure of gaseous reactants (i.e. hydrogen in hydroprocessing) in the reactor. This would be important for ensuring hydrogen-rich condition at catalyst surface along the entire length of the reactor (Shah, 1979).

Because of the important of trickle bed reactors to the petroleum, petrochemical, chemical and other industries, numerous review papers have appeared in the literature, emphasizing on the development of various empirical correlations to describe hydrodynamics and transport phenomena within the reactor. Among of these are contributions by Satterfield (1975), Hofman (1977), Herskowitz and Smith (1983), Ng and Chu (1987), Zhukova (1990), Gianetto and Specchia (1992), and Dudukovi et al. (1999).

2.3.1 Modeling of TBR

Since the two flowing phases in a trickle bed reactor make the reactor behavior complex, involving mass and heat transfer processes between gas and liquid and between liquid and catalyst particle, a large number of researches have been done to obtain a model for describing its behavior.

In general, the mathematical models of the reactor with fixed bed catalyst can be classified into two groups: a pseudo-homogeneous and heterogeneous model, depending

on whether or not heat and mass transfer between the phases is considered. In the pseudo-homogeneous model, the difference of state variables i.e. concentration and temperature, between the phases are neglected whereas in the heterogeneous model, such a difference is significant and cannot be neglected; mass and heat balances are written for each of the phases. However, most of the trickle bed reactor models reported in the literature have been developed based on the heterogeneous models since they usually give results with good accuracy.

Many researchers have attempted to develop rigorous models for explaining the behavior of the trickle bed reactor and computation techniques for solving the resulting model equations.

Warna and Salmi (1996) developed dynamic models based on the three-film theory for describing trickle bed reactors operating under non-isothermal conditions. Reactor simulation was illustrated with a case study: the hydrogenation of toluene. The gas and liquid phases are assumed to be plug flow conditions. The model equations for the gas, liquid and catalyst phases consisted of a set of partial differential equations (PDEs) and ordinary differential equations (ODEs). The solution of these equations was obtained by the method of lines technique using finite difference approximation to discretize the spatial derivative terms. The approximate ordinary differential equations (ODEs) obtianed were solved by using the backward difference method.

Korsten and Hoffmann (1996) provided the model of a trickle bed reactor, operated under isothermal condition, for hydrotreating reactions. It included correlation for determining mass transfer coefficients, gas solubilities and the properties of oils and gases under process conditions. The mass balances for reactor models is based on the two-film theory (gas-liquid and liquid-solid interfaces). The models was tested with data from pilot plant where the hydrodesulfurization of gas oil occur. The simulation showed a good agreement with experiment results carried out in a wide range of temperature and pressure.

Hanika and Lange (1996) proposed a new idea for approximation of an adiabatic trickle bed reactor behavior by employing a cascade of connected continuous stirred tank reactors with the same volume (tank-in-series models) to describe the dynamics

of the reactor. A set of ordinary differential equations was numerical solved using the Runge-Kutta method. The modeling results were compared to the experimental data obtained from a laboratory-scale reactor where cyclohexene hydrogenation on palladium catalyst is used as a case study.

Devetta et al. (1997) simulated a high pressure trickle bed reactor using a pseudo homogeneous two dimensional model. The model equations consisted of partial differential equations which were solved by an orthogonal collocation method. The reaction studied was the hydrogenation of organic substrates, using supercritical CO_2 as a solvent to increase the solubility of hydrogen in the liquid reactants. It was found that modeling results agreed with the experimental data obtained in a pilot plant unit.

Recently, a trickle bed reactor model that takes into account the contributions of partial wetting and stagnant liquid hold-up effects in addition to external and intraparticle mass transfer resistances for a complex reaction scheme was proposed by Chaudhari et al. (2002). Performance of the reactor was studied experimentally and theoretically for an exothermic multistep hydrogenation of 1,5,9-cyclododecatriene. A comparison of the model prediction with experimental data showed excellent agreement.

Chapter 3

Computational Method of Model Predictive Control

As mentioned in Chapter 2, model predictive control refers to a class of control algorithms in which current manipulated variables are obtained by solving on-line an open loop optimal control problem using the current state of a system. The optimization gives a sequence of optimal control input; however, only the the first control is implemented to the system.

This chapter examines the direct optimization approach, which is the method used in this thesis, to the solution of the open loop optimal control problem. First, the basic formulation of MPC problem which comprises of an objective function, system constraints, and state and control constraints is introduced. Then, two general strategies within the framework of the direct method: sequential and simulataneous approach, are explained, The advantages and limitations of both strategies are also discussed.

3.1 Formulation of Model Predictive Control Problem

In this research, we consider the formulation of model predictive control (MPC) problem in continuous time fashion. Mathematically, this problem can be stated as: find the control $u(t)$ minimizing the objective function:

$$J = \int_{t}^{t+T_P} F\left(x(t), u(t); p\right) dt \tag{3.1}$$

subject to process models:

$$\dot{x}(t) = f\left(x(t), u(t); p\right) \tag{3.2}$$

$$x(t_0) = x(0) \tag{3.3}$$

where x is a vector of state variables, $\dot{x}$ denotes the derivative of x with respect to time (t), u is a vector of control variables, f represents a vector of process model functions that is continuously differentiable, p is model parameters, T_P is a prediction time horizon and J defines a desired objective function.

Equations (3.1) to (3.3) provide a basic formulation in the MPC that the control input is determined to minimize the objective function (performance index) subject to process model constraints. However, for some situations, other constraints can be involved in this problem. These include:

Control constraints:

$$u_L \leq u(t) \leq u_U \tag{3.4}$$

State constraints (path constraints):

$$g_L \leq g(x(t), u(t), t) \leq g_U \tag{3.5}$$

Terminal constraints (end-point constraints):

$$h_L \leq h(x(T_p), u(T_p), T_p) \leq h_U \tag{3.6}$$

where u_U and u_L are an upper and lower bound on control variables, g_U and g_L are an upper and lower bound on state constraints, h_U and h_L are an upper and lower bound on terminal state constraints, respectively.

Control constraints generally appear in the MPC problem because, in real application, an ability to manipulate the control variables is always limited. Path constraints are included in the MPC formulation if some of state variables cannot exceed a given limit during the course of process operation. In addition, in some circumstances where the states are necessary to be satisfied in a specific range at the final time, there also arise the terminal constraints of the form as in Equation 3.6 in the MPC problem.

It is evident from the above formulation that the MPC requires the on-line solution of a optimal control problem at each sampling time to determine the manipulated inputs. This problem type involves an optimization of the dynamic systems subject to process constraints concerning state and control variables.

There are several different computational techniques available for giving the solution of such a problem. One approach is based on a classical variation method in which the optimal control is obtained indirectly through the solution of necessary conditions for optimality (Ray, 1981). However, it has been found that such conditions result to a two-point boundary value problem which is difficult to solve. Another class of solution, known as a dynamic programming approach, applies the principle of optimality to develop Hamilton-Jacobi-Bellman partial differential equations, leading to the solution of optimal control problem. The limitation of this approach concerns large computational burden especially in high dimensional systems. The further detail of these solution methods is given in Appendix A.

During the last two decades, the method that uses discretization technique has been received much attention and considered as an efficient technique. The concept of this approach is to transform the original optimal control problem to a finite dimension optimization problem, typically a nonlinear programming problem (NLP). Then, the optimal control solution is given by applying a standard NLP solver to solve the optimization problem directly. For this reason, this approach is known as *a direct method*. The transformation of the problem can be made by using discretization techniques either on only control variables (partial discretization) or on both state and control variables (complete discretization). Based on this consideration, the approach can be classified into two categories: sequential and simultaneous strategy.

3.2 Sequential Strategy

In the sequential strategy, a control (manipulated) variable profile is discretized over a time interval. The discretized control profile can be represented as a piecewise constant, a piecewise linear, or a piecewise polynomial function. The parameters in such functions and the length of time subinterval become decision variables in optimization problem. This strategy is referred to *a control vector parameterization (CVP)*.

The basic concept of the sequential approach consists of a two-step procedure; the
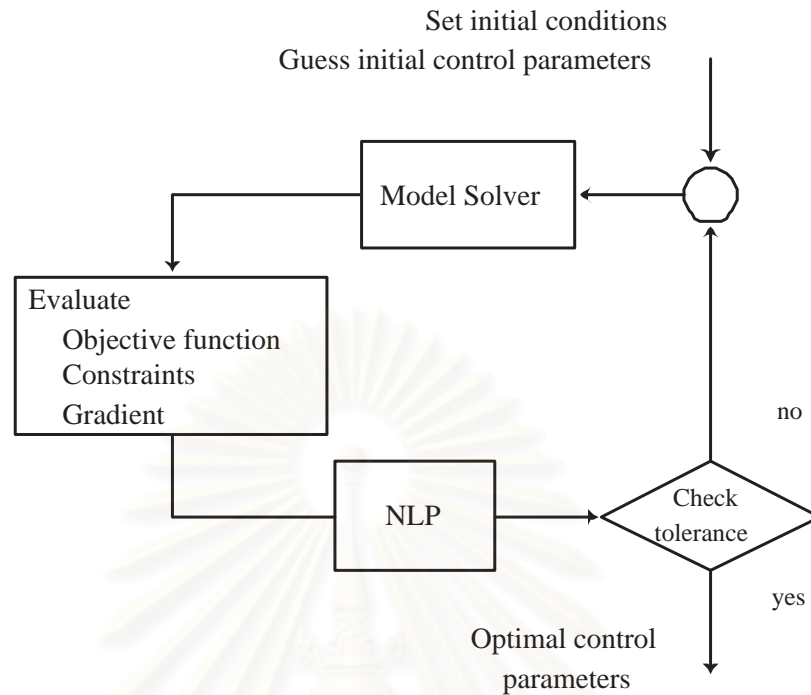
Figure 3.1: The sequential solution approach

first one deals with an integration of process models and the second one involves a solution of optimization problem, as illustrated in Figure 3.1. These procedures are proceed sequentially; that is, given the initial conditions for state variables (dependence variables) and the initial guess for a set of control parameters (decision variables), the process dynamic models are solved (an initial value problem, IVP) to determine the trajectory of state variables at each iteration of optimization. This provides information of the objective function and constraints to the nonlinear programming solver (NLP). Then, the optimization is performed in order to choose the new set of optimal control parameters. This process is repeated until the optimum is satisfied within a specified accuracy. Since in every iteration of the optimization algorithm the process models are satisfied, the sequential strategy is commonly known as a feasible path approach.

Since most NLP algorithms require the gradient of both the objective function and constraints with respect to the control parameters, this information can be calculated by several methods, e.g. *i)* numerical differentiation through finite differences involving repeated call to the routine that solves the dynamic models with different step size, *ii)*

direct solution of sensitivity equation which can be derived from the process equations, and *iii)* integration of the adjoint equations which are determined from the variation approach. However, the gradient information obtained by the finite difference method is not recommended. This is because the integration error during repeated calling can be occurred and may affect to the accuracy of the gradient information obtained. The accurate value has an important to the efficiency of the NLP solver. Macauley and Macgregor (1992) stated that the number of iterations required in the sequential approach to obtain the optimal control solution could be substantial reduced if the accurate value of the gradient information is provided. A comparison on these different methods to evaluate the gradient within the sequential framework has been studied by many researchers. For instance, Fikar et al. (1998) applied the CVP method with different gradient calculations: finite difference and adjoint approach, to determine optimal control policy for a binary distillation. They found that the CVP method was able to solve such a control problem; however, the adjoint-based approach showed superiority over the finite difference-based one.

It should be noted that some methods used in NLP algorithms are not necessary to need the evaluation of gradient; however, they commonly require many function evaluations and this may result in excessively large computation time. Thus, the use of gradient to determine a search direction gives an advantage to increasingly improve the rate of convergence in optimization algorithms.

One advantage in the sequential approach is that only the parameters used to discretize the control profile are considered as the decision variables. The optimization formulated by this approach is a small scale NLP that makes it attractive to apply for solving the optimal control problem with large systems which are modeled by a large number of differential equations. In addition, this approach can take advantages of the available IVP solvers.

However, the limitation of the sequential method is a difficulty to handle a constraint on state variables (path constraints). This is because the state variables are not directly included in NLP. To handle state constraints within the sequential approach, several methods have been proposed and developed.

The first approach used to address the inequality path constraints relies on defining a function that measures the violation of the constraints. The use of constraint violation appears in the following different ways. Firstly, it is used as a penalty term over the entire time horizon in the objective function; however, this approach may cause the numerical difficulties since the value of weighting factor on the penalty term is necessary to be high to ensure that the constraints are satisfy. Secondly, the violation function is defined over the entire time domain as end-point constraints which are forced to be zero at the final time. Since the gradient of the end-point constraints are zero at the optimum, this may decrease a convergence rate when the solution is approaching. Thirdly, the violation term is enforced through interior point constraints to be zero instead of forcing them at the final time as in the previous method. The interior points are the result of the application of the discretization of these constraints at a finite number of points. The main disadvantage of this method is that a large number of interior points are needed if the path constraints are not to be violated during the optimal trajectory. That results in a large scale optimization problem.

Another approach to cope with the inequality path constraints is to transform them into equality constraints by using a slack variable. The drawback of this approach is that it can generate high-index problems which need a special index reduction technique. Furthermore, all inequality constraints require additional computational effort, even though they are never active during the solution trajectory.

3.2.1   Optimization Formulation of the Sequential Approach

To pose the dynamic optimization problem as a nonlinear programming problem with the sequential approach (CVP), the control $u(t)$ is approximated by a finite dimensional representation. The time interval $[t_0, t_f]$ is divided into a finite number of subintervals (P). In each subinterval, the control $u(t)$ is represented by a set of basis functions involving a finite number of parameters (z_j)

$$u(t) = \phi^j(t, z_j) \qquad t \in [(t_{j-1}, t_j), j = 1, 2, \ldots, J] \qquad (3.7)$$

where $t_J = t_f$. The control profile is defined by the parameters z_j and switching times t_j. However, the piecewise constant control policy (zero order polynomial function) is

assumed and used because the form of the solution is ideally suited for implementation on a digital computer. Thus the set of decision variables for the nonlinear program can be written as

$$y = \{z_1, z_2, \ldots, z_J, t_1, t_2, \ldots, t_J\} \tag{3.8}$$

Computational procedure of the sequential approach is presented in Figure 3.1. With the initial guess of the decision variables (y), the integrator is used for solving the process models providing the value of the objective function and constraints. Once gradient information is given, the NLP solver determines a new set of control parameters and sends it back to the model solver. This procedure is repeated until the optimal value is found satisfying the specified accuracy.

3.3   Simultaneous Strategy

In contrast to the sequential approach, the simultaneous strategy solves the process dynamic models and the optimization problem at the same time. This avoids solving the model equations at each iteration in the optimization algorithm as in the sequential approach.

With this approach, the dynamic process model constraints in the optimal control problem are transformed to a set of algebraic equations which is treated as equality constraints in NLP problem. As a result, the optimal control problem is reduced to a constrained nonlinear optimization problem. To solve this problem, optimization algorithms based on a sequential quadratic programming (SQP) technique (also known as successive or iterative quadratic programming) are widely used in this approach. In the SQP, at each iteration of optimization, a quadratic program (QP) is formed by using a local quadratic approximation to the objective function and a linear approximation to the nonlinear constraints. The resulting QP problem is solved to determine a search direction and with this search direction, the next step length of the decision variables is specified. The SQP is known as *an infeasible path optimization algorithm* since it does not require that nonlinear constraints are satisfied until the optimal control is found; that is, only a linearized set of nonlinear equality constraints is solved

and as the SQP converges to the optimum, the solution of the linearized set converges to the solution of the nonlinear equality constraints.

To apply the simultaneous strategy, both state and control variable profile are discritized by approximating functions and treated as decision variables in the optimization problem. Since the process models are embedded in the optimization as equality constraints, a discretization technique used to approximate differential equations obtained from process models to a set of algebraic equations should be chosen properly to compromise between the accuracy of the approximation and the size of the optimization problem.

Although finite difference techniques through the Euler formulation can be used for this purpose, it needs a small step size to give a satisfactory solution that results in a large scale optimization problem with many variables. To avoid such a problem, the state variables are approximated by polynomial functions using a weighted residual method e.g. Galerkin's method and collocation method. However, the collocation method is used by a number of researchers because it does not require the evaluation of integral terms of the control variables (Tsang et al., 1975). The use of polynomial approximation to the state solution in the collocation method can be defined over either the entire time horizon (Global collocation method) (Tsang et al., 1975; Biegler, 1984) or parts of each subinterval that provides an approximation over the whole time domain (Cuthrell and Biegler, 1987; Renfro et al. 1987). The latter is referred to the collocation method on finite elements.

The control variables can be discretized and represented either by polynomial continuous function or by piecewise control policy as in the sequential approach if the collocation method on finite elements is used to approximate the state profile. It should be noted that the function used to discretize state and control variables is not necessary to be the same function (Eaton and Rawlings, 1990)

The main advantage of the simultaneous approach is a capability in handing constraints on state variables. This is because these constraints can be dealt with by including them directly in the optimization problem as additional constraints. However, due to the discretization on both state and control variables, this leads the

simultaneous approach to a large scale optimization problem consisting of a large set of algebraic constraints and decision variables

3.3.1   Optimization Formulation of the Simultaneous Approach

In the simultaneous method, a continuous time optimal control problem is transformed into a finite dimensional nonlinear programming problem by approximating state and control profiles. An orthogonal collocation method on finite elements is applied to discretize the state profile since it allows accurate representation of the state profile without using high order polynomial and is able to solve a wide range of problems (e.g. stiff and boundary value problems) as pointed out by Renfro et al. (1987).

In order to apply the orthogonal collocation method on finite elements, the prediction time horizon (T_p) is divided into NE elements that each finite element equals to one sampling time as can be seen in Figure 3.2. Within each element, we apply a Lagrange polynomial to convert differential model equations into algebraic equations. The approximate relation of differential variables can be defined by linear summation of state values at each collocation point as shown by the following equation (for element k):

$$\left(\frac{dx}{dt} \right)_{t=t_i} = \frac{1}{h_k} \sum_{j=1}^{ncol} A_{ij} x(t_j) \tag{3.9}$$

where $x(t_j)$ represents a value of state variable x at discreted point t_j, which is chosen as the roots of an orthogonal polynomial, h_k is the length of element k, A is the weighting matrix for first derivative term and *ncol* is a number of collocation points in each element.

Additionally, the control profile is represented by piecewise constant function; the value of control u is assumed to be constant in each element as shown below (Equation (3.10)). The reason of using this representative form of the control variables contributes to its appropriateness for computer control implementation. Figure 3.2 illustrates the discretization of control input as well as state profile with 2 internal collocation points for each element.

$$u(t) = \{u_1, u_2, u_3, \dots, u_{NE}\} \tag{3.10}$$
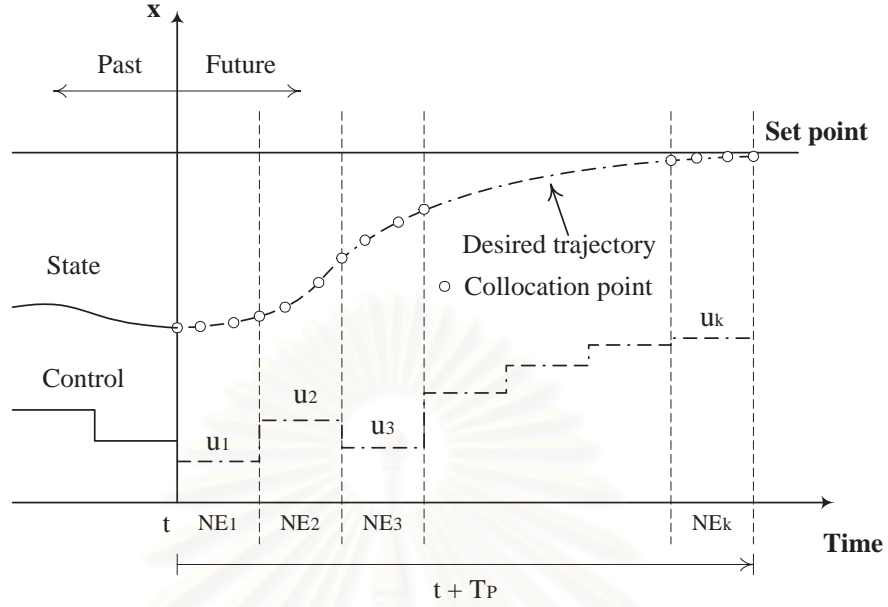
Figure 3.2: The simultaneous solution approach

To pose the optimal control problem in a standard form of constrained optimization problem, the integral term in the objective function (Equation (3.1)) is needed to be further modified. Here, Radau quadrature formulation is chosen to approximate this integral term (Villadsen and Michelsen, 1978). As a result, the NLP problem can be stated as:

$$\min_{\{x,\,u\}} J = \sum_{i=1}^{NE} \sum_{j=1}^{ncol} w_j F_{ij}(x, u, p) \tag{3.11}$$

subject to (for k^{th} element: $k = 1, , NE$)

discreted process models:

$$\frac{1}{h_k} \sum_{j=1}^{ncol} A_{ij} x(t_j) = f\left(x(t_i), u_k, p\right) \quad 1 \le i \le ncol \tag{3.12}$$

algebraic equations:

$$g(x_i, u_i, p) = 0 \quad 1 \le i \le ncol \tag{3.13}$$

state and control constraints:

$$x_L \le x_i \le x_U \tag{3.14}$$

$$u_L \le u_i \le u_U \tag{3.15}$$

continuity equations:

$$x(t_1) \text{ at } \text{k}^{\text{th}} \text{ element} = x(t_{ncol}) \text{ at } (\text{k} - 1)^{\text{th}} \text{ element} \tag{3.16}$$

where w_j is Radau quadrature weights. It should be mentioned that an alternative approach to convert the integral term in the objective function into a standard form can be done by defining a new additional state variable representing the integral function (see e.g. Renfro et al., 1987 for detail). However, this way should be avoided in the simultaneous optimization strategy because it will increase a number of unnecessary state variables in the optimization problem.

Chapter 4

Modeling of Trickle Bed Reactor for Selective Hydrogenation of Pyrolysis Gasoline*

Developing a mathematical model for describing chemical systems has been the main focus of research for many years because it can be employed as a useful tool to study, design and improve the systems. In addition, the model can be used in the formulation of advanced model-based control techniques.

This chapter presents the development of dynamic distributed models for a trickle bed reactor, one of most commonly used reactors in industrial processes. The reactor model is demonstrated by the catalytic hydrogenation of pyrolysis gasoline produced from an olefin plant. The formulation of an optimization problem is given to estimate kinetic parameters. Finally, the prediction of the state variables obtained from the reactor model is validated with actual plant data. It should be noted here that the models developed in this chapter will be used in the formulation of a model predictive control strategy to regulate the reactor.

4.1 Catalytic Hydrogenation of Pyrolysis Gasoline

A catalytic hydrogenation is an important industrial process which is involved many petroleum fractions in refining and petrochemical industries. The purpose of this process is to stabilize unsaturated and reactive hydrocarbons i.e. diolefins in order to

---

*Portions of this chapter were appeared in Arpornwichanop et al. (2002a) and Kittisupakorn and Arpornwichanop (1999).

avoid the formation of undesired products during downstream processing. In addition, the hydrogenation process can be used to remove sulfur content in petroleum products.

Pyrolysis gasoline is one of the products produced by a steam cracking process in an olefin production plant. Typical pyrolysis gasoline has a boiling range of 40-120 ^{o}C and usually contains C5-C9 hydrocarbons (Cheng et al., 1986). Due to high content of olefins and aromatics, the pyrolysis gasoline is suitable either as high-octane blending components for motor gasoline fuel or as high-aromatic feedstock for an aromatic extraction. However, the raw gasoline cut from steam cracking is unstable because of the presence of a large amount of unsaturated hydrocarbons, known as gum-forming compounds, such as diolefins and styrenes.

To prevent gum formation during downstream processing or storage, the pyrolysis gasoline is stabilized by a selective hydrogenation process. The advantage of this process is that it can efficiently remove most of unstable compounds and convert them to desired olefins and aromatics, thus increasing overall yield (Derrien et al., 1974).

The hydrogenation processing of pyrolysis gasoline can be classified into two groups depending on type of the desired final products. That is, if the purpose is in order to obtain a gasoline fuel blendstock, only the first stage hydrogenation where the selective hydrogenations of diolefins and alkenylaromatics occur without saturating other unsaturated hydrocarbon i.e. olefins and aromatics, is used. If the process is aimed to obtain a product for further aromatics extraction, the second stage hydrogenation (total hydrogenation) where the further hydrogenations of olefins and hydrodesulphurization occur without aromatics hydrogenation, is followed by the first stage hydrogenation (Derrien,1986). Figure 4.1 shows the simplified flow diagram of gasoline hydrogenation process.

In this work, we concentrate on the first stage hydrogenation process; the main unit of this process is a gasoline hydrogenation reactor. Owing to that the hydrogenation reaction is an exothermic, two schemes for operating the reactor are possible: isothermal and adiabatic reactor. The former consists of multi-tubular reactors externally cooled by a cooling fluid. However, the cost of investment is high and it is impractical to make in situ regeneration. The latter is operated in adiabatic condition. The

(A)

First stage reactor

Fuel gas

Hydrogenated gasoline

Fuel gas

Hydrogen

Feed

Residue

(B)

First stage reactor

Second stage reactor

Fuel gas

Fuel gas

Fuel gas

Fuel gas

Stabilizer

Heater

Pyrolysis gasoline

Hydrogen

Feed
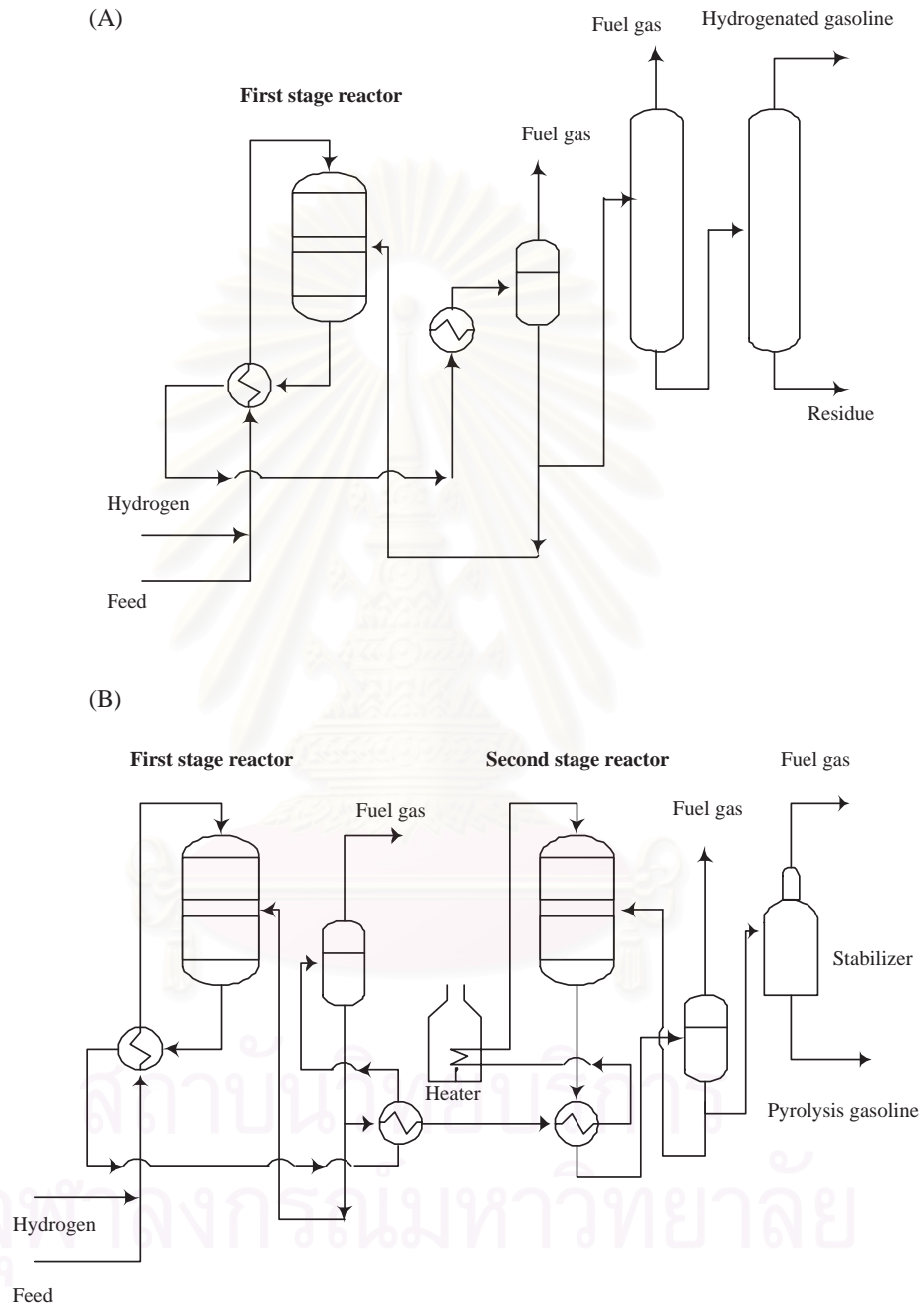
Figure 4.1: Simplified flow diagram of the pyrolysis gasoline hydrogenation. (a) First stage hydrogenation (b) Second stage hydrogenation

increment of temperature resulting from heat of reactions is avoided either by quench injection or by feed dilution.

In general, hydrogenation of pyrolysis gasoline is conducted in liquid phase in the presence of Ni or Pd supported catalyst. These catalysts are appropriate for the operation at low temperature and high pressure in order to maintain the hydrocarbon stream in liquid phase. The liquid phase operation is beneficial to reduce pressure drop through the catalyst bed and also to wash high molecular weight species i.e. polymer, which otherwise deposit on the surface of catalyst and then accelerate the loss of its activity.

4.2 Process Description of the First Stage Hydrogenation

Figure 4.2 illustrates the simplified schematic diagram of the first stage hydrogenation studied in this research. First, raw pyrolysis gasoline (C5+) from ethylene plant is combined with makeup and recycle hydrogen, and diluent (hydrogenated gasoline product). After heating against the reactor effluent, the mixed stream of gasoline (raw gasoline, hydrogen and diluent) is delivered to the first stage reactor in which hydrogenations of diolefins and alkenylaromatics occur in liquid phase. The inlet temperature varies between 60 and 120 ^{o}C and the reactor is approximately operated at pressure of 30 atm.

Since hydrogenations are exothermic causing an temperature increase in the reactor, some of hydrogenated gasoline (quench stream) is added directly to the reactor between the two catalyst beds in order to maintain the reactor temperature at an operable level. The reactor effluent is passed to a heat exchanger to heat up the gasoline feed and then is flashed in a hot separator. The vapor from the separator is sent to further process in order to make recycle hydrogen while the bottom liquid hydrogenated gasoline is passed through the second stage reactor. However, a portion of the hydrogenated gasoline is recycled to the first stage reactor, which is used as diluent and quench stream.

First stage reactor

Quench

Fuel gas

Fuel gas

H2 Recycle

H2 Make up

Raw gasoline feed

Diluent

Product to
the second stage reactor
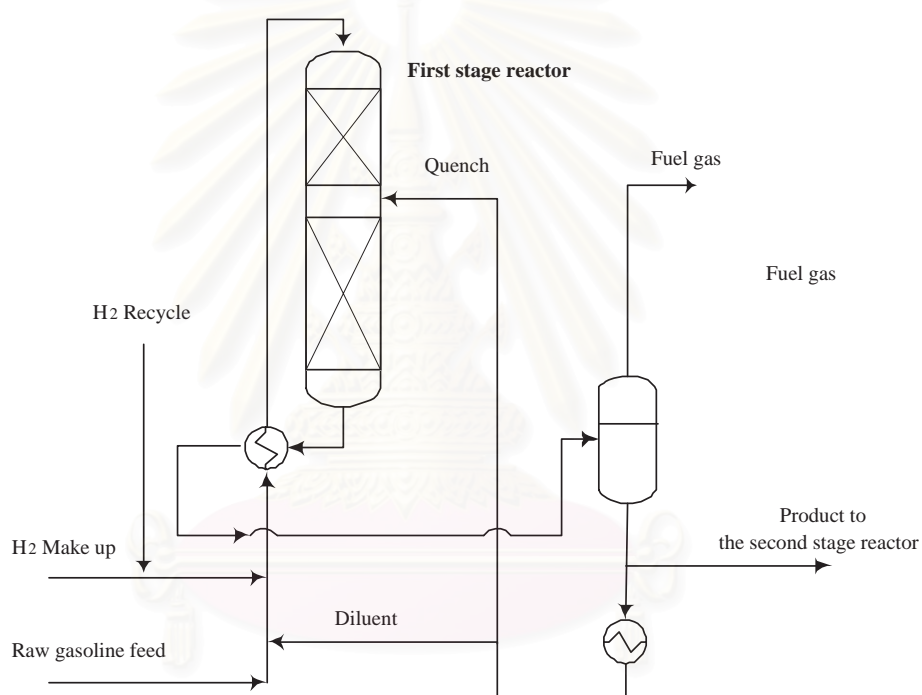
Figure 4.2: Schematic representative of the first stage hydrogenation studied in this work

Table 4.1: The configuration of the trickle bed reactor and properties of catalyst particles in this study

Reactor	
height of the top catalyst bed	7.9 m
height of the bottom catalyst bed	15.75 m
diameter	1.8 m
Catalyst particles	
shape	sphere
diameter	3 mm
void fraction	0.4
volume of the top bed	20 m^3
volume of the bottom bed	40 m^3

As mentioned earlier, the typical pyrolysis gasoline is a complex mixture of diolefins, alkenylaromatics, olefins, aromatics, paraffins and naphthenes, mostly within C5 and C9. It has been known that stabilization of the pyrolysis gasoline involves the elimination of unstable compounds i.e. diolefins and alkenylaromatics. Nevertheless, other unsaturated hydrocarbons i.e. olefins may also be hydrogenated. It is noted that chemical reactions within the reactor primarily involve the consecutive hydrogenations of diolefins to olefins and then to paraffins within the same carbon number group. Figure 4.3 represents the main reactions in the gasoline hydrogenation reactor.

The objective of this research is to develop dynamic models for the first stage hydrogenation reactor in which hydrogen and raw pyrolysis gasoline cocurrently flow through a fixed bed of catalyst. This type of reactor is known as a trickle bed reactor (TBR). The reactor has a diameter of 1.8 m and contains approximately 60 m^3 of Ni/Al$_2$O$_3$ catalyst which is divided into two beds. Table 4.1 shows the configuration of the reactor as well as the properties of catalyst particles studied in this work.

1. Hydrogenation of diolefins

  e.g.   CH2=CH-CH=CH-CH3 + H2 $\longrightarrow$ CH3-CH=CH-CH2-CH3
           (1,3 Pentadiene)   (2 Pentene)

2. Hydrogenation of cyclodiolefins

  e.g.

       (Cyclohexadiene)   + H2 $\longrightarrow$ (Cyclohexene)

3. Hydrogenation of alkenylaromatics

  e.g.   (Styrene)   + H2 $\longrightarrow$ (Ethylbenzene)

4. Hydrogenation of olefins

  e.g.   CH2=CH-CH2-CH2-CH3 + H2 $\longrightarrow$ CH3-CH2-CH2-CH2-CH3
           (1 Pentene)   (n Pentene)

       (Cyclopentene)   + H2 $\longrightarrow$ (Cyclopentane)

5. Olefins isomerization

  e.g.   CH2=CH-CH2-CH2-CH3 $\longrightarrow$ CH3-CH=CH-CH2-CH3
              (1 Pentene)   (2 Pentene)

Figure 4.3: Main reactions in the first stage hydrogenation reactor

4.3   Mathematical Model of Trickle Bed Reactor

To develop a dynamic model of a trickle bed reactor for the hydrogenation of pyrolysis gasoline, the following assumptions have been made:

1. The reactor operates at transient condition under adiabatic and isobaric condition.

2. The gas and liquid phase are supposed to be in a plug flow condition.

3. Axial dispersion in both gas and liquid phases is negligible.

4. The gas-liquid mass transfer resistance is considered whereas mass transfer resistance at the liquid-solid interface and the resistance to pore diffusion can be ignored. They are assumed to be included in the effective kinetic expressions.

5. The catalyst particles are assumed to be completely wetted with the liquid.

6. All the reactions are assumed to take place in the liquid phase.

7. The vaporization of hydrocarbons is negligible.

8. The interphase and intraparticle heat transfer limitation are assumed to be negligible. The heat generated from the reactions is assumed to be carried away by the flowing liquid.

9. Physical properties of reacting components and the heat of reactions are constant.

Furthermore, due to that a large number of reactions and components take part in the reactor system, the model will be complex. To reduce the complexity of the reactor model, all hydrocarbon components in the system are refined into three hydrocarbon classes (Somer et al. (1976); Cheng et al. (1986)). Each class represents a single compound. The classification of hydrocarbons from C4 to C9 of pyrolysis gasoline in each pseudocomponent is shown in Table 4.2 which comprises of diolefins, olefins and

Table 4.2: Lumped hydrocarbon components in the study

Carbon number	Diolefins	Olefins	Parafins	Aromatics
C4	Butadiene	Butene	Butane	
C5	Cyclopentadiene	Cyclopentent	Cyclopentane	
	Isoprene	Methylbutene	Isopentane	
	Pentadiene	Pentene	Pentane	
C6	C6-diolefins	C6-olefins	C6-parafins	Benzene
C7	C7-diolefins	C7-olefins	C7-parafins	Toluene
C8		C8-olefins	C8-parafins	Styrene
				Ethylbenzene

paraffins. The following kinetic model scheme has been considered to represent the hydrogenation in the present study:

$$Diolefins \xrightarrow{k_1} Olefins \xrightarrow{k_2} Paraffins$$
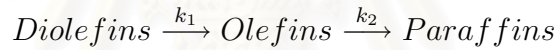
The concentration dependence of each pseudocomponent on the rate expression is based on that proposed in the literature for selective hydrogenation of pyrolysis gasoline. It was observed that the hydrogenation showed irreversible reaction and first order with respect to hydrogen and unsaturated reactant concentration. In addition, from experimental results, it appeared that the disappearance of olefins is influenced from a number of diolefins in the reaction system; hydrogenation of olefins occurs after the diolefins are completely hydrogenated. This indicates that the diolefins are strongly absorbed on the catalyst surface. Hence, the rate of olefins hydrogenation contains the adsorption term of diolefins (Somer et al., 1976; Bressa et al., 2003). Based on the available information, the rate expressions as given below are utilized.

$$r_1 = k_1 C_{di} C_{H_2} \tag{4.1}$$

$$r_2 = \frac{k_2 C_{ole} C_{H_2}}{1 + k_{ad} C_{di}} \tag{4.2}$$

where r_1 and r_2 are hydrogenation rate of diolefins and olefins, respectively. k_1 and k_2 are specific reaction rate constant. k_{ad} is adsorption constant. The temperature dependency of these kinetic parameters is described by the Arrhenius correlation.
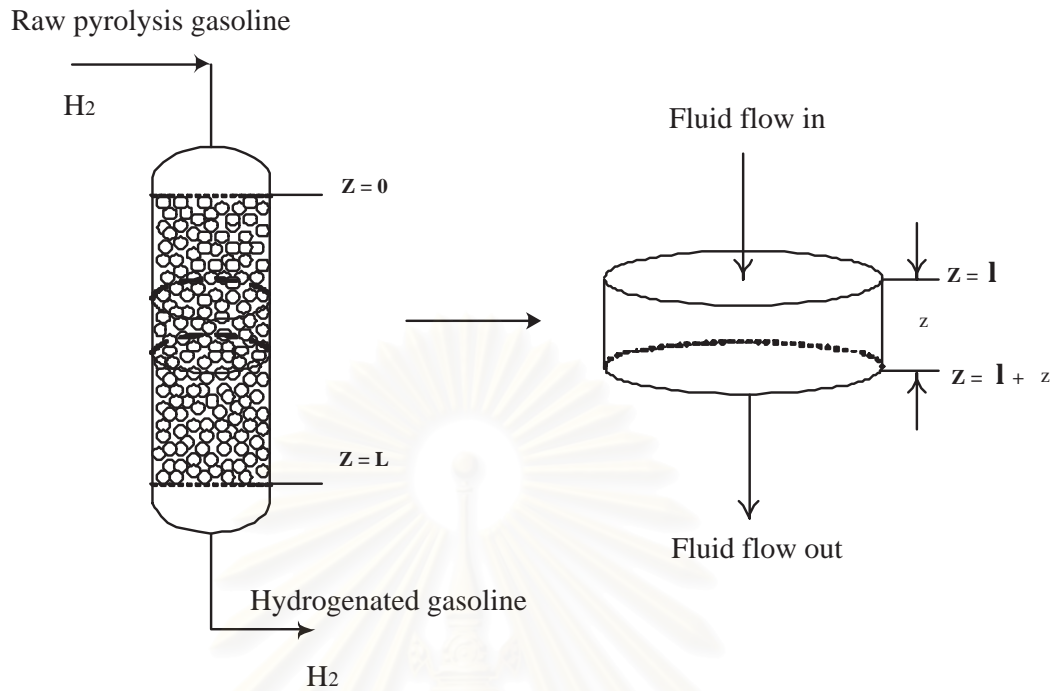
Figure 4.4: Development of mathematical models for a trickel bed reactor

4.3.1 Reactor Models

Let us consider a trickle bed reactor of length L and cross sectional area A, which gas and liquid cocurrently down flow through pack bed catalyst as shown in Figure 4.4. Performing a mole and energy balance for component i around an increment Δz leads to the following equations:

Mole balances

Gas phase

H$_2$:

$$A\Delta z\varepsilon_g \frac{dC_{H_2,g}}{dt} = u_g A \left(C_{H_2,g}|_{z=l} - C_{H_2,g}|_{z=l+\Delta z} \right) - A\Delta z K_{l,H_2} a_i \left(C_{H_2,g} - C_{H_2,l} \right) \quad (4.3)$$

Liquid phase

H$_2$:

$$A\Delta z\varepsilon_l \frac{dC_{H_2,l}}{dt} = u_l A \left(C_{H_2,l}|_{z=l} - C_{H_2,l}|_{z=l+\Delta z} \right) + A\Delta z K_{l,H_2} a_i \left(C_{H_2,g} - C_{H_2,l} \right)$$
$$- A\Delta z(1-\varepsilon)(r_1 + r_2) \quad (4.4)$$

HC: diolefins, olefins, parafins

$$A\Delta z\varepsilon_l\frac{dC_{HC,l}}{dt} = u_lA\left(C_{HC,l}|_{z=l} - C_{HC,l}|_{z=l+\Delta z}\right) - A\Delta z(1-\varepsilon)(R_{HC}) \tag{4.5}$$

where R_{HC} is net reaction rate for each hydrocarbon component.

Dividing both side of Equations (4.3) to (4.5) by $A\Delta z$ and taking limits as $\Delta z = 0$, we have

Gas phase

H$_2$:

$$\frac{dC_{H_2,g}}{dt} = -\frac{u_g}{\varepsilon_g}\frac{dC_{H_2,g}}{dz} - \frac{K_{l,H_2}a_i}{\varepsilon_g}\left(C_{H_2,g} - C_{H_2,l}\right) \tag{4.6}$$

Liquid phase

H$_2$:

$$\frac{dC_{H_2,l}}{dt} = -\frac{u_l}{\varepsilon_l}\frac{dC_{H_2,l}}{dz} + \frac{K_{l,H_2}a_i}{\varepsilon_l}\left(C_{H_2,g} - C_{H_2,l}\right) - \frac{(1-\varepsilon)}{\varepsilon_l}(r_1 + r_2) \tag{4.7}$$

HC: diolefins, olefins, parafins

$$\frac{dC_{HC,l}}{dt} = -\frac{u_l}{\varepsilon_l}\frac{dC_{HC,l}}{dz} - \frac{(1-\varepsilon)}{\varepsilon_l}(R_{HC}) \tag{4.8}$$

The correlations used for evaluation of hydrodynamics and mass transfer parameters for the trickle bed reactor are taken from the literature. The liquid hold up in the catalyst bed is calculated by the following correlation (Tarhan, 1983):

$$\varepsilon_l = 9.9\left(\frac{G_ld_p}{\mu_l}\right)^{\frac{1}{3}}\left(\frac{d_p^3g\rho_l^2}{\mu_l^2}\right)^{-\frac{1}{3}} \tag{4.9}$$

The overall external mass transfer resistance between gas and liquid phases can be written as:

$$\frac{1}{K_la_i} = \frac{1}{Hk_ga_i} + \frac{1}{k_la_i} \tag{4.10}$$

For slightly solution gases, such as hydrogen, the value of Henrry's constant (H) exceeds unity and gas mass transfer resistance can be negligible (Zhukova et al., 1990). Therefore, the total mass transfer can approximately equal to liquid phase mass transfer coefficient as:

$$\frac{1}{K_la_i} = \frac{1}{k_la_i} \tag{4.11}$$

The liquid phase mass transfer coefficient ($k_l a_i$) for H_2 is calculated using the correlation reported by Korsten and Hoffmann (1996).

$$\frac{k_{l,H_2}a_i}{D_{l,H_2}} = 0.4\left(\frac{G_l}{\mu_l}\right)^7\left(\frac{\mu_l}{\rho_l D_{l,H_2}}\right)^{\frac{1}{2}} \tag{4.12}$$

Energy balance

$$
\begin{aligned}
(\varepsilon_g \rho_g C_{p,g} + \varepsilon_l \rho_l C_{p,l})A\Delta z\frac{dT}{dt} &= (u_g A C_{p,g}\rho_g + u_l A C_{p,l}\rho_l)\left(T|_{z=l} - T|_{z=l+\Delta z}\right) \\
&\quad -(\Delta H)A\Delta z(1-\varepsilon)(r_1 + r_2)
\end{aligned} \tag{4.13}
$$

Dividing both side of Equation (4.13) by $A\Delta z$ and taking limits as $\Delta z = 0$, we obtain

$$\frac{dT}{dt} = \frac{-(u_g C_{p,g}\rho_g + u_l C_{p,l}\rho_l)\frac{dT}{dz} - (\Delta H)(1-\varepsilon)(r_1 + r_2)}{(\varepsilon_g \rho_g C_{p,g} + \varepsilon_l \rho_l C_{p,l})} \tag{4.14}$$

where ΔH is the heat of hydrogenation which is approximated to 30 kcal/mole for each double bond reaction (Hanika, 1977).

4.3.2 Quench Section

Within the trickle bed reactor studied here, a pack bed catalyst is divided into two beds between which a quench stream is added directly. Thus, the fluid from the top catalyst bed and the quench stream are mixed and then enter the second bed. Here, the space between successive beds is treated as the quench section which is assumed to be a perfectly stirred tank as demonstrated in Figure 4.5. It is also assumed that the mixing process reaches steady state instantaneously. Therefore, the steady state model of the stirred tank is employed to compute initial inlet conditions of reactant concentrations and temperature for the bottom catalyst bed, as given:

$$(Q_f + Q_q)C^{B2}_{H_2,l} = Q_f C^F_{H_2,l} + Q_q C^Q_{H_2,l} \tag{4.15}$$

$$(Q_f + Q_q)C^{B2}_{di,l} = Q_f C^F_{di,l} + Q_q C^Q_{di,l} \tag{4.16}$$

$$(Q_f + Q_q)C^{B2}_{ole,l} = Q_f C^F_{ole,l} + Q_q C^Q_{ole,l} \tag{4.17}$$
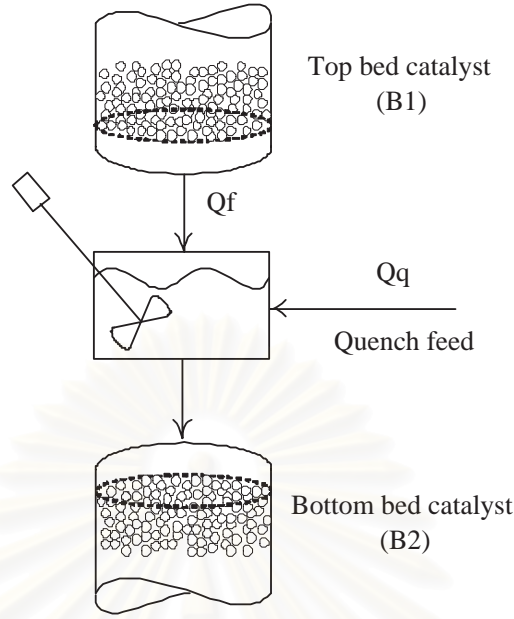
Figure 4.5: The model of quench section

$$(Q_f + Q_q)C_{para,l}^{B2} = Q_f C_{para,l}^F + Q_q C_{para,l}^Q \tag{4.18}$$

$$T^{B2} = \frac{u_g A \rho_g C_{p,g} T^F + \rho_l C_p (Q_f T^F + Q_q T^Q)}{(u_g A \rho_g C_{p,g} + (Q_f + Q_q)\rho_l C_{p,l})} \tag{4.19}$$

4.4 Numerical Solution

The dynamic models of the trickle bed reactor developed in the earlier section result to a set of partial differential equations (PDEs) describing the mass and energy balances. In this work, the partial differential equations are solved numerically using a *method of lines* technique; the spatial derivative terms in Equations (4.6) to (4.8) and (4.14) are discretized by an orthogonal collocation method on finite elements. The following equation is used to approximate the spatial derivative terms.

$$\frac{dx^i}{dz} = \frac{1}{h_k} \sum_{j=1}^{NP} A_{ij} x^j \tag{4.20}$$

where x^i represents a vector of state variables at position i in each element, h_k is a length of element k, NP is a number of collocation points in each element (k), and A is the weighting matrix for the first derivative term. Detail regarding the orthogonal collocation method is given in Appendix B.

Here, each packed bed of catalyst in the reactor is divided into 10 elements with an equal space and 2 internal collocation points are used for each finite element. Collocation points and weighting coefficients are determined using the algorithms of Villadsen and Michelsen (1978). On each element, applying Equation (4.20) in the dynamic reactor models (Equations (4.6) to (4.8) and (4.14)) leads to:

$$\frac{dC_{H_2,g}^i}{dt} = -\frac{u_g}{\varepsilon_g}\left(\frac{1}{h_k}\sum_j^{NP} A_{ij}C_{H_2,g}^j\right) - \frac{k_{l,H_2}a_l}{\varepsilon_g}\left(C_{H_2,g}^i - C_{H_2,l}^i\right) \tag{4.21}$$

$$\frac{dC_{H_2,l}^i}{dt} = -\frac{u_l}{\varepsilon_l}\left(\frac{1}{h_k}\sum_j^{NP} A_{ij}C_{H_2,l}^j\right) + \frac{k_{l,H_2}a_i}{\varepsilon_l}\left(C_{H_2,g}^i - C_{H_2,l}^i\right)$$
$$-\frac{(1-\varepsilon)}{\varepsilon_l}(r_1^i + r_2^i) \tag{4.22}$$

$$\frac{dC_{HC,l}^i}{dt} = -\frac{u_l}{\varepsilon_l}\left(\frac{1}{h_k}\sum_j^{NP} A_{ij}C_{HC,l}^j\right) - \frac{(1-\varepsilon)}{\varepsilon_l}(R_{HC}^i) \tag{4.23}$$

$$\frac{dT^i}{dt} = \frac{-(u_gC_{p,g}\rho_g + u_lC_{p,l}\rho_l)\left(\frac{1}{h_k}\sum_j^{NP} A_{ij}T^j\right) - (\Delta H)(1-\varepsilon)(r_1^i + r_2^i)}{(\varepsilon_g\rho_gC_{p,g} + \varepsilon_l\rho_lC_{p,l})} \tag{4.24}$$

where HC stands for diolefins, olefins and paraffins.

An approximation of the spatial derivative terms make the partial differential equations reduce to a system of differential and/or algebraic equations (DAEs). In this work, the DAEs are solved by means of the backward difference method using the well-known differential equation solver, DASSL (Petzold, 1982).

4.5 Kinetic Parameter Estimation

Before performing the solution of the models developed in the previous section, specific reaction rate constants (k_1, k_2) and adsorption coefficient (k_{ad}) in the rate expression, Equations (4.1) and (4.2), for hydrogenation of diolefins and olefins have to be determined. These variables are dependent on temperature according to the Arrhenius relation as follows:

$$k_1 = k_{0,1}\exp\left(\frac{-Ea_1}{RT}\right) \tag{4.25}$$

$$k_2 = k_{0,2}\exp\left(\frac{-Ea_2}{RT}\right) \tag{4.26}$$

$$k_{ad} = k_{0,ad} \exp\left(\frac{-Ea_{ad}}{RT}\right) \tag{4.27}$$

where k_0 is the apparent pre-exponential factor and Ea is the apparent activity energy.

Therefore, the unknown kinetic parameters consist of $k_{0,1}, k_{0,2}, k_{0,ad}, Ea_1, Ea_2$ and Ea_{ad}. All of these parameters will be estimated based on plant data. In this work, the industrial plant data in the gasoline hydrogenation unit (GHU) of the Thai Olefin Company's plant located at Map Ta Phut industrial estate, Rayong is collected for gasoline hydrogenation reactor.

Under normal operation, the reactor is usually operated within a narrow region in which the reactor operating condition is smooth and has a little change with time, so the data observed is assumed to be at a quasi-steady state condition.

4.5.1 Formulation of the Parameter Estimation Problem

The following optimization problem is solved to find the kinetic parameters which minimize the sum of residual squares between the prediction taken from the models and the plant data of the temperature profile in the reactor and the concentration of hydrocarbon components at the outlet of the reactor.

The objective function to be optimized is as follows:

$$\min_{\substack{k_{0,1},\ k_{0,2},\ k_{0,3} \\ Ea_1,\ Ea_2,\ Ea_{ad}}} J = \sum_{i=1}^{N} (T_i^{actual} - T_i^{model})^2 + \sum_{j=1}^{k} (C_{j,out}^{actual} - C_j^{model})^2 \tag{4.28}$$

subject to the steady state reactor models:

$$u_g \frac{dC_{H_2,g}}{dz} = -k_{l,H_2} a_l (C_{H_2,g} - C_{H_2,l}) \tag{4.29}$$

$$u_l \frac{dC_{H_2,l}}{dz} = k_{l,H_2} a_i (C_{H_2,g} - C_{H_2,l}) - (1-\varepsilon)(r_1 + r_2) \tag{4.30}$$

$$u_l \frac{dC_{di,l}}{dz} = -(1-\varepsilon)(r_1) \tag{4.31}$$

$$u_l \frac{dC_{ole,l}}{dz} = -(1-\varepsilon)(-r_1 + r_2) \tag{4.32}$$

$$u_l \frac{dC_{para,l}}{dz} = (1-\varepsilon)(r_2) \tag{4.33}$$

$$\frac{dT}{dz} = \frac{-(\Delta H)(1-\varepsilon)(r_1 + r_2)}{(u_g C_{p,g} \rho_g + u_l C_{p,l} \rho_l)} \tag{4.34}$$

Table 4.3: Estimated kinetic parameters

	Reaction rate constant and adsorption constant		
	k_1	k_2	k_{ad}
k_0	7345	7839	2.057
Ea	22500	35370	14907

$$r_1 = k_{0,1} \exp\left(\frac{-Ea_1}{RT}\right) C_{di,l} C_{H_2,l} \tag{4.35}$$

$$r_2 = \frac{k_{0,2} \exp\left(\frac{-Ea_2}{RT}\right) C_{ole,l} C_{H_2,l}}{1 + k_{0,ad} \exp\left(\frac{-Ea_{ad}}{RT}\right) C_{di,l}} \tag{4.36}$$

where i denotes the location of temperature measurement within the reactor and j denotes the hydrocarbon components: diolefins, olefins and paraffins, respectively.

The simultaneous approach as described in Chapter 3 is employed to solve such the optimization problem. With such an approach, the SNOPT software (Gill et al., 1998) is utilized for solving the resulting nonlinear programming problem. It applies a sparse SQP technique, using limited memory quasi-Newton approximations to the Hessian of the Lagrangian. The estimated kinetic parameters in the model equations were computed and given in Table 4.3.

4.6   Modeling Results

The reactor models incorporated kinetic models with the estimated rate parameters obtained from the previous section have been evaluated against the plant data. Two different plant data sources are investigated. First, the concentration of each reactant taken from plant design data is compared with that predicted from the reactor models. Based on the lumped chemical components: diolefins, olefins and paraffins, a comparison of the observed and calculated value is shown in Table 4.4. The result indicated that the models give a good prediction in the concentration of the major components.

Next, the model results are validated with the plant production data. The calculated outlet temperature from top and bottom catalyst beds and the concentration

Table 4.4: Comparison of calculated concentration of diolefins, olefins and paraffins at the outlet of the reactor with plant design data

Components	Plant	Calculated
Diolefins ($kmol/m^3$)	0.00	0.028
Olefins ($kmol/m^3$)	2.20	2.18
Paraffins ($kmol/m^3$)	3.13	3.43

Table 4.5: Comparison of the reactor temperature and diolefins concentration predicted from the models with plant production data

Case studies	Outlet T from top bed (^oC)		Outlet T from bottom bed (^oC)		Diolefins ($kmol/m^3$)	
	Plant	Calculated	Plant	Calculated	Plant	Calculated
1	174.97	173.11	189.91	182.07	Nil	0.0027
2	184.99	181.66	193.09	194.49	Nil	0.0029
3	181.61	180.18	186.98	191.26	Nil	0.0027
4	175.04	176.78	191.07	195.68	Nil	0.0034
5	179.86	183.86	192.10	201.75	Nil	0.0028

of diolefins at the reactor outlet for five case studies are presented in Table 4.5. It is shown that the prediction of outlet temperature from the top and bottom catalyst bed agree with the plant data. Furthermore, the diolefins concentration at the exit of the reactor calculated from the reactor models matches very well with the plant values. Since the available plant data do not provide information on the concentration of other hydrocarbon components such as olefins and paraffins, a comparison in these components is not given.

Figure 4.6 shows the concentration profiles along the reactor at steady state condition based on information from the case study 1. This case study is served as a base case for simulation study. It can be seen from Figure 4.6 that the hydrogenation of diolefins results in an increase in the olefins concentration. However, the concentration of olefins in the bottom catalyst bed trends to decrease slowly due to the disappearance of the diolefins in the reactor. There is an insignificant increase in paraffins concentration in both top and bottom catalyst beds.

The steady state temperature profile for the same case study is illustrated in Figure 4.7. It can be seen that the temperature predicted by the models agrees quite well with that obtained from the plant data. The reaction heat from hydrogenation causes an increase in the temperature along the length of reactor. However, after adding some quench feed at the quench section, the temperature drops at the entrance of the bottom catalyst bed. It is also observed that the temperature increase in the top bed of catalyst is steeper than that in the bottom bed. This is explained by the decrease of the concentration of diolefins within the reactor.

Figures 4.8 to 4.11 show typical dynamic responses of the concentration of diolefins olefins and paraffins and the reactor temperature, respectively, for the case study 1. In these figures, the process models are simulated for a reactor start-up.

4.7 Conclusions

In this chapter, a dynamic model for an industrial adiabatic trickle bed reactor in which catalytic hydrogenations of a pyrolysis gasoline from an olefin production plant

occur, has been developed. To reduce the complexity of the model, all hydrocarbon components in the system were lumped into three pseudocomponents: diolefins, olefins and paraffins. The dynamic model results to a system of partial differential equations which was solved numerically by the method of lines. The orthogonal collocation method was used to discretize the spatial derivative terms.

Kinetic parameters were determined based on industrial plant data using optimization technique. The reactor model with the estimated kinetic parameters was validated with plant data. It is observed that although the model contained some simplifying assumptions, it has found to be in good agreement with plant data; the model gave a good prediction of temperature and lumped components in the reactor. This showed that the model adequately approximates the real system and can be used to formulate a model-based control technique to control the reactor.
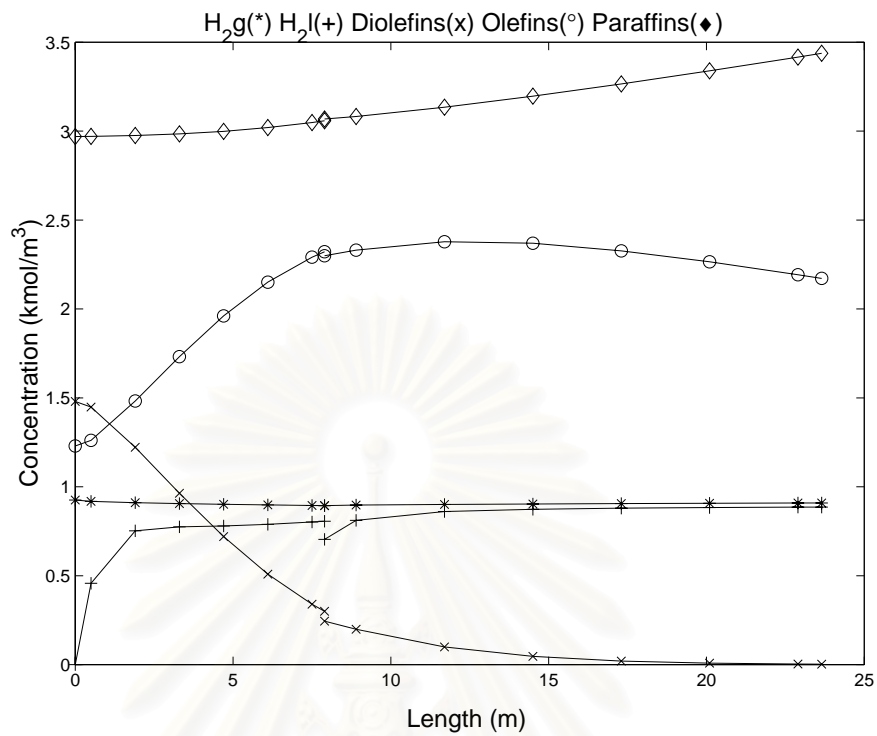
Figure 4.6: Steady state concentration profiles for the case study 1.
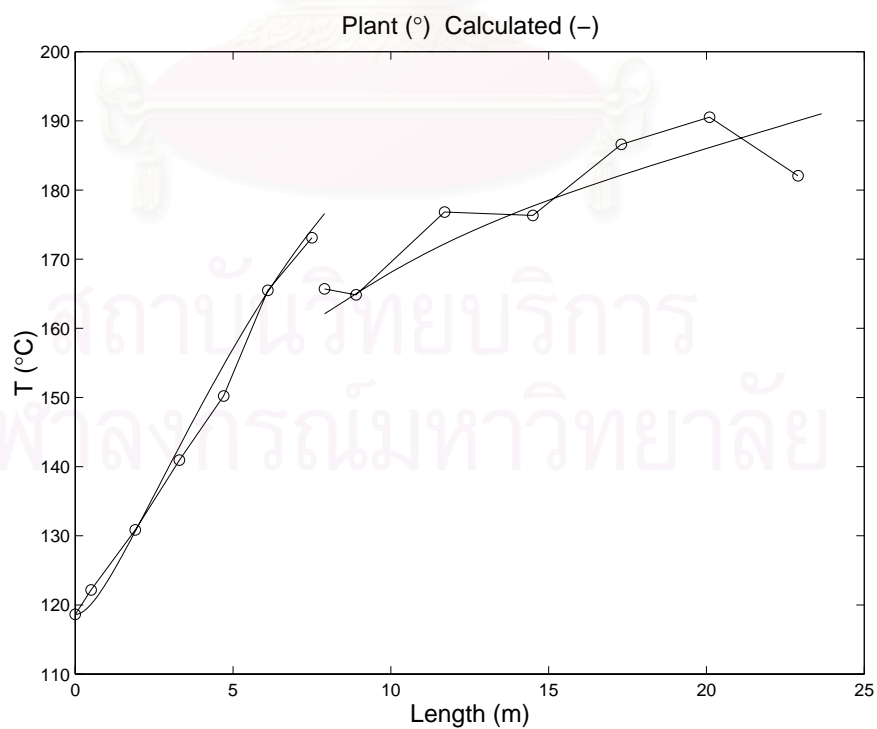
Figure 4.7: Steady state temperature profile for the case study 1.
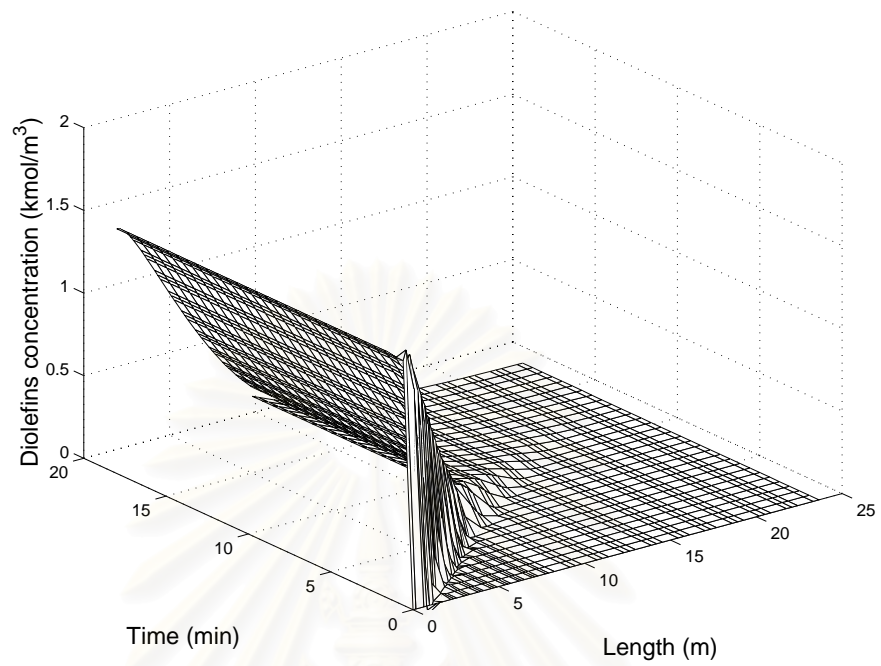
Figure 4.8: Diolefins concentration profile for the case study 1.
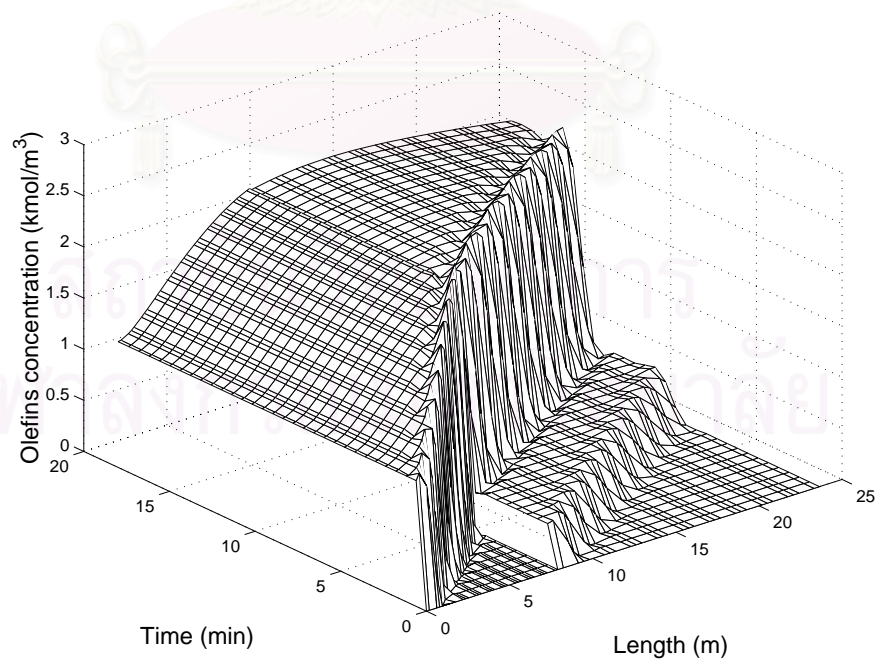
Figure 4.9: Olefins concentration profile for the case study 1.
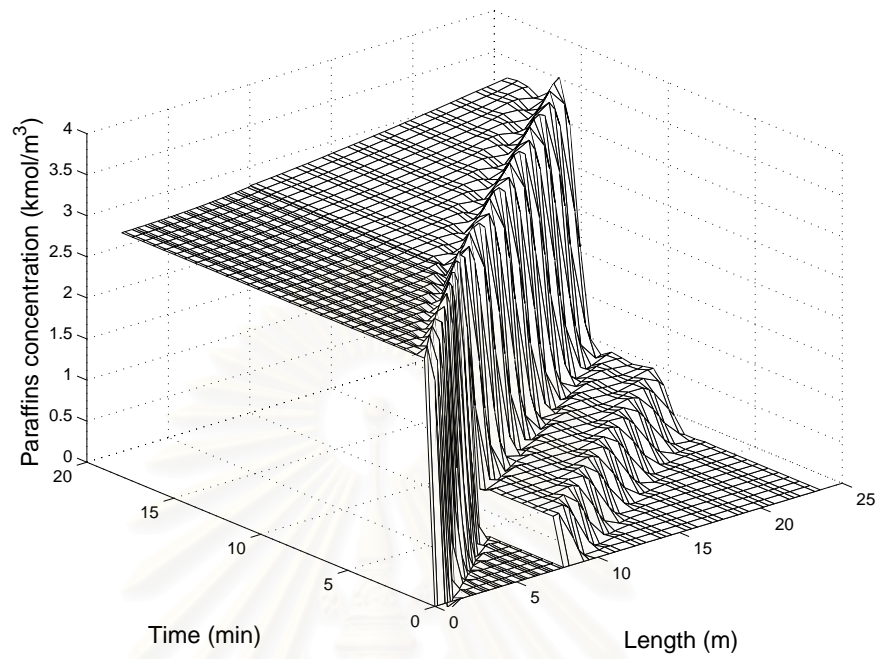
Figure 4.10: Paraffins concentration profile for the case study 1.
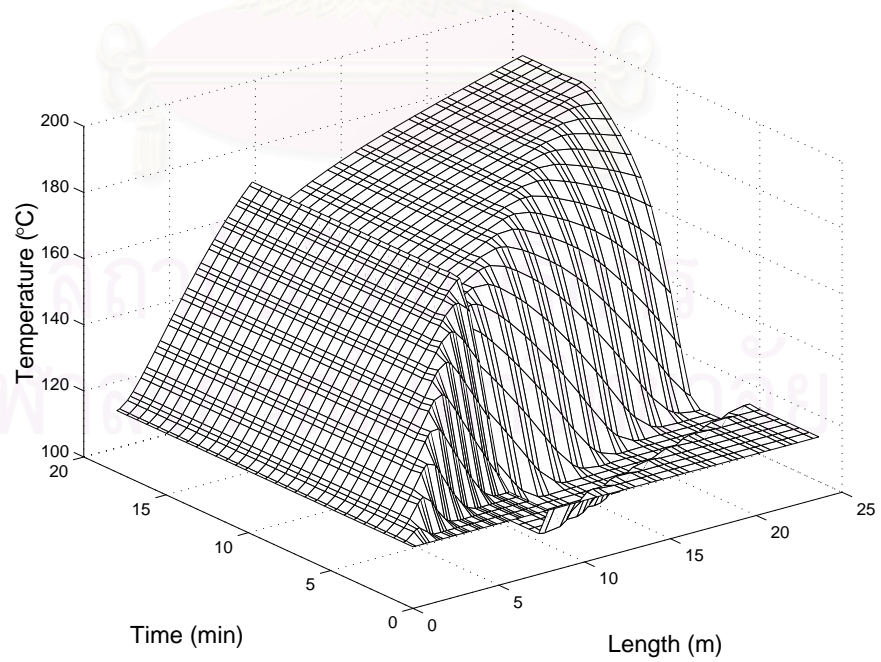
Figure 4.11: Temperature profile for the case study 1.

Chapter 5

Application of Model Predictive Control to Batch and Continuous Reactor: A Case Study[*]

Prior to implementing a model predictive control (MPC) strategy to control a trickle bed reactor in which the dynamic behavior is described by partial differential equations, it is interesting to examine the proformance of MPC to control less complicated processes which their response is described by ordinary differential equations.

This chapter presents the implementation of the MPC to reactor systems. Control studies on two types of chemical reactor: batch reactor and continuous stirred tank reactor (CSTR), are investigated. For the batch reactor, the MPC problem is formulated to on-line modify an optimal temperature set point profile. Once the optimal temperature profile is updated, a local controller i.e. a generic model control (GMC) controller, is applied to drive the reactor temperature to follow the desired profile. For the CSTR, the MPC controller is applied to control a product concentration in the reactor. In addtion, we also address the application of a dual mode model predictive control, an extended version of the MPC. This control strategy integrates the MPC with a local linear control algorithm.

---

[*]Portions of this chapter were appeared in Arpornwichanop et al. (2002b) and Arpornwichanop and Kittisupakorn (2002).

5.1 Batch Reactor

5.1.1 Introduction

In many chemical industries, there is an increasing trend to place a consideration on the production of high value products (e.g. polymers, pharmaceuticals, and specialty chemicals) in batch processes. As an important main unit in such processes, a batch reactor is generally involved in manufacturing of these products. The use of batch reactors offers many advantages. Firstly, a batch reactor is quite flexible, it can adapt to small volume production of various products, which are greatly submitted to the rapid changes in market conditions and the advent of new technology. Secondly, the batch reactor provides the natural way to scale-up processes from laboratory experiments where a synthesis of complex chemicals is studied, to industrial manufacturing. Finally, it is especially suitable to carry out reactions where materials involved are dangerous and difficult to handle (Rotstein and Lewin, 1992).

Since batch reactors are used to produce a wide variety of expensive products, it is known that this process is very complicated and involves complex chemical reaction mechanisms, and may include side reactions that produce undesired products. As a result, there is a great deal of interest to enhance batch operation to achieve high quality and purity products while minimizing the conversion of undesired by-products. Recently, the use of process optimization in the control of batch reactors has been received much attention in the literature. This provides a useful tool for operating batch reactors efficiently and optimally. For this purpose, it is desirable to optimize the process conditions during the reactor operation in order to meet desired products and safety specification whereas a control system is an essential part to ensure that the desired operating conditions can be maintained as close as possible during the course of batch run.

However, achieving such a proposed method for an optimal operation of batch reactors is quite difficult, and still provides challenging and interesting problems. This is mainly due to the inherent complexity of batch reactors which can be characterized by i) highly nonlinear behavior resulting from the dependence of reaction rates

on concentration and temperature, *ii*) time-varying system; the process variables (e.g. concentration, temperature) and parameters change with time, *iii*) no steady state operating condition; batch reactors are unstable under open loop condition so that control failure can make the reactor runaway, *iv*) imperfect model; complex kinetic reactions occurred within batch reactors are rarely well understood that leads to an inaccuracy in developing the system model, and *v*) lack of measurement information; the product qualities or key properties to be controlled (e.g. molecular weight) cannot be measured until the end of batch run or even if they can be measured (e.g. concentration), there is a significant time delay. Only a few of physical quantities such as temperature and pressure are available for direct on-line measurement. That makes direct control of product properties difficult (Bonvin, 1998). Although, in recent years there has been significant advance in developing new sensors for measuring these product properties, they have rarely been used in industrial processes due to high operating cost and expensive investment on the measuring devices. Thus, the usual practice is to control other variables that can be measured rapidly in order to obtain desired product properties instead.

In general, optimal batch reactor operation can be carried out by two-step approach; firstly, determining an optimal set point profile of key operating process variables such as temperature (Aziz and Mujtaba, 2002) and secondly, tracking the desired profile by a control system (Aziz et al., 2000). The optimal profile can usually be determined off-line by solving an optimal control problem. This problem is formulated based on fundamental models of the system and is often referred to a dynamic optimization problem. This is because it involves an optimization of a dynamic system. However, as mentioned above, because of the complexity of chemical reaction schemes, modeling error is always present and in addition, process disturbance can occur during the process operation. Due to the existence of this error and disturbance, the final product may significantly differ from the desired value, even though the pre-specified optimal profile is tracked perfectly (Loeblein, et al., 1997). To realize this fact, it is necessary to recalculate the optimal profile as an on-line optimization strategy whenever new feedback information is available. This strategy could compensate the modeling error leading to process operation improvement.

In order to perform the on-line optimization strategy, the knowledge of current state variables and/or parameters in process models is required. Due to the fact that some of these variables cannot be known exactly or sometimes can be measured with time delay, it is essential to include an on-line estimator to estimate these process variables using available process measurements as well. The sequence of an estimation and optimization procedure is known as an estimation-optimization task (Ruppen et al., 1998). Among several estimation techniques, an extended Kalman filter (EKF) has become increasingly popular because it is relatively easy to implement. It has been found that the EKF can be applied to a number of chemical process applications with great success. Once the estimate of unknown process variables is determined and then the models are updated, the optimization is performed on-line to generate a new optimal input profile. With the modified optimal profile, a designed controller is used to control the system to follow this profile until the new one is available.

Apart from specifying the optimal set point profile, a control system used to track such a profile is another important issue to be considered. This is because the deviation from the desired profile may cause an off-spec product. However, since it is well known that the control of batch reactors is difficult due to the inherently nonlinear behavior, the use of a linear control technique may give a poor performance. For this reason, many advanced control techniques have been developed and applied to the control of batch reactors. These include, for example, nonlinear feedforward-feedback control (Kravaris et al., 1989), generic model control (Cott and Macchietto, 1989), adaptive control (Rotstein and Lewin, 1992), globally linearizing control (Liu and Macchietto, 1995), dynamic matrix control (Yuce et al., 1999), linear model predictive control (Arpornwichanop et al., 2002), or inverse model control (Aziz et al., 2001). A review on the progress in control methodologies that have been applied to batch reactors as well as their importance and performance is given by Berber (1996). Among these advanced control methods, a generic model control (GMC) technique is one of the most studied control algorithm. This is because nonlinear process models can be interpreted straightforwardly in the GMC control algorithm so that they do not need to be linearized. Furthermore, its implementation is relatively easy when compared to other model-based control methods; consequently, the application of this control

technique appears in many chemical processes.

In this study, we develop an approach based on the idea of model predictive control (MPC), an on-line dynamic optimization strategy, to modify optimal temperature set point profile for improving batch operation performance. To demonstrate the effectiveness of the developed approach, the batch reactor studied by Cott and Machietto (1989), where two parallel exothermic reactions occur, is chosen here as a simulation case study. For solving the on-line optimization problem, it needs the knowledge of the current states of the system. Although most physical quantities (e.g. temperature, flowrate) can be measured frequently and available for on-line measurement, some other properties (e.g. concentration) are measured infrequently with time delay. To overcome this difficulty, the extended Kalman filter (EKF) is incorporated into the proposed strategy in order to estimate the concentrations from their delayed measurements.

The optimal control problem is solved by the sequential solution and optimization method, as described in Chapter 3, via the PREOP package (Morison, 1984). The successive reduced quadratic programming algorithm (Chen, 1988) is used to solve the resulting nonlinear program. Detailed discussion on the sequential solution algorithm can be further seen in Morison (1984).

Once the optimal temperature profile is modified, a controller based on generic model control algorithm (GMC) is applied to control the batch reactor temperature following the desired profile. In the GMC formulation, the EKF is also used to estimate the heat released from reactions. It is noted that the proposed strategy would be one of several strategies studied to promote the applicability of on-line dynamic optimization with set point tracking for improving of a batch reactor.

5.1.2 Dynamic Models of Batch Reactor

A reactor system considered by Cott and Macchietto (1989) which consists of a batch reactor and jacket cooling system is chosen here as a case study. The typical diagram of this system is shown in Figure 5.1. It is assumed that two parallel highly exothermic
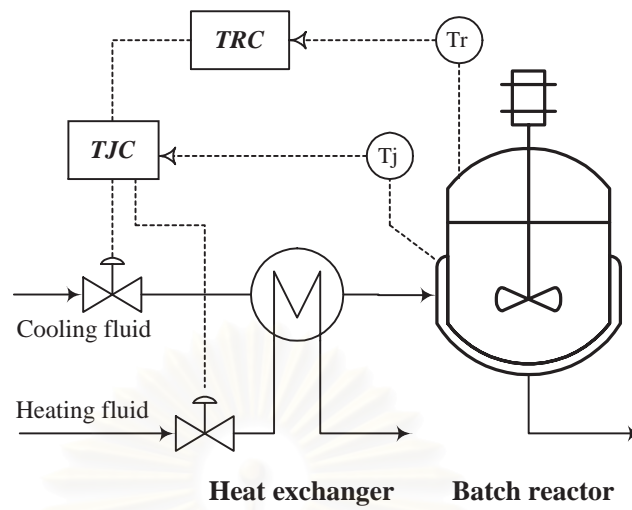
Figure 5.1: Batch reactor system

reactions occur in the reactor:

$$A + B \xrightarrow{k_1} C$$
$$A + C \xrightarrow{k_2} D$$
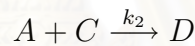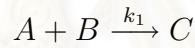
where A and B are raw material, C and D are the desirable product and undesirable by-product, respectively. The rate constants k_1 and k_2 are temperature dependence according to the Arrhenius relation.

The batch reactor is modeled by the following equations:

Material balances in the reactor:

$$\frac{dM_A}{dt} = -k_1 M_A M_B - k_2 M_A M_C \tag{5.1}$$

$$\frac{dM_B}{dt} = -k_1 M_A M_B \tag{5.2}$$

$$\frac{dM_C}{dt} = +k_1 M_A M_B - k_2 M_A M_C \tag{5.3}$$

$$\frac{dM_D}{dt} = +k_2 M_A M_C \tag{5.4}$$

Energy balances around the reactor:

$$\frac{dT_r}{dt} = \frac{Q_r + Q_j}{M_r C p_r} \tag{5.5}$$

$$\frac{dT_j}{dt} = \frac{F_j \rho_j C p_j (T_j^{sp} - T_j) - Q_j}{V_j \rho_j C p_j} \tag{5.6}$$

with
$$k_1 = \exp\left(k_1^1 - \frac{k_1^2}{T_r + 273.15}\right)$$

$$k_2 = \exp\left(k_2^1 - \frac{k_2^2}{T_r + 273.15}\right)$$

$$W = MW_A M_A + MW_B M_B + MW_C M_C + MW_D M_D$$

$$M_r = M_A + M_B + M_C + M_D$$

$$Cp_r = (Cp_A M_A + Cp_B M_B + Cp_C M_C + Cp_D M_D)/M_r$$

$$Q_r = -\Delta H_1(k_1 M_A M_B) - \Delta H_2(k_2 M_A M_C)$$

$$Q_j = UA(T_j - T_r)$$

$$A = 2W/\rho r$$

where M_i is the amount of mole of component i, T_r is the reactor temperature, T_j is the jacket temperature, and T_j^{sp} is a set point value of the jacket temperature control system. The meaning of other variables and parameters are explained in the nomenclature.

The dynamic behavior of the reactor can be simulated by solving Equations (5.1) to (5.6). The differential-algebraic solver DASSL (Petzold, 1982) is used here to give the solution of these equations. The initial conditions for M_A, M_B, M_C, M_D are 12, 12, 0, and 0 kmol, respectively. The initial values of both reactor and jacket temperature are set at 20 ^oC. The batch operation time (t_f) is 200 minutes. Other process parameter values used in the reactor models are listed in Table 5.1.

In this work, it is assumed that the temperature is measured frequently without delay. The sampling time of 0.2 min is used for temperature measurement. It is also assumed that the concentration (amount of mole) of reactants in the reactor is measured infrequently and has a sampling time and measurement delay of 10 min.

5.1.3   MPC as On-line Dynamic Optimization Strategy

The aim of a dynamic optimization is to determine a control profile minimizing (or maximizing) a given objective function subject to process constraints. With the optimal control policy, the controlled system is driven from an initial state to a final desired state in an optimal way. However, as mentioned earlier that in the presence of modeling error, the pre-specified control profile may lose its optimal character (Bonvin,

Table 5.1: Process parameter values

MW_A	$= 30$	$[kg/kmol]$	Cp_A	$= 75.31$	$[kJ/(kmol.^oC)]$
MW_B	$= 100$	$[kg/kmol]$	Cp_B	$= 167.36$	$[kJ/(kmol.^oC)]$
MW_C	$= 130$	$[kg/kmol]$	Cp_C	$= 217.57$	$[kJ/(kmol.^oC)]$
MW_D	$= 160$	$[kg/kmol]$	Cp_D	$= 334.73$	$[kJ/(kmol.^oC)]$
k_1^1	$= 0.9057$		ΔH_1	$= -41840$	$[kJ/kmol]$
k_1^2	$= 10000$		ΔH_2	$= -25105$	$[kJ/kmol]$
k_2^1	$= 38.9057$		ρ	$= 1000$	$[kg/m^3]$
k_2^2	$= 17000$		ρ_j	$= 1000$	$[kg/m^3]$
r	$= 0.5$	$[m]$	Cp_j	$= 1.8828$	$[kJ/(kg.^oC)]$
F_j	$= 0.348$	$[m^3/min]$	V_j	$= 0.6912$	$[m^3]$
U	$= 40.842$	$[kJ/(min.m^2.^oC)]$			

1998). For this reason, an on-line optimization strategy through a model predictive control (MPC) scheme is employed in this work to compensate such an error. The basic concept is to compute the optimal control profile based on current feedback information. However, only the initial value of the optimal trajectory is sent to the system as a set point for a local controller. After new information of states is available from either measurement or estimation, the optimization is repeated again to generate updated optimal set point profile at the next time interval.

The method proposed for improving the batch operation can be divided into two phases: on-line modification of the temperature trajectory and on-line tracking of the desired temperature trajectory. The first phase involves determining an optimal temperature set point profile by solving the on-line dynamic optimization strategy based on the delayed measurement of the amount of mole of reactants (M_A, M_B, M_C, and M_D) in the reactor. The other phase involves designing a nonlinear controller for tracking of the optimal reactor temperature.

Problem Formulation

Two major optimization problems related to batch operation: maximization of product concentration and minimization of batch operation time are studied to determine an optimal temperature profile, which highly influences the rate of reactions. The obtained optimal temperature profile has to satisfy the specified objective function and other desired process constraints. Such optimization problems can be described as follows.

Maximum Product Concentration Problem (P1)

In this type of the problem, the objective is to compute the optimal temperature policy maximizing the amount of a desired product concentration for a given fixed batch time subject to bounds on the reactor temperature. The problem can be written mathematically as:

$$\max_{T(t)} J = X(t_f)$$

subject to:

$$
\begin{aligned}
\dot{x} &= f\left(x(t), T, p, t\right) \\
x(t_0) &= x(0) \\
T_L \leq T &\leq T_U \\
t_f &= t_f^*
\end{aligned}
$$

where X is the amount of the desired product at a given final batch time , x is state variables, $\dot{x}$ is the derivative of x with respect to time (t), T is the reactor temperature, p is process parameters, t_f is the fixed batch time, and T_L and T_U are lower and upper bounds of the reactor temperature.

Minimum Batch Time Problem (P2)

The purpose of this optimization problem is to determine the optimal temperature profiles to achieve the desired final product concentration in minimum batch time, thus

the performance index is the final time whereas the desired product concentration is defined as a terminal constraint. The formulation of the minimum batch time problem can be shown as:

$$\min_{T(t)} J = t_f$$

subject to:

$$
\begin{aligned}
\dot{x} &= f\left(x(t), T, p, t\right) \\
x(t_0) &= x(0) \\
T_L \leq T &\leq T_U \\
X(t_f) &= X^*
\end{aligned}
$$

where X^* is the desired product concentration at the end of batch run and t_f is final batch time.

5.1.4   State and Parameter Estimation

The implementation of the on-line optimization strategy requires the knowledge of current states and/or parameters in nonlinear process models in order to modify a new optimal profile defined as the set point for a controller. However, it is known that in many processes, some measurements i.e. concentration are available at low sampling rate with significant time delay. To overcome this difficulty, state and parameter estimation is incorporated into the proposed on-line optimization algorithm.

In this study, an extended Kalman filter (EKF) is used to reconstruct the current state variables from their delayed state measurements. The detail of the EKF algorithm can be found in Appendix C.

Application to the Batch Reactor

Since the concentration of reactants (M_A, M_B, M_C and M_D) in the batch reactor is assumed to be measurable with a delay of one sampling time; that is, at time k, only information at time $k-1$ is available. Thus, the EKF is applied to estimate the

value of reactant concentration at current time k from their delayed measurements at sampling time $k - 1$. However, since it is expected to exhibit uncertainty in reaction rate constants (i.e. k_2^1 and k_2^2) in real plant, the EKF is also used to estimate these uncertain parameters. The following equations, therefore, are appended for parameter estimation.

$$\frac{dk_2^1}{dt} = 0 \tag{5.7}$$

$$\frac{dk_2^2}{dt} = 0 \tag{5.8}$$

Equations (5.1) to (5.4) and (5.7) to (5.8) correspond to Equation (C.1) in the EKF algorithm. Based on the estimate of the current information, the dynamic optimization problem is resolved to generate a new optimal temperature trajectory.

5.1.5 Generic Model Control (GMC)

The success of the proposed strategy for an on-line modification of the reactor temperature set point profile is associated with designing a controller to control the reactor temperature to track the desired temperature trajectory. It is accepted that the use of linear control techniques in highly nonlinear chemical processes e.g. batch chemical reactors is quite limited to their performances and may give a poor control response. Therefore, in this work a nonlinear control technique based on a generic model control (GMC) is utilized. This control methodology has been received much interest during the last decade and a number of applications of GMC to the control of batch processes have been reported in the literature (e.g. Cott and Machietto, 1989; Kershenbaum and Kittisupakorn, 1994; Shen et al., 1999; Aziz et al, 2000, etc.). However, most of these works focus on using the GMC to track the pre-determined optimal profile (off-line calculation) of a reactor temperature. No effort has been made to apply the GMC to implement an on-line optimal set point profile. Therefore, in this work, the performance of the GMC controller with the optimal temperature set point determined by on-line optimization strategy is evaluated and compared to that of the GMC controller with pre-determined set point.

Control Algorithm

Let us consider a process based on the following model equations:

$$\frac{dx}{dt} = f(x, p, t) + g(x, t)u \tag{5.9}$$

$$y = h(x) \tag{5.10}$$

where x is a vector of state variables, y is a vector of output variables, u is a vector of input variables, p is a vector of process parameters, and f, g, and h are generally nonlinear functions.

The general form of the GMC algorithm can be written as

$$\frac{dy}{dt} = K_1 \left(y^{sp} - y \right) + K_2 \int_0^{t_f} \left(y^{sp} - y \right) dt \tag{5.11}$$

The GMC control response can be designed via the tuning parameters K_1 and K_2 based on the tuning curve given by Lee and Sullivan (1988). The use of Equation (5.11) forces y toward its set point, y^{sp}, with zero offset. If Equation (5.10) is differentiated, and the Equation (5.11) is substituted into Equation (5.9), the GMC control law is

$$u = \frac{\left[K_1 \left(y^{sp} - y \right) + K_2 \int \left(y^{sp} - y \right) dt - \frac{dh}{dx} f\left(x, d, t \right) \right]}{\left(\frac{dh}{dx} g(x, t) \right)} \tag{5.12}$$

Application of GMC Controller to the Batch Reactor

To implement the GMC, an energy balance around the reactor is required; it gives the relation between the reactor temperature (controlled variable) and the jacket temperature (manipulated variable). Based on an assumption that the amount of the heat accumulated in the wall of the reactor is negligible compared to the heat transferred in the reactor, the energy balance equation becomes

$$\frac{dT_r}{dt} = \frac{Q_r + U_r A_r (T_j - T_r)}{W_r C p_r} \tag{5.13}$$

where U_r is the heat transfer coefficient, A_r is the heat transfer area, W_r is the mass of the reactor contents, Cp_r is the mass heat capacity of the reactor content, and Q_r is the heat released by the reactions.

Rearranging the Equation (5.13) as in the form of GMC algorithm, the following functions f, g, and h can be defined

$$f(x,p,t) = \frac{Q_r - U_r A_r T_r}{W_r C p_r} \tag{5.14}$$

$$g(x,t) = \frac{U_r A_r}{W_r C p_r} \tag{5.15}$$

$$h(x) = T_r \tag{5.16}$$

Replacing the above equations in Equation (5.12), we have

$$T_j = T_r + \frac{W_r C p_r}{U_r A_r} \left(K_1 (T_r^{sp} - T_r) + K_2 \int_0^t (T_r^{sp} - T_r) dt \right) - \frac{Q_r}{U_r A_r} \tag{5.17}$$

The discrete form of Equation (5.17) for on-line implementation at k^{th} time interval is given as

$$T_j(k) = T_r(k) + \frac{W_r C p_r}{U_r A_r} \left(K_1 (T_r^{sp} - T_r(k)) + K_2 \sum_0^k (T_r^{sp} - T_r(k)) \Delta t \right) - \frac{Q_r(k)}{U_r A_r} \tag{5.18}$$

where Δt is the sampling time.

However Equation (5.18) gives the actual jacket temperature $[T_j(k)]$ required at the next sampling time to control the reactor temperature $[T_r(k)]$ at the desired trajectory $[T_r^{sp}]$. In usual practice, the reactor temperature control is cascaded with the jacket temperature control (heating and cooling system); the output of the reactor temperature controller (master loop) is the set point value of the jacket temperature controller (slave loop), as demonstrated in Figure 5.2. Additionally, the model of a heat exchanger system for heating and cooling is not included in Equation 5.13. If $T_j(k)$ is applied directly as the set point for the jacket temperature control system without considering its dynamic, the resulting control response would be sluggish. To accommodate such an effect, it is reasonable to assume that the dynamic of the jacket control system can be approximated by a first order model with time constant (τ_j) (Liptak, 1986). Consequently, the $T_j^{sp}(k)$ can be computed by:

$$T_j^{sp}(k) = T_j(k-1) + \tau_j \left(\frac{T_j(k) - T_j(k-1)}{\Delta t} \right) \tag{5.19}$$

With this jacket temperature set point, the jacket temperature controller (setting as a PI controller) through a heat exchanger system opens or closes control valve
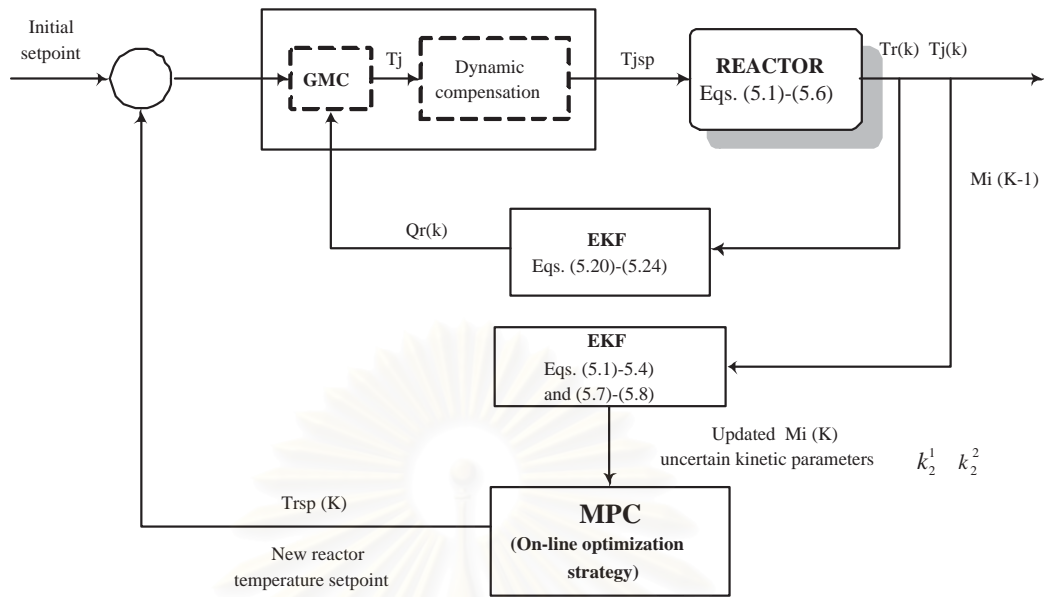
Figure 5.2: The proposed control strategy for on-line update and control of reactor temperature profile

reflecting to the flowrate of heating and cooling fluid. However in reality the ability of the heat exchanger in adjusting the jacket temperature is always limited, thus, in this work the jacket temperature is bounded between 0 ^oC and 120 ^oC. The tuning parameters of the GMC controller are given in Table 5.2.

<div align="center">

Table 5.2: Parameters in GMC algorithm

</div>

W_r	$= 1560 \ [kmol]$	τ_j	$= 2 \ [min]$
Cp_r	$= 1.8828 \ [kJ/(kmol.^oC)]$	K_1	$= 2.4$
U_r	$= 40.842 \ [kJ/(min.\,m^2.^oC)]$	K_2	$= 10^{-4}$
A_r	$= 6.42 \ [m^2]$		

As can be seen from Equation (5.18), the knowledge of heat released $[Q_r(k)]$, which cannot be measured, is needed in the GMC algorithm. Here, the EKF technique coupled with the simplified reactor model, given by Kittisupakorn (1995), is also applied here to estimate the heat released $[Q_r(k)]$. The reason of using the simplified models, not the exact model of the plant, is because if the exact model were used, too many uncertain/unknown parameters as well as too many unmeasurable states would be in-

volved. That may lead to poor performance of the EKF. Hence, the simplified model with less uncertain/unknown parameters and unmeasurable states as shown below is used instead.

$$\frac{dT_r}{dt} = \frac{Q_r + U_r A_r (T_j - T_r)}{W_r C p_r} \tag{5.20}$$

$$\frac{dT_j}{dt} = \frac{F_j \rho_j C p_j (T_j^{sp} - T_j) - U_r A_r (T_j - T_r)}{V_j \rho_j C p_j} \tag{5.21}$$

$$\frac{dN}{dt} = -bNT_r \tag{5.22}$$

$$\frac{dQ_r}{dt} = N\frac{dT_r}{dt} + T_r \frac{dN}{dt} \tag{5.23}$$

$$\frac{db}{dt} = 0 \tag{5.24}$$

where $N = -bM_r(\Delta H)$, b is a pseudo reaction rate constraint, M_r is the total reactant concentration, and ΔH is heat of reaction. It should be noted that the variable N representing two unknown parameters M_r and ΔH can be estimated instead of these parameters so that the number of state equations for estimation decrease and an error of estimation corresponding to the uncertainty of each parameters can be reduced.

Equations (5.20) to (5.24) correspond to Equation (C.1) in the EKF algorithm. Once the reactor and jacket temperature measurement are available, the EKF with the simplified model estimates the heat released from reactions $[Q_r(k)]$. Table 5.3 summarizes the initial conditions and tuning parameters of the EKF used in this simulation work.

5.1.6 Simulation Results

Maximum Conversion Problem (P1)

All simulation results given here are based on the optimization problem P1, in which the objective is to find the optimal reactor temperature profile, such that the amount of mole of the product C is maximized in a fixed batch time with respect to a constraint on the temperature.

In this case study, the specified final batch time (t_f) of 200 min is used and the reactor temperature is bounded according to $20 \leq T(^oC) \leq 120$.

Table 5.3: Parameters and initial conditions in EKF

For the estimation of M_i, k_2^1 and k_2^2	

$M_A(0)$ $= 12 \ [kmol]$ $\qquad$ P $= \text{diag}[100 \ 10 \ 100 \ 100 \ 100 \ 10^5]$

$M_B(0)$ $= 12 \ [kmol]$ $\qquad$ Q $= \text{diag}[100 \ 1 \ 100 \ 1 \ 500 \ 5 \times 10^8]$

$M_C(0)$ $= 0 \ [kmol]$ $\qquad$ R $= \text{diag}[10 \ 10 \ 10 \ 10]$

$M_D(0)$ $= 0 \ [kmol]$

k_2^1 $\qquad = 38.9057$

k_2^2 $\qquad = 17000$

For the estimation of Q_r

$T_r(0)$ $= 20 \ [^oC]$ $\qquad$ P $= \text{diag}[1 \ 1 \ 100 \ 20 \ 10]$

$T_j(0)$ $= 20 \ [^oC]$ $\qquad$ Q $= \text{diag}[10 \ 10 \ 2000 \ 100 \ 100]$

$N(0)$ $= 1.8462$ $\qquad$ R $= \text{diag}[10 \ 10]$

$Q_r(0)$ $= 0$

$b(0)$ $= 1.8386 \times 10^{-6}$

Temperature Set Point Profile Determined Off-line with Perfect Tracking

The first set of simulation studies has investigated the case where the theoretical optimal temperature profile is determined by off-line computation and perfect tracking of such a profile is assumed. This results in the maximum product (maximum conversion) that can be achieved at the end of batch run and is served as a reference to be compared with results obtained from the proposed strategy. The optimal control problems are solved using time interval with equal length varied from one to 40 intervals to discretize the profile. The switching time is fixed and the length of each interval is specified by dividing the fixed batch time (t_f) with a number of time intervals (P). Therefore, the problem is to find only optimal temperature value in each subinterval.

Simulation results with different time interval (P) are reported in Table 5.4. Optimal reactor temperature policy for each case is shown in Figure 5.3. As seen in Table 5.4, when one time interval ($P = 1$) is used, the product C obtained at the final time ($t_f = 200$ min) is 7.0171 kmol and the optimal temperature (isothermal operation) set point is 88.01 ^oC whereas using $P = 20$, the product C achieved is 7.0379 and computa-
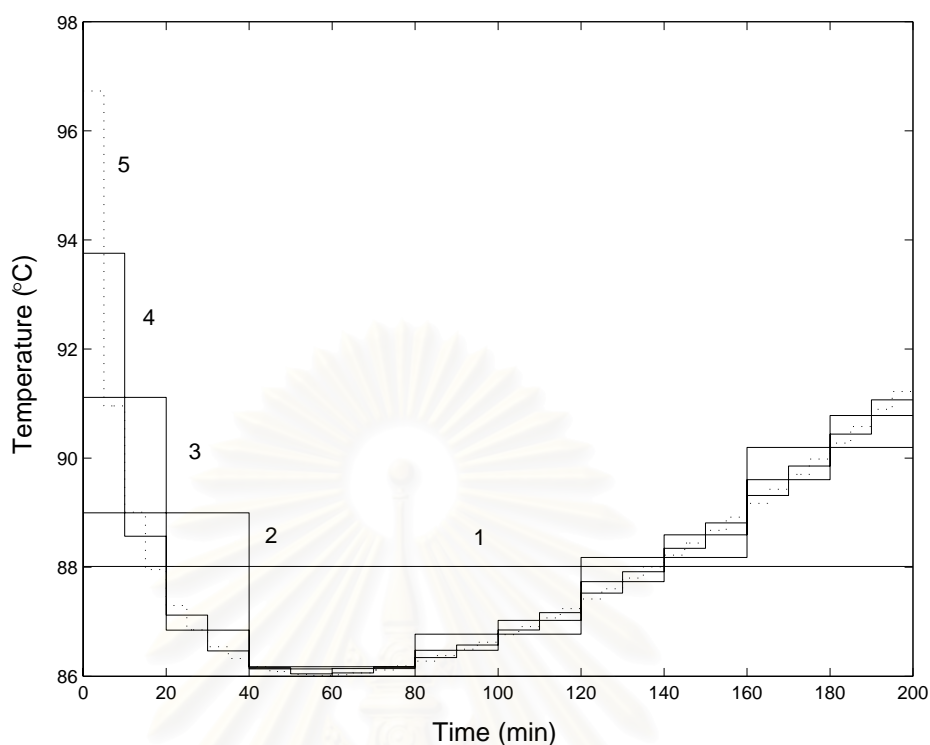
Figure 5.3: Optimal temperature profile: 1 interval (1), 5 intervals (2), 10 intervals (3), 20 intervaLs (4), 40 interval (5)

tional time is approximately 2.80 sec. It was found from these results that the amount of the desired product C increases as a number of time intervals increases. This can be explained that as the number of intervals enlarges, the approximate optimal profile with piecewise constant policy is closed to the actual optimal profile.

Temperature Set Point Profile Determined On-line with GMC Controller

Next, the proposed strategy using an on-line dynamic optimization to update optimal temperature set point profile is implemented. Rather than assuming the reactor temperature trajectory can be tracked perfectly as in the previous studies, the GMC controller is applied here to drive the system to follow the desired trajectory. Regarding to the time elapsed in the determination of the optimal control problem, with $P = 20$, the temperature set point profile is updated every 10 min. By this is meant that, to apply this strategy on-line, the computational time for the updated temperature set point profile must be less than 10 minutes. It was found that the computational time

based on Pentium III/850 mHz is approximately 3 sec. As a result, this strategy is applicable for on-line implementation. Regarding to the GMC control performance, it was found that the GMC controller can drive the system from the current set point to a new one within 10 min. Therefore, the GMC controller can be used for tracking the profile obtained from the strategy.

Results in term of the amount of the desired product C from on-line optimization strategy are compared with those from off-line strategy. Simulation results have been evaluated under nominal condition with perfect model that all parameters are specified correctly, and plant/model mismatch condition by changing parameters in the plant model i.e. pre-exponential rate constant (k_0) decreased by 50% and activity energy (E_a) increased by 20% from their nominal values, as shown in Table 5.5.

In the nominal case, the product obtained from the off-line strategy ($C = 6.9459$) is close to that obtained by the on-line strategy ($C = 6.9585$). Figures 5.4 and 5.5 show the response of the GMC controller to track the reactor temperature trajectory that is pre-specified by off-line calculation, and the comparison of the actual and estimated heat released by reactions, respectively. It can be seen that the EKF provides excellent estimation of the heat released and with this heat released, the GMC controller can give reasonably good temperature control. Similarly, in the case that the optimal temperature is modified via the on-line optimization strategy based on the current information of M_i, k_2^1, and k_2^2 obtained from delayed measurements of M_i, the GMC controller is able to track the reactor temperature (Figure 5.6). The performance of the EKF to predict the amount of M_A, M_B, M_C, and M_D at current time from their measurements with time delay 10 min is illustrated in Figure 5.7. Also, the EKF gives good estimation of k_2^1 and k_2^2 as shown in Figure 5.8. It is interesting to note that since the initial reactor temperature starts at 20 ^oC, to start up the reactor, the GMC controller heats the reactor temperature from this condition to the desired set point value as quickly as possible. As a result, the reactor temperature deviates from its set point at the beginning of batch time causing that the product C obtained from both on-line and off-line strategy with the GMC controller is slightly lower than that obtained for the case of $P = 20$ ($C = 7.0379$), as shown in Table 5.4.

For the mismatch in k_2^1, the value of the desired product $C = 7.8839$ can be achieved

Table 5.4: Summary of the results: off-line optimization and perfect tracking cases

Time interval	Product C(kmol)	By-product D (kmol)	CPU time (s)
1	7.0171	1.3464	0.1591
5	7.0281	1.3605	1.2600
10	7.0339	1.3594	1.9778
20	7.0379	1.3585	2.8066
40	7.0402	1.3579	5.0519

Table 5.5: Comparison of the results obtained from off-line and on-line optimization strategy with GMC controller (Problem P1)

Case studies	Product C (kmol)	
	Off-line	*On-line*
1. Nominal case		
(a) all parameters specified correctly	6.9459	6.9585
2. Plant/model mismatch case		
(a) -50% k_0 of Reaction 2 in plant model ($k_2^1 = 38.2125$)	7.6673	7.8839
(b) $+20\%$ E_a of Reaction 2 in plant model ($k_2^2 = 20400$)	8.5660	10.2024
(c) -50% k_0 and $+20\%$ E_a of Reaction 2 in plant model	8.5658	10.2029

Note that: $k_0 = exp(k_2^1)$ and $E_a = k_2^2(R)$ where k_0 is pre-exponential rate constant, E_a is activity energy and R is ideal gas constant.

at the end of batch time for the on-line strategy which is higher than that obtained from the off-line strategy where the mismatch is not noticed ($C = 7.6673$). Similar results can be observed under the case of plant model mismatch in k_2^2 as shown in Table 5.5. These results indicate clearly that the performance of batch reactor operation is improved via the proposed strategy. Due to similarity in their control responses, only the result for change in k_2^1 is shown in Figure 5.9.

Finally, with a change in both k_2^1 (-50% k_0) and k_2^2 ($+20\%$ E_a) in the plant model, the result using the on-line optimization strategy shows that the GMC controller is able to accommodate this change very well as can be seen in Figure 5.10. Figure 5.11 presents the performance of the EKF for estimation of k_2^1 and k_2^2. Since the EKF estimates these parameters closed to the true values, the mismatch is eliminated. That leads to high product C obtained at the final batch time ($C = 10.2029$) compared to the value of $C = 8.5958$ obtained from the off-line strategy

Minimum Time Problem (P2)

The results presented here correspond to the case where the objective is to minimize the batch time of operation subject to a terminal constraint on the desired amount of mole of product C ($M_C(t_f) = 6.00$ kmol). The reactor temperature constraint is the same as in problem P1.

Several simulations have been carried out under process parameter uncertainties i.e. in pre-exponential rate constant (k_0) and activity energy (Ea). In all case studies we considered 10 time intervals that the reactor temperature and switching time are optimized while minimizing the final batch operation time. Results, reported in the value of minimum batch time to obtain the desired product C and the amount of the desired product C at the end of batch operation, from the on-line dynamic optimization strategy are compared with those from the off-line strategy.

With an 20% increase of parameter k_2^1 in the plant model, it can be seen from Table 5.6 that the final batch time needed to achieve the desired product C from the proposed on-line modification of temperature set point profile ($t_f = 49.6$ min) is shorter compared to the result with the off-line strategy ($t_f = 65.0$ min). This is because the

Table 5.6: Comparison of the results obtained from off-line and on-line optimization strategy with GMC controller (Problem P2)

Case studies	Final time (min)/Product C (kmol)	
	Off-line	*On-line*
(1) -50% k_0 of Reaction 2 in plant model ($k_2^1 = 38.2125$)	65.0/6.0070	49.6/6.0052
(2) $+20\%$ E_a of Reaction 2 in plant model ($k_2^2 = 20400$)	56.2/6.0027	42.6/6.0114
(3) -50% k_0 and $+20\%$ E_a of Reaction 2 in plant model	56.5/6.0021	42.3/6.0129

EKF can acknowledge this parameter uncertainty, so that the temperature set point profile is updated corresponding to the modified parameter value closed to the actual value. Figure 5.12 shows the control response of the GMC controller to deliver the reactor temperature form initial condition to the desired temperature set point determined off-line for this mismatch. For the on-line temperature set point modification, as expected, the GMC controller can also control the reactor corresponding to the set point changes as can be seen in Figure 5.13

The results for other case studies are summarized in Table 5.6. The important aspect obtained from these results is that in all cases, the minimum batch time to obtain the desired product concentration in the on-line set point modification strategy decreases. This points out the effectiveness of the proposed method to improve the operation of batch reactor.

5.1.7 Conclusions

In this study, the method using an on-line dynamic optimization and control strategy to enhance batch reactor operation has been proposed. The on-line dynamic optimization through the idea of MPC scheme was performed, based on the updated current information of states of the reactor which are estimated from the delayed measurement of an amount of reactants using an extended Kalman filter (EKF) technique, at specified time interval to provide a new updated optimal reactor temperature set point profile. Two types of optimization formulation related to batch operation (maximum

concentration and minimum time problem) were considered in the proposed on-line set point modification strategy. The reactor temperature set point obtained was implemented using a generic model control (GMC). The EKF was also incorporated into the GMC algorithm in order to estimate the heat released by reactions using direct measurements of the reactor and jacket temperature. A batch reactor with highly exothermic reactions was used as a simulation case study to demonstrate the effectiveness of the proposed approach. Simulation studies have been carried out in both nominal case and plant/model mismatch case and the results showed that the performance of the batch reactor in terms of the amount of a desired product and of batch operation time can be improved significantly by the proposed strategy. In addition, they also clearly indicate the capability of the GMC controller to control the reactor temperature along the specified trajectory and that of the EKF to estimate the states and parameters of the system.
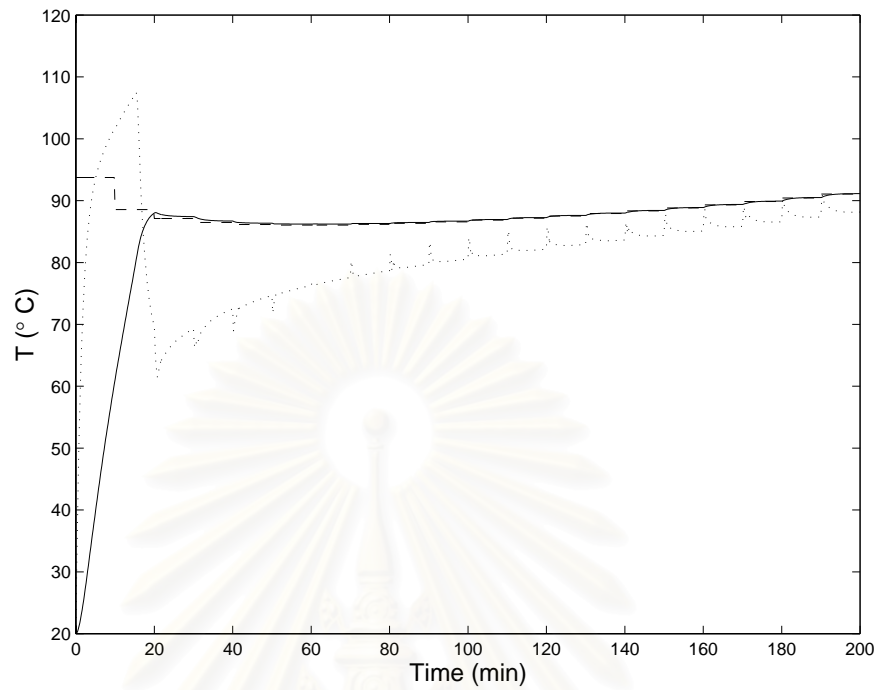
Figure 5.4: Control response (off-line, nominal case): T_r^{sp} (dash), T_r (solid), T_j (dot)
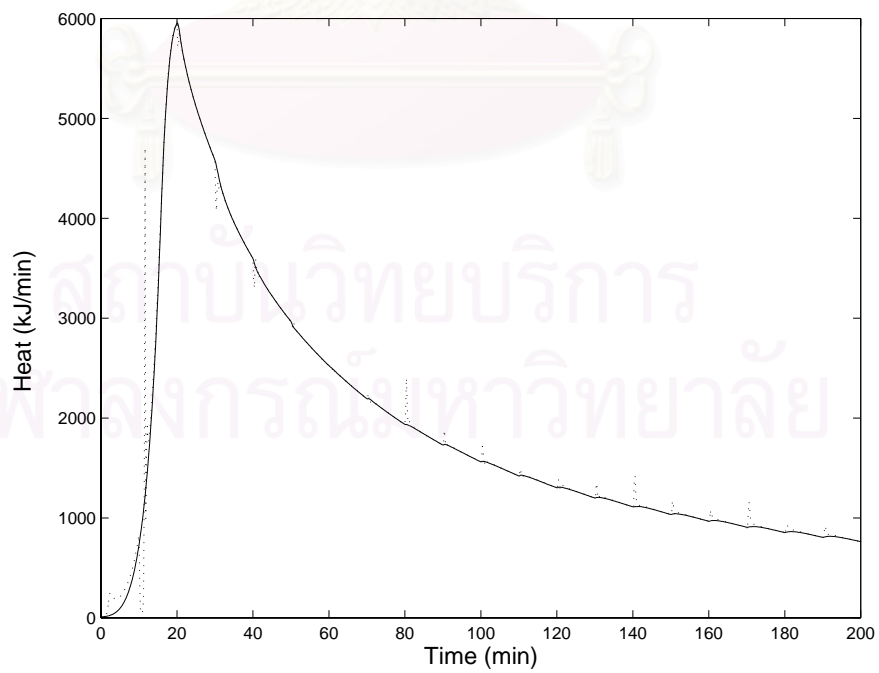
Figure 5.5: Heat released (off-line, nominal case): actual (solid), estimate (dot)
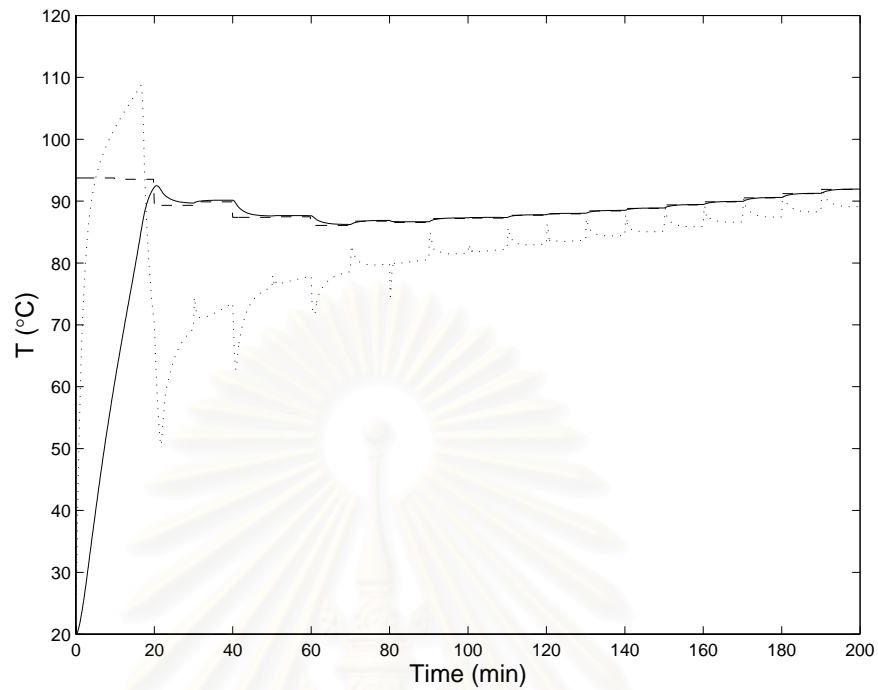
Figure 5.6: Control response (on-line, nominal case): T_r^{sp} (dash), T_r (solid), T_j (dot)
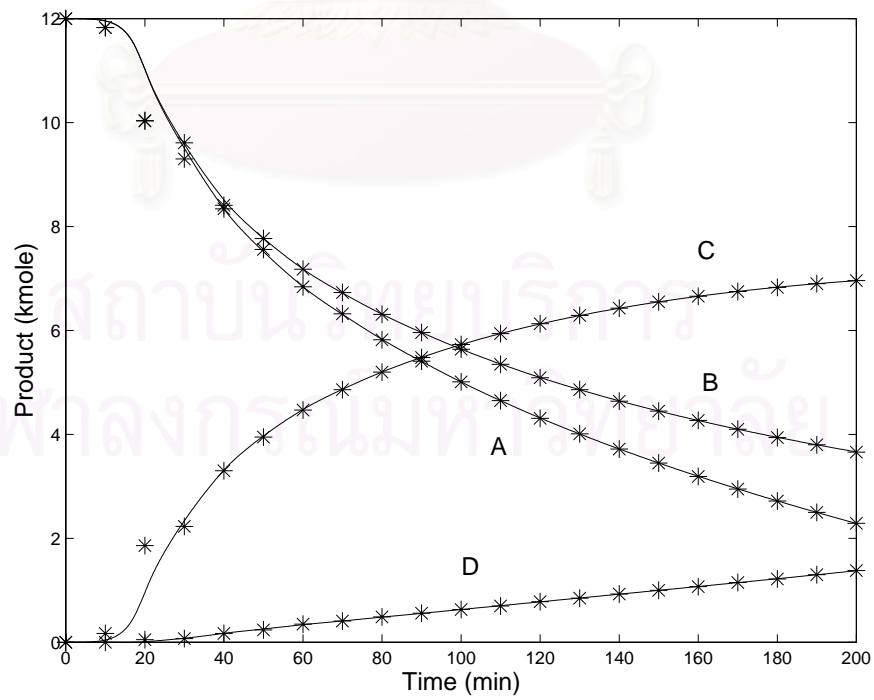
Figure 5.7: Product profile (on-line, nominal case): actual (solid), estimated (*)
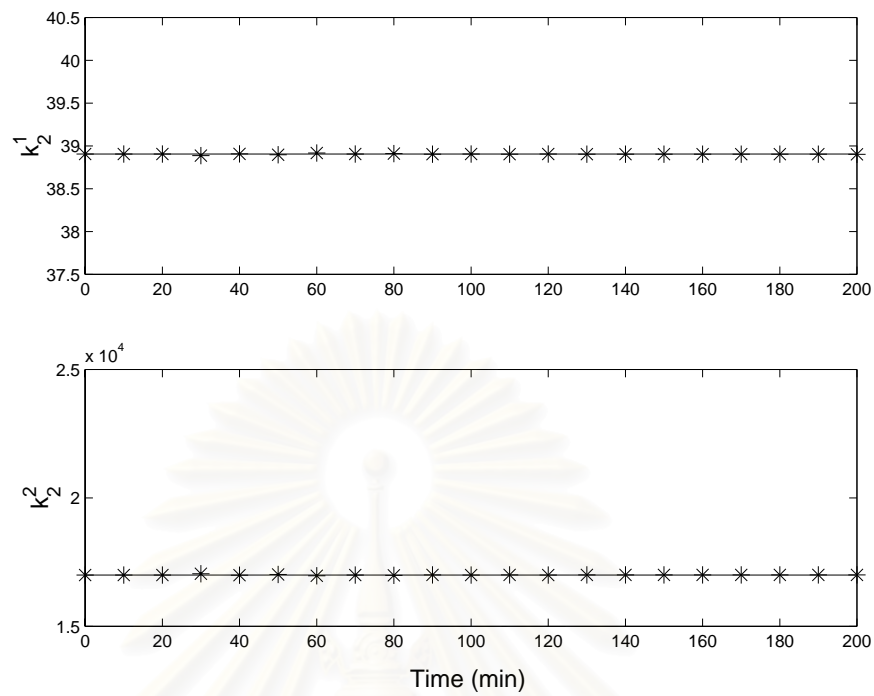
Figure 5.8: Estimate of k_2^1 and k_2^2 (on-line, nominal case): actual (solid), estimate (*)
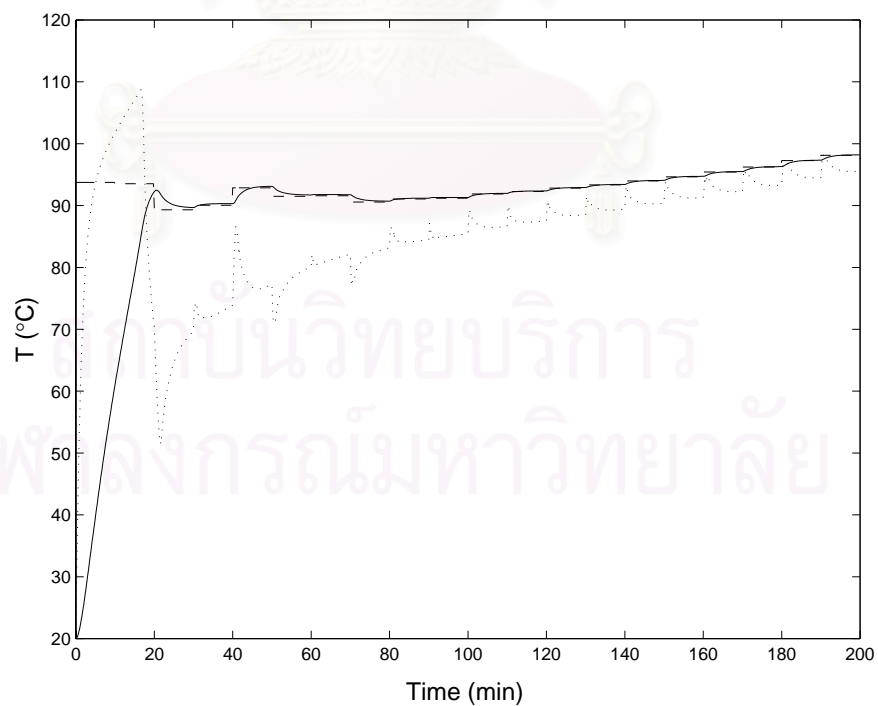
Figure 5.9: Control response (on-line, mismatch in k_2^1): T_r^{sp} (dash), T_r (solid), T_j (dot)
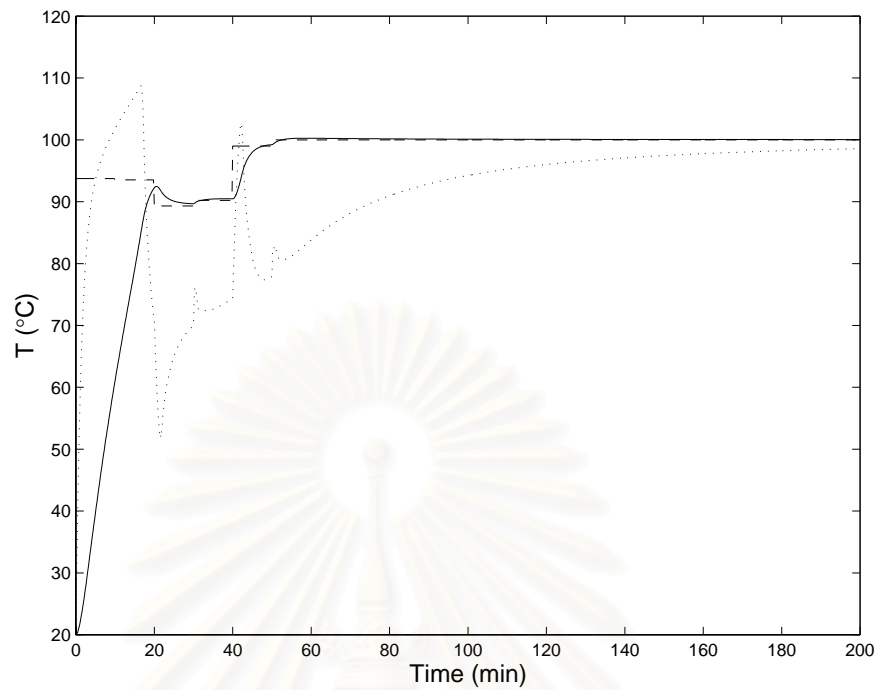
Figure 5.10: Control response (on-line, mismatch in k_2^1 and k_2^2): T_r^{sp} (dash), T_r (solid), T_j (dot)
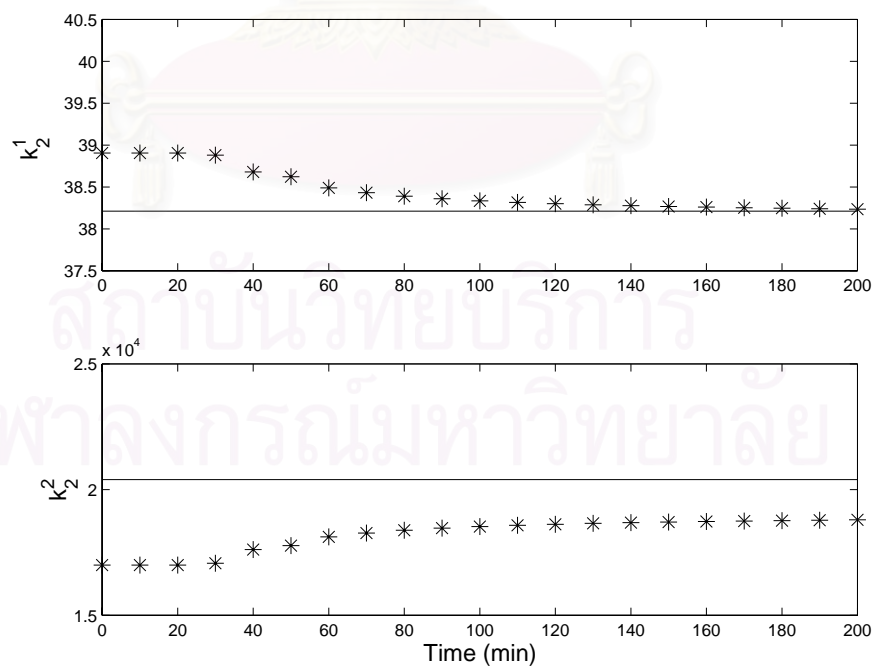
Figure 5.11: Estimate of k_2^1 and k_2^2 (on-line, mismatch in k_2^1 and k_2^2): actual (solid), estimate (*)
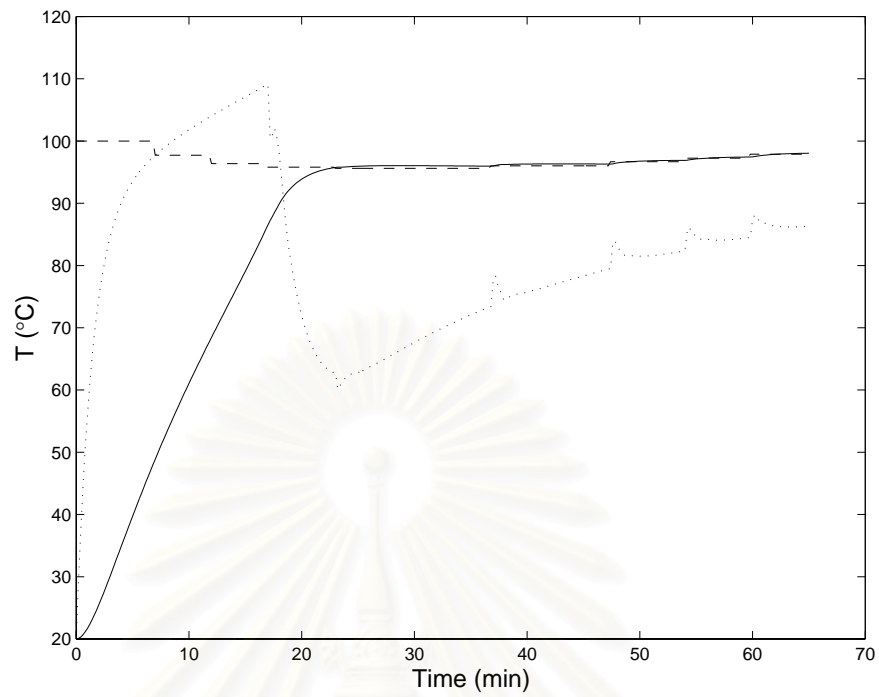
Figure 5.12: Control response (off-line, mismatch in k_2^1, Problem P2): T_r^{sp} (dash), T_r (solid), T_j (dot)
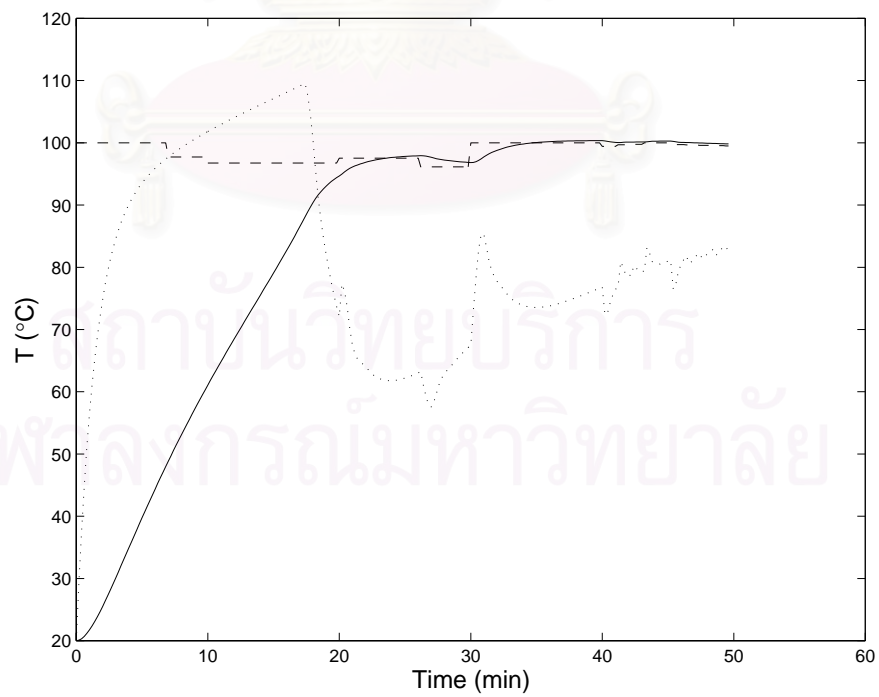
Figure 5.13: Control response (on-line, mismatch in k_2^1, Problem P2): T_r^{sp} (dash), T_r (solid), T_j (dot)

5.2   Continuous Stirred Tank Reactor (CSTR)

5.2.1   Introduction

The control of chemical reactors such as a continuous stirred tank reactor (CSTR) has received major attention over the past decades. Inherently nonlinear and complex dynamic behavior i.e. strong parametric sensitivity and multiple steady state behavior posts some of the most challenging control problems that are difficult to handle with linear controllers. However, most chemical reactors have been traditionally controlled using linear control techniques. This mainly contributes to their simplicity, well establishment of linear control theory, and successful applications in real industries. Since it is known that linear controllers usually provide satisfactory control performance especially when a process is operated in the vicinity of a nominal operating condition, a number of nonlinear process control methodologies has emerged for nonlinear processes with wide range of operation (Bequette, 1991). This characteristics is prevalently found in many process control problems, for examples, controlling systems during startup and shutdown, and tackling set point changed due to different product specification.

Model predictive control (MPC), one of advanced feedback control techniques, is widely recognized as an efficient control strategy to deal with many challenging nonlinear control problems. It has been increasing adopted in industries. Many successful applications as well as an overview of commercial MPC algorithms are reported by Qin and Badgwell (1997). The key advantage of MPC over other control methods is that various process constraints concerning state and manipulated variables can be explicitly handled in the formulation of a MPC problem. Furthermore, MPC is also well suited for control of multivariable processes in an optimal way.

However, there are some important issues that need to be taken into account in the practical implementation of MPC. The first one lies on the fact that the MPC requires an availability of the process model to be used in its algorithm and also the knowledge of all system states to incorporate feedback. However, in most industrial processes, it is accepted that the perfect model is rarely available; a modeling error

is unavoidable, and the state variables are not all measurable. Thus, the use of MPC should account for these requirements. Apart from that, stability is an important issue to be considered since the closed loop stability property of the system under MPC is desirable (Mayne et al., 2000). It is to be noted that most control techniques used in process industries do not meet this demand (Henson, 1998). Additionally, the computational method of an optimization problem in the MPC formulation is another difficult problem. An efficient and reliable optimization technique is needed so that the computational time is sufficient small for on-line implementation. All of these concerns will be addressed through this simulation study.

The objective of this study is aimed to investigate the performance of a nonlinear MPC and a hybrid control strategy using a nonlinear MPC and a linear control methodology through a dual mode control approach. Using the dual mode approach takes an advantage of combining an advanced nonlinear control design and a linear control technique in that the linear controller with simple control algorithm and less computation demand is applied within the area around a desired condition which satisfies its design specification while, outside this area, the nonlinear MPC with guaranteed stability is applied instead. In the nonlinear MPC algorithm, a simultaneous model solution and optimization technique is used for solving an on-line optimization problem at each time interval to determine manipulated variables.

To demonstrate the implementation of both nonlinear MPC and dual mode nonlinear MPC, we consider the control of a continuous stirred tank reactor (CSTR) with a single irreversible, exothermic reaction. Although there exists many research studies on the control of a CSTR, most of the previous works mainly attempt to control a reactor temperature. The direct control of concentration in a CSTR is sometimes necessary in order to satisfy different product specification, environmental requirement, safety consideration, etc., so that we focus our attention to the control of product concentration. Nevertheless, major difficulties associated with such a control problem are that the measurement of concentration is often not available for the control point of view and a process model used always presents the uncertainty of model parameters e.g. in kinetic parameters. To overcome these obstacles, an on-line extended Kalman filter (EKF) is coupled with the nonlinear MPC to estimate the unmeasured

concentration and to compensate a model mismatch due to the uncertainty in process parameters.

5.2.2   Dual Mode Nonlinear MPC Approach

The basic concept of the dual mode nonlinear MPC algorithm can be divided into two modes of operation as illustrated in Figure 5.14. That is, in the first mode, the nonlinear MPC with a terminal inequality constraint, is applied whenever the state $x(t)$ lies outside the terminal space E, while a local controller in the second mode is employed inside the terminal region to bring the state to a desired set point. The main benefit of the dual mode MPC is that, under nominal operating condition where the state are usually located within the pre-determined area (around a desired set point), any reliable linear control techniques, which can stabilize the system and require less computational effort, is utilized to achieve satisfactory control performance. This is because, in this region, the nonlinear dynamic behavior of the systems can be sufficiently described by linear relation. However, for the case where the system is driven far away from the desired condition, the MPC with guaranteed stability over a wide range of operation is activated to steer the states of the system back to the region E. In other words, an advanced control algorithm is integrated with a conventional linear control technique in an efficient dual mode scheme. Due to such advantage, the dual mode MPC is an attractive control methodology for process control applications.

Local Linear Control Technique

In the present study, two types of well developed linear control methodologies: state feedback linearizing control (SFC) and conventional proportional-integral-derivative technique (PID) are studied via the dual mode control framework. In general, the SFC has often been used in the dual mode control approach (Michalska and Mayne, 1993; Allgower adn Ogunnaike, 1997) since it can asymptotically stabilize a closed loop system within the small region E. However, the SFC controller still requires a reliable process model used in the control algorithm. Alternatively, the PID controller, which has long history in control engineering and is widely used for many real applications,
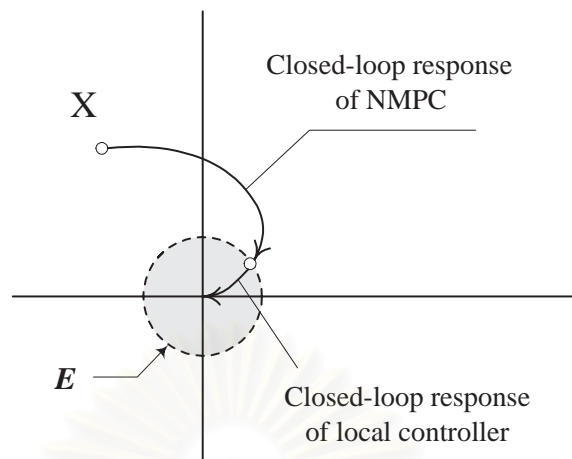
Figure 5.14: The concept of dual mode NMPC technique

is considered in the dual mode control approach. The advantage of the PID controller over the SFC controller is that the knowledge of process models is not necessary in the PID control law. This alternative approach has not been previously addressed in the literature. Furthermore, it has been accepted that the PID controller can effectively control processes near or within nominal operating regimes in which control parameters are tuned.

Dual Mode Nonlinear MPC Algorithm with EKF

In this section, we present the extension of dual mode nonlinear MPC concept to include an extended Kalman filter (EKF) in its control algorithm. Since the dual mode nonlinear MPC incorporates a feedback mechanism to update current states for computing a future prediction of system behavior in the control algorithm, the acquirement of current process information is an essential part in the nonlinear MPC algorithm as well.

Generally, the knowledge of the system states is often obtained through on-line measurements; however, in practice only some of states can be directly measured. In such a case, a state estimation can be employed to obtain the value of unmeasured state variables from available output measurements. Various methods of state estimation for linear and nonlinear systems exist in process control area, for example,

Kalman filter, Luenberger observer and Moving horizon estimator. A review of these estimation techniques and their applications can be seen in Soroush (1998) and Muske and Edgar (1997). However, the EKF, which is an optimal recursive estimation technique, is applied here due to the main contributions in that the EKF requires only a current measurement and allows to use prior knowledge of a system for estimation with unsophisticated algorithm. As a consequence, the EKF is appropriate for on-line implementation. The detail of the EKF is given in Appendix C.

With an inclusion of the EKF, the capability of the dual mode nonlinear MPC to handle systems in which some state variables are not measurable, can be enhanced. Besides, in some situations where process parameters are not known exactly, we can apply the EKF to estimate these uncertain parameters, thus increasing the robustness of the dual mode MPC as well.

The proposed dual mode nonlinear MPC integrating with the EKF algorithm can be described as follows:

Step 0 Specify a terminal region (E) around a desired operating condition.

Step 1 Measure outputs and estimate unmeasured states/uncertainty process parameters using the EKF.

Step 2 Examine the value of the state variable to be controlled i.e. if the state lies inside the region E, a linear controller is activated. Otherwise, a nonlinear MPC controller is implemented.

Step 3 Apply the first element of calculated control input to the system.

Step 4 Repeat from step 1 for the next sampling time interval.

5.2.3   CSTR Case Study

In this work, we consider a continuous stirred tank reactor in which a first order, irreversible exothermic reaction ($A \rightarrow B$) is carried out, as an illustrative case study. The reactor model studied by Limqueco and Kantor (1990) has been modified here to include the dynamic of product concentration (B). Under the following assumptions;

Table 5.7: The definition of dimensionless variables and parameters

x_1	$= \frac{C_A}{C_f}$	v	$= \frac{\gamma q}{T_{f0}}(T_f - T_{f0})$	γ	$= \frac{E}{RT_{f0}}$
x_2	$= \frac{C_B}{C_f}$	τ	$= \frac{Q_0}{V}t$	ϕ	$= \frac{V}{Q_0}k_0 e^{-\gamma}$
x_3	$= \frac{T - T_{f0}}{T_{f0}}\gamma$	β	$= \frac{-\Delta H C_f}{\rho C_p T_{f0}}\gamma$	q	$= \frac{Q}{Q_0}$
u	$= \frac{\gamma\delta}{T_{f0}}(T_c - T_{f0})$	δ	$\frac{U_r A_r}{\rho C_p Q_0}$		

the reactor is perfectly mixed and no heat loss occurs; all model parameters and physical properties are constant at nominal operation, the material and energy balances of the CSTR can be written as:

$$\frac{dC_A}{dt} = -k_0 C_A \exp\left(-\frac{E}{RT}\right) + \frac{F}{V}(C_{Af} - C_A) \tag{5.25}$$

$$\frac{dC_B}{dt} = k_0 C_A \exp\left(-\frac{E}{RT}\right) - \frac{F}{V}C_B \tag{5.26}$$

$$\frac{dT}{dt} = -\frac{\Delta H}{\rho C_p}k_0 C_A \exp\left(-\frac{E}{RT}\right) + \frac{F}{V}(T_f - T) + \frac{UA}{\rho C_p V}(T_c - T) \tag{5.27}$$

where C_A and C_B are the concentration of component A and B, T is reactor temperature, T_f and T_c are feed temperature and coolant temperature, respectively.

With the dimensionless parameters and variables as defined in Table 5.7, the reduced dimensionless models are given by:

$$\frac{dx_1}{d\tau} = -\phi x_1 \exp\left(\frac{x_3}{1 + x_3/\gamma}\right) + q(1 - x_1) \tag{5.28}$$

$$\frac{dx_2}{d\tau} = \phi x_1 \exp\left(\frac{x_3}{1 + x_3/\gamma}\right) + qx_2 \tag{5.29}$$

$$\frac{dx_3}{d\tau} = \beta\phi x_1 \exp\left(\frac{x_3}{1 + x_3/\gamma}\right) - (q + \delta)x_3 + u + v \tag{5.30}$$

where x_1 is the dimensionless concentration of component A (reactant), x_2 is the dimensionless concentration of component B (product), x_3 is the dimensionless reactor temperature, u and v represent the dimensionless cooling temperature and the dimensionless feed temperature, respectively. The meanings of the other variables and parameters are given in the nomenclature.

The values of process parameters and initial conditions chosen in this case study are shown in Table 5.8. We assume that the initial feed temperature (T_f) and the

nominal feed temperature (T_{f0}) are equal at 300 K. For these process parameters and conditions, the dynamic behavior of the CSTR system exhibits multiple steady state conditions as shown in Figure 5.15 where the intersections between the total rate of heat generated and that of heat removed are the steady states. According to Figure 5.15, the system has three (two stable and one unstable) steady states and the operating condition in Table 5.8 corresponds to the higher stable steady state. It should be noted that, without any control, when there is a small disturbance, for example, an decrease in feed temperature of 5 K from its nominal temperature of 300 K, the system will move to a new steady state as can be clearly seen from Fig. 5.15.

Table 5.8: Process parameters and initial conditions

β	$= 8$	$x_1(0)$	$= 1$
δ	$= 0.3$	$x_2(0)$	$= 0$
γ	$= 20$	$x_3(0)$	$= 2$
ϕ	$= 0.072$	u	$= 0$
q	$= 1$	v	$= 0$

5.2.4 Control Implementation

This section demonstrates the application of the EKF-based dual mode nonlinear MPC algorithm proposed to a CSTR system for the control of product concentration. To investigate the benefit of this control strategy, we also compare the control performance of the developed control strategy with other different predictive control schemes as explained in Table 5.9. The controller **I** and **II** based on the EKF-based dual mode control approach consist of nonlinear MPC (NMPC) technique in conjunction with SFC and PID method, respectively, whereas the controller **III** and **IV** are original NMPC approach, which includes zero terminal constraint to guarantee stability, with and without the EKF, respectively. To control the dimensionless of the product concentration (x_2), the jacket cooling temperature (u) is used as a control manipulated input and is assumed to be directly manipulated without delay. The input u is bounded between 0 and 2. The frequency of updated control action and estimation is chosen
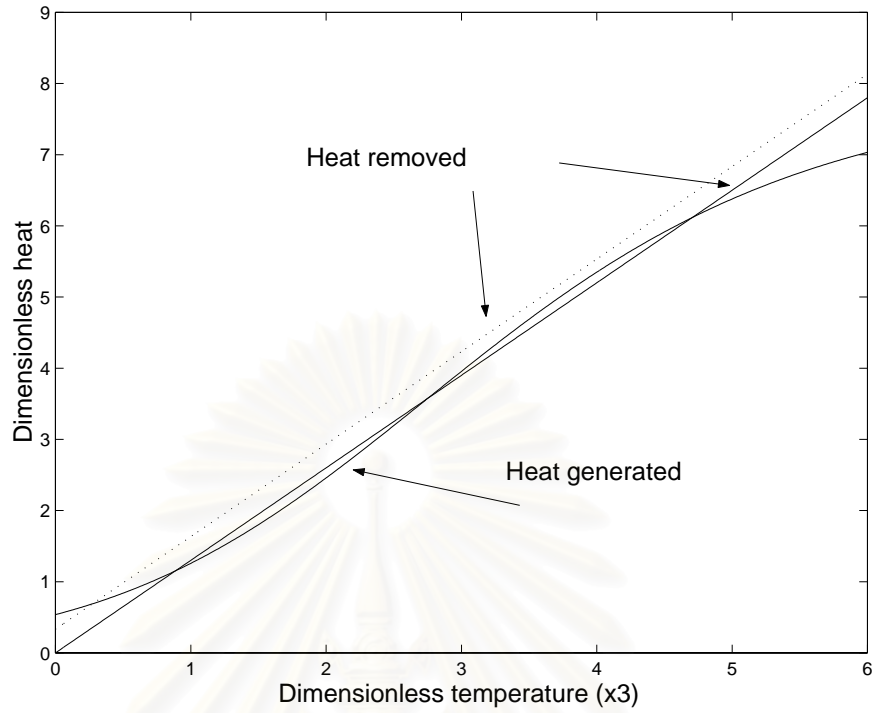
Figure 5.15: Steady state operating condition with change in feed temperature

to be equivalent to the measurement sampling time ($\Delta\tau = 0.2$).

The formulation of the MPC can be described as follows:

$$\min_{u(\tau)} \int_{\tau}^{\tau+T_p} \left(x_2^{sp} - x_2(\tau)\right)^2 d\tau \tag{5.31}$$

subject to:

process model equations:

$$\text{Equations (5.28) to (5.30)} \tag{5.32}$$

control and state constraints:

$$0 \leq \quad u(\tau) \quad \leq 2 \tag{5.33}$$

$$0 \leq \quad x_3(\tau) \quad \leq 6.7 \tag{5.34}$$

and the terminal (region) state constraint:

$$|x_2^{sp} - x_2(T_p)| \leq 0.115 \quad \text{for the controller } \mathbf{I} \text{ and } \mathbf{II} \tag{5.35}$$

$$x_2^{sp} - x_2(T_p) = 0 \quad \text{for the controller } \mathbf{III} \text{ and } \mathbf{IV} \tag{5.36}$$

Table 5.9: Different predictive control strategies

Controller	Control strategy	Stability constraints in NMPC	Estimator
Type I	Dual mode approach (NMPC with SFC)	Terminal region (E)	EKF
Type II	Dual mode approach (NMPC with PID)	Terminal region (E)	EKF
Type III	NMPC	Zero terminal	EKF
Type IV	NMPC	Zero terminal	not included

where the prediction horizon (T_p) equals to 10. Equation (5.34) represents path constraint on reactor temperature which is equivalent to the maximum allowable temperature of 400 K. The region state stability constraint is defined in Equation (5.35) corresponding to approximately 10% deviation around its desired set point value while the terminal zero constraint is given in Equation (5.36). Note that to keep the concentration at the desired set point, the reactor temperature sometimes needs to be raised. However, it is essential to keep the reactor temperature within a certain limit to avoid a runaway reaction. The resulting optimal control problem is solved using the simultaneous strategy as described earlier.

As a local controller in the dual mode control scheme, both SFC controller through a linear quadratic control approach and PID controller in velocity form are investigated. The idea of the SFC is to compute the control $u(t)$ as shown in the following equation, at each sampling time based on linearized nonlinear process models around the current state condition.

$$u(\tau) = -K(\tau)x(\tau) \tag{5.37}$$

where the feedback controller gain $K(\tau) = -R^{-1}B^T P(\tau)$ and $P(\tau)$ is determined by solving the following Riccati equation:

$$-P(\tau)A(\tau) - A(\tau)^T P(\tau) - Q + P(\tau)B(\tau)R^{-1}B(\tau)^T P(\tau) = 0 \tag{5.38}$$

where A and B are the Jacobi-linearized system matrix corresponding to process models (Equations (5.28) to (5.30)), Q and R are SFC tuning parameter matrix. Table

Table 5.10: The value of tuning parameters for SFC and PID

The SFC controller		
$Q \quad = \mathrm{diag}[1\ 1\ 5]$	$R \quad = 0.05$	
The PID controller		
$K_c \quad = 13$	$\tau_i \quad = 1.2$	$\tau_d \quad = 0.5$

5.10 shows the tuning parameter value of the SFC and PID controller. These tuning parameters are adjusted to make the control action less drastic.

In all case studies, only the measurement of the dimensionless reactor temperature (x_3) is assumed to be available. Accordingly, the EKF is utilized to on-line estimate the dimensionless concentration $(x_1$ and $x_2)$ using the measurement of x_3. That makes the dual mode NMPC possible to control the unmeasured concentration. However, this assumption is omitted when the controller **IV** is applied; for this case the value of all dimensionless states $(x_1, x_2$ and $x_3)$ can be acknowledged.

Simulation results are evaluated in case of disturbance rejection studies under nominal condition where all process parameters in the controller model are specified correctly and under model mismatch condition due to uncertainties in kinetic parameter (ϕ) and heat transfer coefficient (δ). Since these parametric uncertainties can affect the control performance, the EKF is also employed to estimate ϕ and δ. To do this, the Equations (5.39) and (5.40), as shown below, are augmented to the CSTR models (Equations (5.28) to (5.30)) and utilized in the EKF algorithm. The parameter value is, therefore, estimated along with state variables. The use of parameters as additional system states is found to be a suitable approach (Semino et al., 1996). The EKF parameters: P, Q and R are tuned to reflect the accuracy of estimation of the unmeasured concentration as well as of the uncertain parameters $(\phi$ and $\delta)$. The values of these tuning parameters are given in Table 5.11.

$$\frac{d\phi}{d\tau} = 0 \tag{5.39}$$

$$\frac{d\delta}{d\tau} = 0 \tag{5.40}$$

5.2.5   Simulation Results and Discussions

In principle one would like to control the CSTR system at a desired steady state (set point). However, once disturbances e.g. a step change in feed temperature, come into the system, this can cause the system to move from the desired steady state to a new (undesired) steady state point. The control objective of our simulation work is to apply the EKF-based dual mode NMPC techniques to control the dimensionless of the product concentration at its nominal steady state ($x_2^{sp} = 0.7646$). We assume that the CSTR system is initially controlled at its nominal steady state value until a feed temperature disturbance (v) consisting of a decrease in the feed temperature from 300 K to 295 K is introduced to the system at $t = 20$ and is kept throughout the simulation. At this point, the controller is still set at its initial value until at $t = 40$ the controller is then activated. During this open loop period the dimensionless product concentration decreased to a new steady state value ($x_2 = 0.0862$) as shown in Figure 5.16. It can also be seen from Figure 5.16 that the CSTR shows highly nonlinear dynamic behavior.

First, simulation studies are performed on the nominal case in which all model parameters are known exactly. For the controller **I** and **II**, since the feed temperature disturbance causes the dimensionless concentration (x_2) to be outside the area E, the NMPC controller is first activated to drive the state x_2 to the operating region E and then switches to the local controller (SFC or PID) in order to control the system to the desired set point. Figure 5.17 shows a control response of the controller **I** and **II**. It can be seen that both the controller **I** and **II** can bring the product concentration (x_2) back

Table 5.11: Initial state estimates and tuning parameters in EKF

$x_1(0)$	$= 1.0$	P	$= \mathrm{diag}[2\ 1.5\ 1.5\ 0.5\ 0.5]$
$x_2(0)$	$= 0$	Q	$= \mathrm{diag}[9\ 4\ 4\ 0.01\ 0.5]$
$x_3(0)$	$= 2.0$	R	$= \mathrm{diag}[10]$
$\phi(0)$	$= 0.072$		
$\delta(0)$	$= 0.3$		
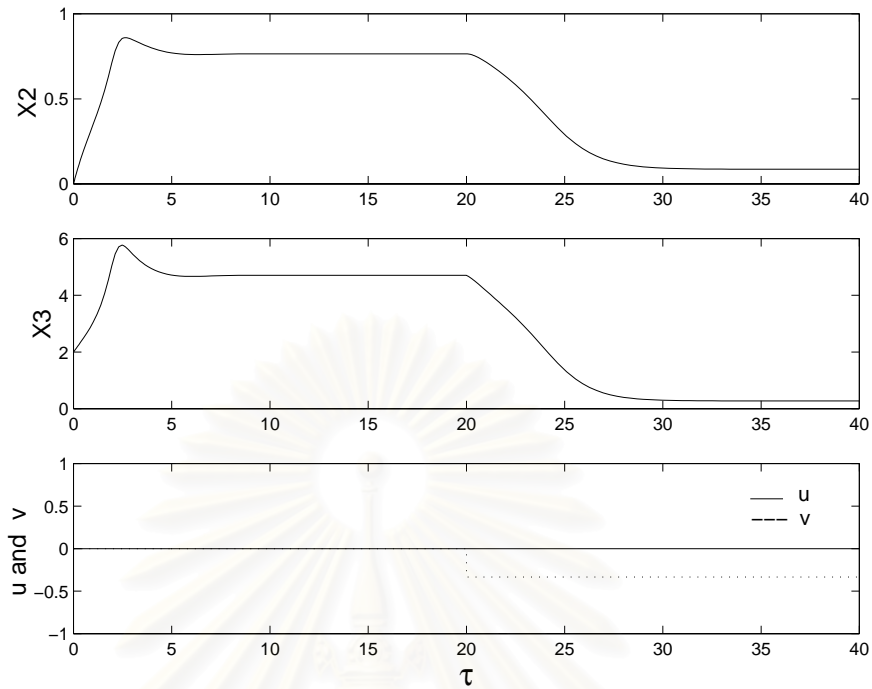
Figure 5.16: Open loop response with feed temperature disturbance

to the desired set point with slightly overshoot in response, even though the controller **II** gives longer setting time (high IAE, see Table 5.12). It should be mentioned that the better control performance of the controller **II** could be achieved by adjusting the PID tuning parameters. Similar results can be observed for the controller **III** and **IV**; the performance of the controller **III** is closely equivalent to that of the controller **IV** as shown in Figure 5.18 and further seen in Table 5.12.

Next, the control performances are investigated with respect to a model mismatch due to parametric uncertainties, i.e. changes in ϕ and δ, in the controller model. As known that, in real practice, a perfect model is hardly to obtain, the control performance should be tested for robustness under the presence of these uncertainties.

Figures 5.19 and 5.20 show the result for the model mismatch in ϕ (25% decrease). It is found that the controller **I**, **II** and **III** are able to control the concentration of B nearly to its desired set point with small overshoot; although, the control response of the controller **II** takes long settling time. This is because the ability of the EKF to estimate the states and process parameter values accurately as can be seen from Figure 5.21. Therefore, such a model mismatch is reduced. On the other hand, the controller

IV cannot manage this mismatch; however, it still provides a reasonably good control response with small offset and more oscillations in the control action compared to the controller **I**, **II** and **III**. This result implies that the controller **IV** can regulate the system within a limit range of a model mismatch. An offset of the controlled system caused by model mismatch is often noticeable; nevertheless, using the EKF can reduce this influence.

In case of a 25% decrease in δ, again the controller **I** is capable to deal with this mismatch and give a better control response while the controller **II** and **III** give a similar control response but with small offset and some oscillation as illustrated in Figures 5.22 and 5.23. The control performance of the controller **I** is found to be better than other controllers as compared in Table 5.12. In comparison to the controller **I**, **II** and **III**, the controller **IV** cannot accommodate this mismatch at all resulting to the state x_2 far away from the desired set point. It is shown that the controller **IV** is strongly sensitive to the mismatch in δ.

Finally, simulations are carried out under parametric uncertainties in ϕ decreased by 25% and δ decreased by 25%. As can be seen from Figure 5.24, the results using the controller **I** and **II** show that they can drive the state x_2 to the desired set point and then keep it at set point; although, there is some oscillation in the controller **II**. The control response of the controller **III** and **IV** shows a similar trend (Figure 5.25). Both the controllers give a good control performance with small offset but the controller **IV** produces more oscillate in control action. Figure 5.26 shows the estimation of the state x_2 and parameters ϕ and δ; it is found that the EKF provides a good estimation of the state x_2 and can estimates these parameters closed to the actual values.

Table 5.12 summaries the results for all case studies in term of the IAE value and the CPU time. It can be noticed from these results that the use of the EKF can improve the performance of the model predictive controller when the models of the system to be controlled is exposed to model mismatch under parametric uncertainty as compared the results of the controller **IV** to the controller **I**, **II** and **III**. In other words, the robustness of the MPC controller coupled with the EKF is enhanced. Another important point to be emphasized is that by comparing the dual mode NMPC (the controller **I** and **II**) and the original NMPC (the controller **III** and **IV**), it indicates

Table 5.12: Summary of control performance (IAE) and elapsed CPU time for different control strategies

Case studies	IAE/CPU time (s)			
	Controller I	Controller II	Controller III	Controller IV
(1) Nominal case	1.2356/49.43	1.3299/48.39	1.2359/106.33	1.2358/100.35
(2) ϕ +25%	1.2366/66.24	1.3360/62.61	1.2481/120.45	5.1083/80.74
(3) ϕ -25%	1.2348/57.78	1.3267/54.21	1.2373/108.42	1.5238/149.01
(4) δ +25%	1.2372/56.25	1.4401/55.25	1.3374/115.84	1.2935/124.74
(5) δ -25%	1.2321/40.15	1.3365/39.33	1.3435/103.75	3.4463/65.86
(6) ϕ and δ +25%	1.2372/59.81	1.4451/56.02	1.3419/123.42	1.6882/102.38
(7) ϕ and δ -25%	1.2330/44.49	1.3363/41.52	1.3725/87.99	1.4784/139.34

the effect on using a terminal region constraint instead of a final zero constraint in the NMPC formulation; the dual mode NMPC requires less computational time than the original NMPC. This can be explained that, within the pre-specified area around the desired set point, the linear control method is utilized and needs little computational effort compared to the NMPC.

5.2.6   Conclusions

In this study, a dual mode control design framework integrating an advanced nonlinear control methodology, i.e. a nonlinear MPC controller, with a conventional linear control technique, i.e. a SFC and PID controller, has been proposed and applied to control a product concentration in a CSTR. An EKF was incorporated into the control algorithm to estimate a concentration and process parameters exposed to model uncertainty. To control the concentration, a reactor temperature is considered as a path constraint in the formulation of MPC problem to ensure that it does not exceed an allowable limit during the course of operation. An open loop optimal control arising from the MPC problem was solved at every sampling time using an efficient simultaneous optimization approach. The performance of the dual mode MPC was compared with an original MPC scheme with/without the EKF. Simulation results have shown

the capability of the proposed control strategies to maintain the product concentration at its desired set point. Stability and robustness of the dual mode MPC controller can be achieved for both the nominal case and the presence of parametric uncertainty. The results also indicated that the PID controller implemented in the dual mode MPC is a reliable and powerful control strategy; the SFC controller can be replaced by the PID controller in order to steer a state to a desired set point. In addition, it can be seen that the EKF performs excellent estimation of the concentration as well as model parameters; combining the EKF with the controller can compensate the effect of model mismatch. In comparison to the original MPC, the dual mode MPC strategy needs less on-line computational time; this clearly indicates the feasibility in employing this controller for real application.
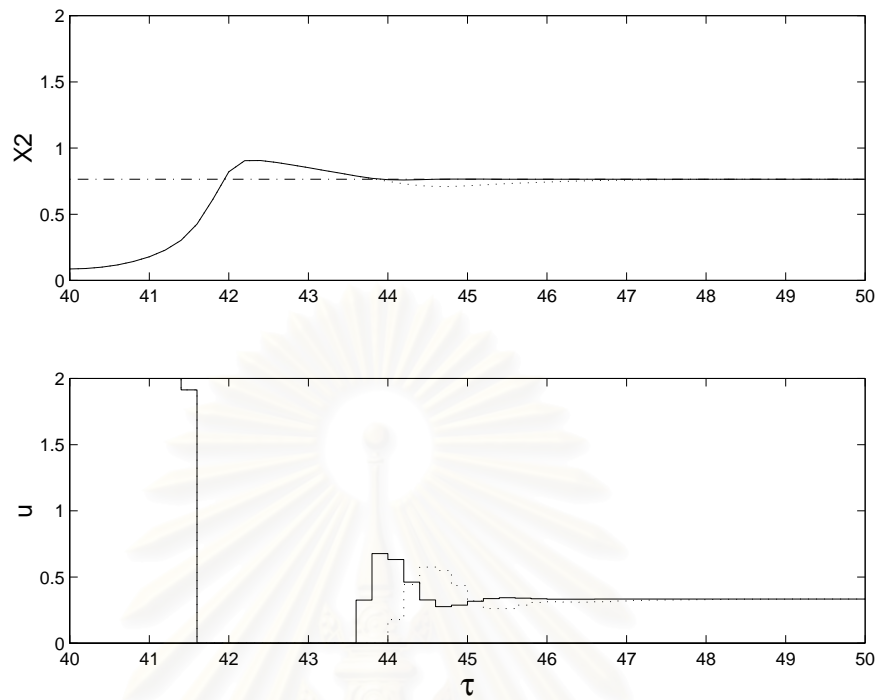
Figure 5.17: Control response for nominal case: controller I (solid) and II (dash)
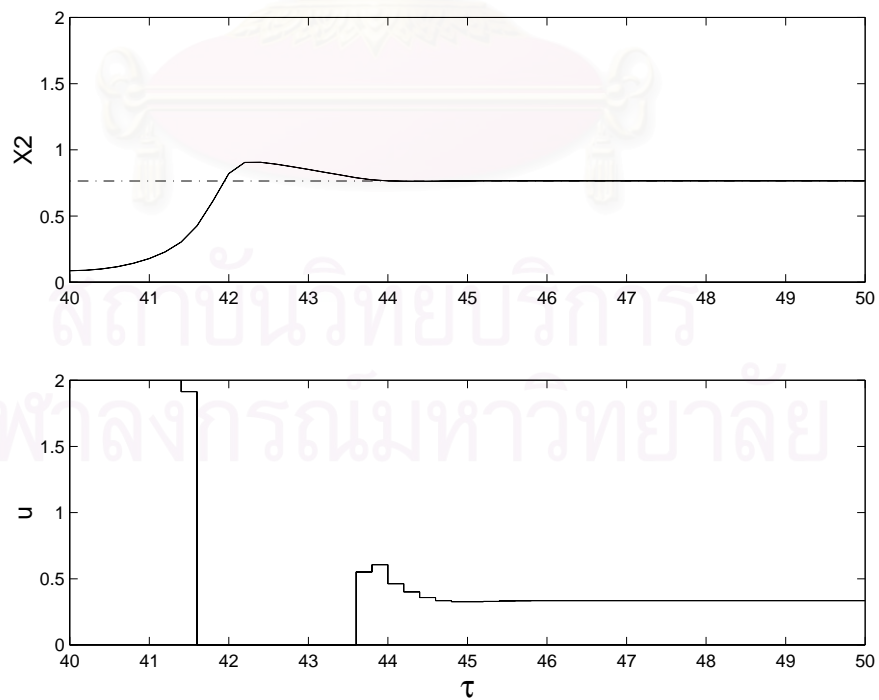
Figure 5.18: Control response for nominal case: controller III (solid) and IV (dash)
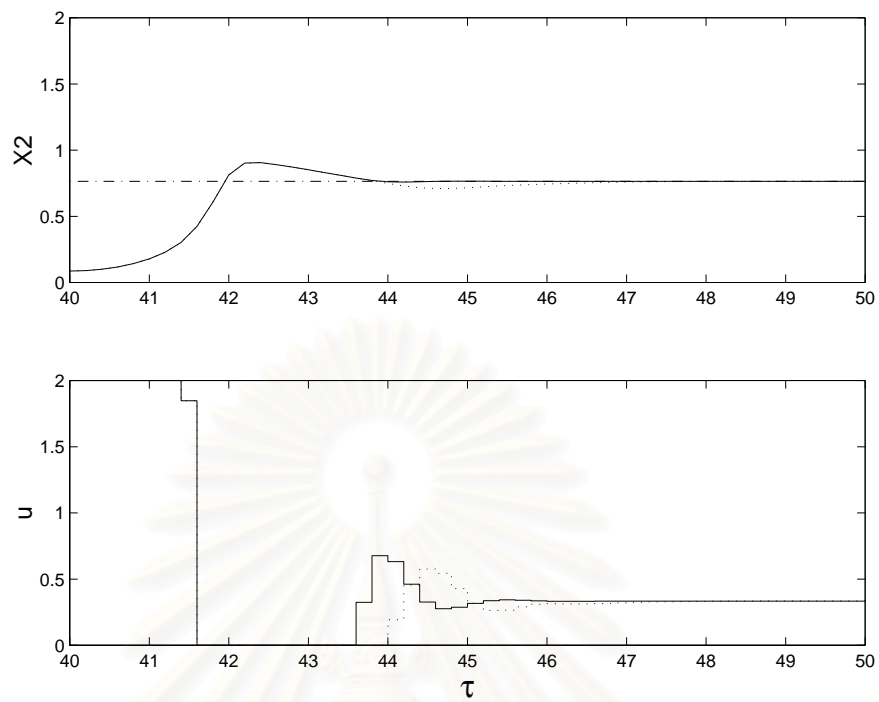
Figure 5.19: Control response for uncertainty in ϕ (25% decrease): controller I (solid) and II (dash)
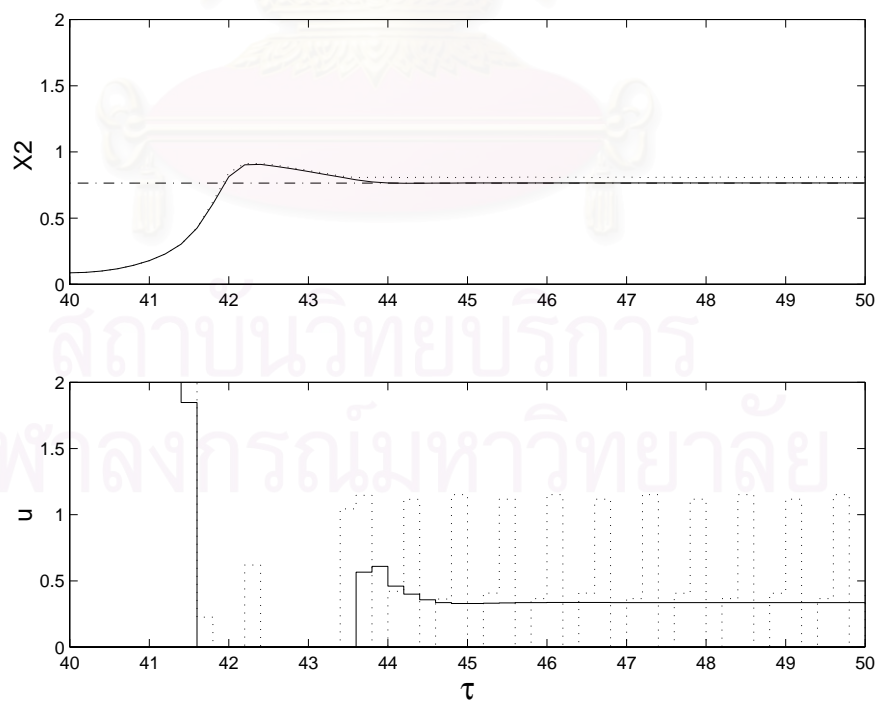
Figure 5.20: Control response for uncertainty in ϕ (25% decrease): controller III (solid) and IV (dash)
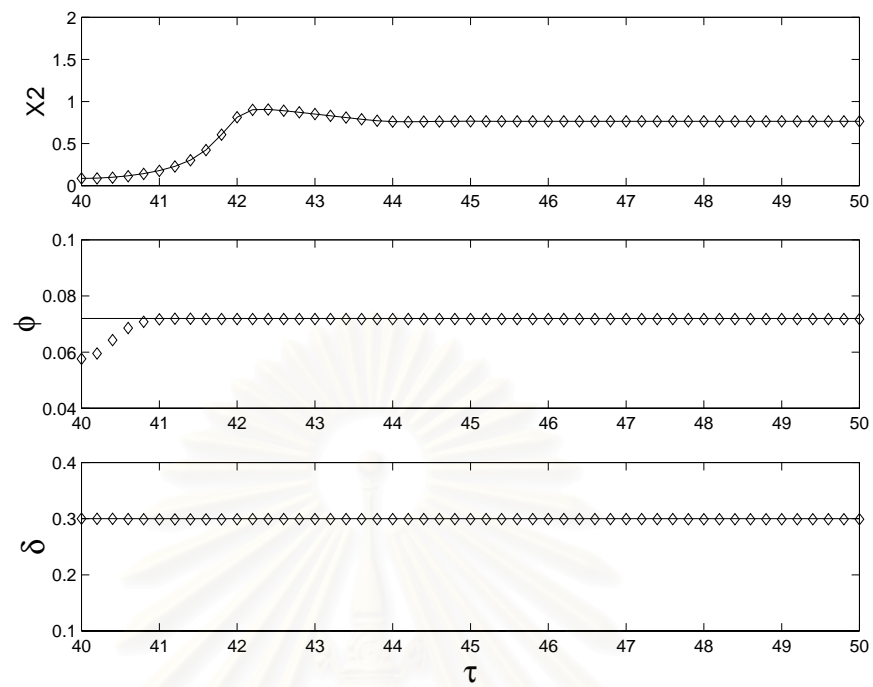
Figure 5.21: Performance of the EKF for uncertainty in ϕ (25% decrease): actual (solid) and estimate ($\diamond$)
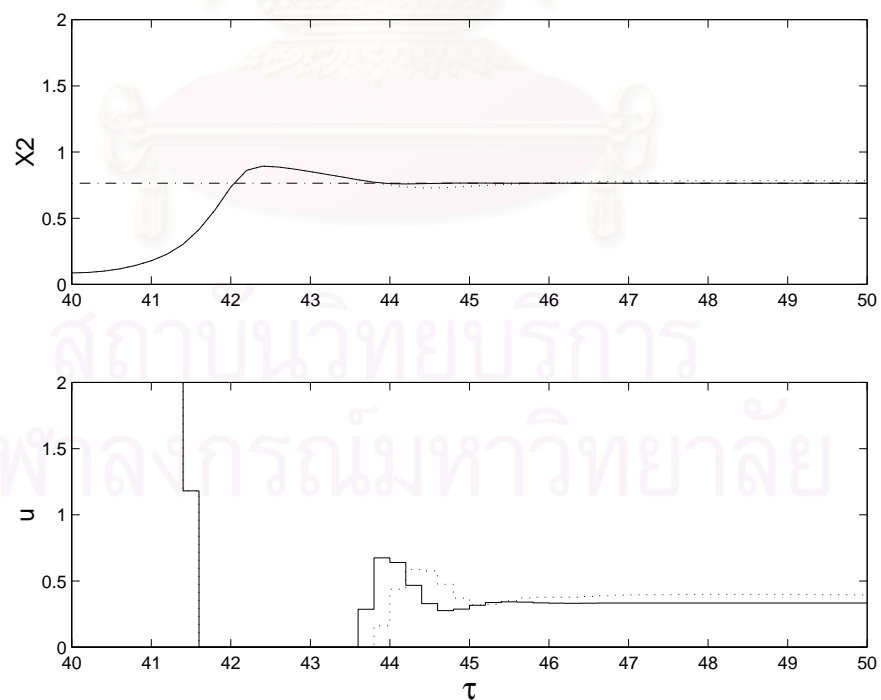
Figure 5.22: Control response for uncertainty in δ (25% decrease): controller I (solid) and II (dash)
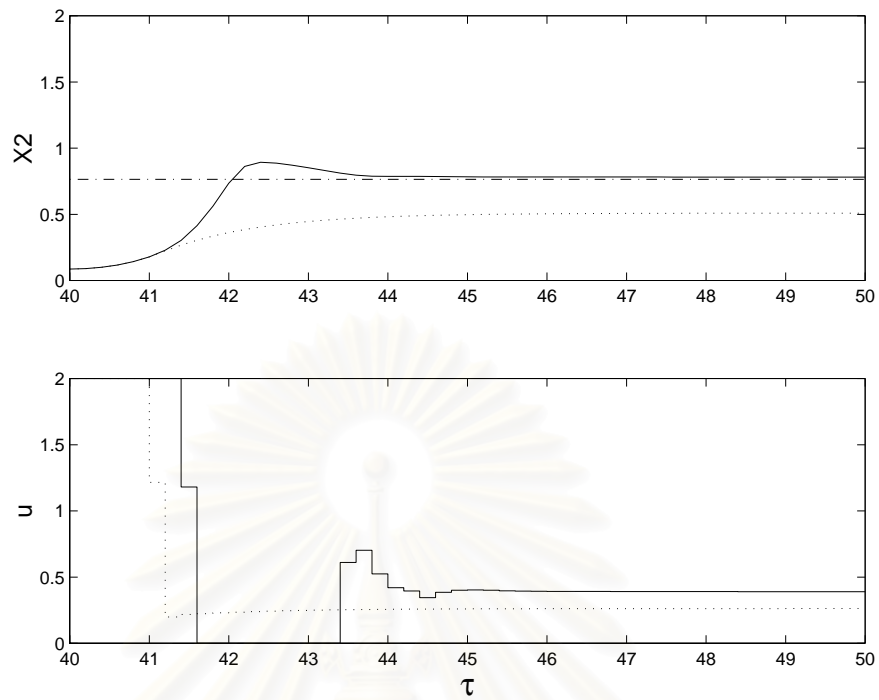
Figure 5.23: Control response for uncertainty in δ (25% decrease): controller III (solid) and IV (dash)
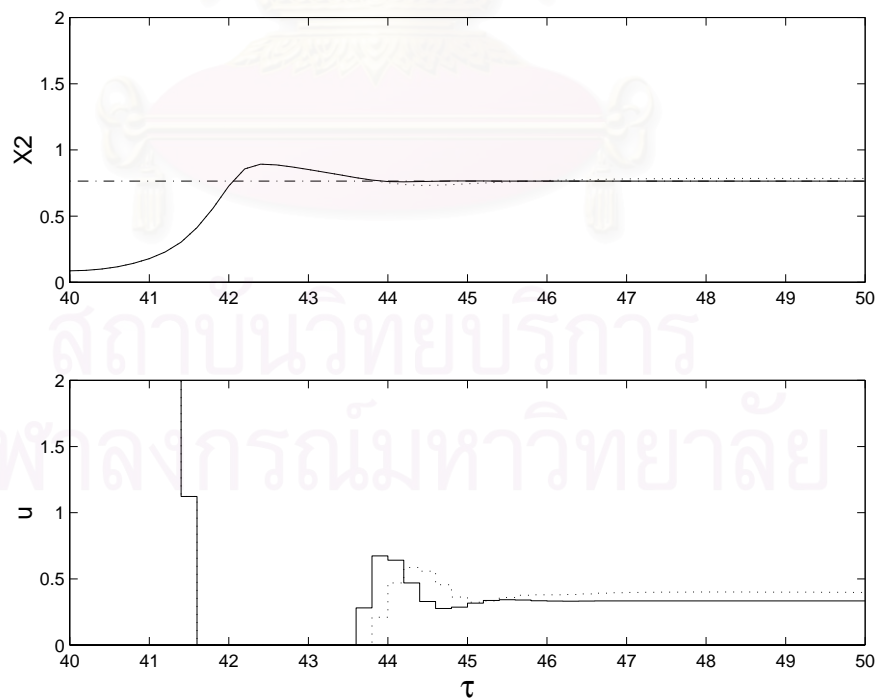
Figure 5.24: Control response for uncertainty in ϕ and δ (25% decrease): controller I (solid) and II (dash)
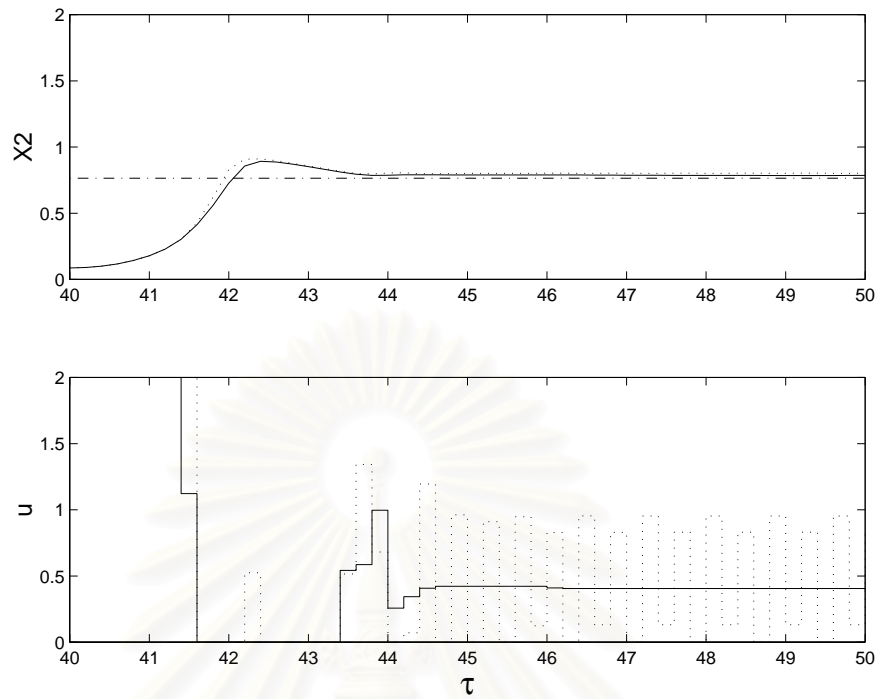
Figure 5.25: Control response for uncertainty in ϕ and δ (25% decrease): controller III (solid) and IV (dash)
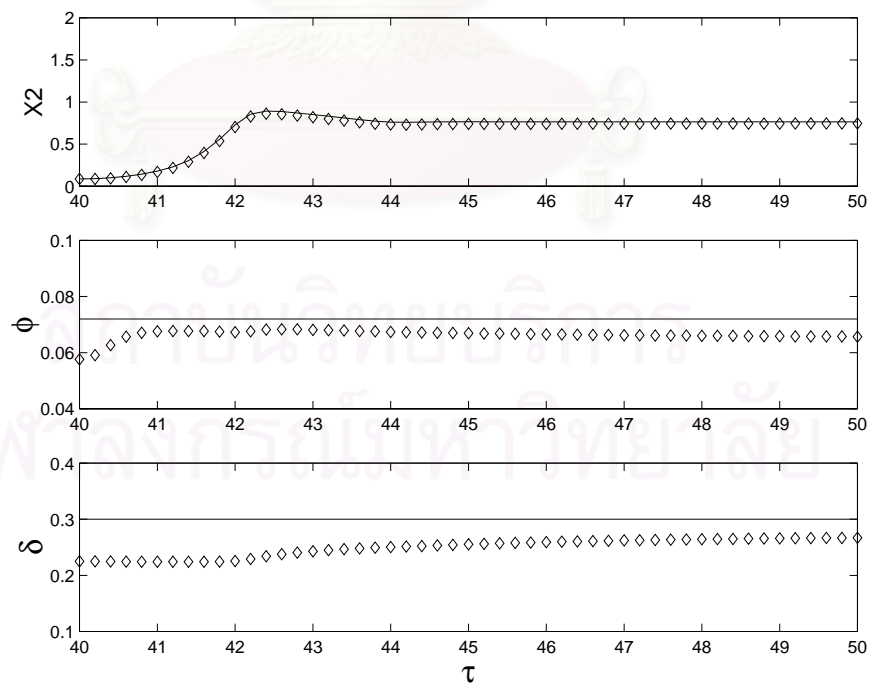
Figure 5.26: Performance of the EKF for uncertainty in ϕ and δ (25% decrease): actual (solid) and estimate ($\diamond$)

<div align="center">

Chapter 6

Model Predictive Control of a Trickle Bed Reactor[*]

</div>

This chapter describes the implementation of a model predictive control (MPC) technique to a trickle bed reactor. The dynamic reactor models developed in Chapter 4 is used here to represent the reactor system and to design the MPC controller. Simulation studies are carried out to investigate the performance of the MPC strategy to control the temperature at outlet of a top catalyst bed within the trickle bed reactor. The performance of the MPC controller is evaluated with set point tracking and disturbance rejection cases under nominal and model mismatch conditions.

6.1   Description of Trickle Bed Reactor

The trickle bed reactor (TBR) in which hydrogenations of pyrolysis gasoline occur, as described in Chapter 4, is utilized for the control study of a model predictive control (MPC) scheme. The schematic diagram of the TBR system is illustrated in Figure 6.1.

The following reactions are assumed to take place within the trickle bed reactor:

$$Diolefins + H_2 \xrightarrow{r_1} Olefins + H_2 \xrightarrow{r_1} Paraffins$$
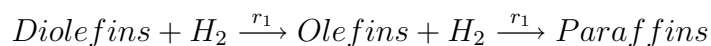
The process models derived from mass and energy balances can be written as (see Chapter 4 for details):

$$\frac{dC_{H_2,g}}{dt} = -\frac{u_g}{\varepsilon_g}\frac{dC_{H_2,g}}{dz} - \frac{k_{l,H_2}a_i}{\varepsilon_g}\left(C_{H_2,g} - C_{H_2,l}\right) \tag{6.1}$$

---

[*]Portions of this chapter were appeared in Arpornwichanop and Kittisupakorn (2003).
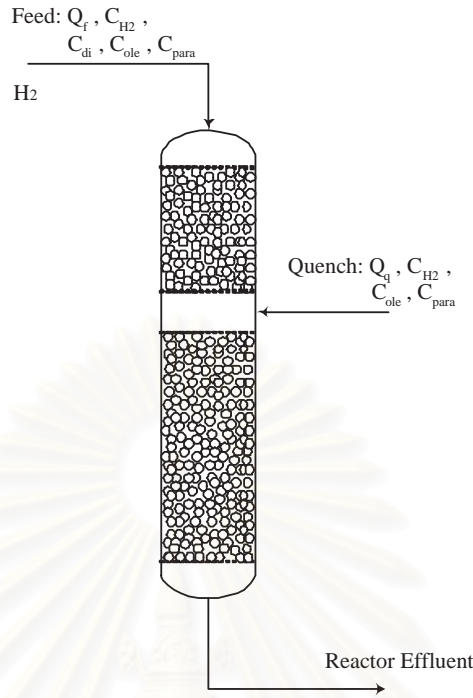
Figure 6.1: Schematic diagram of trickle bed reactor

$$\frac{dC_{H_2,l}}{dt} = -\frac{u_l}{\varepsilon_l}\frac{dC_{H_2,l}}{dz} + \frac{k_{l,H_2}a_i}{\varepsilon_l}\left(C_{H_2,g} - C_{H_2,l}\right) - \frac{(1-\varepsilon)}{\varepsilon_l}(r_1 + r_2) \tag{6.2}$$

$$\frac{dC_{di,l}}{dt} = -\frac{u_l}{\varepsilon_l}\frac{dC_{di,l}}{dz} - \frac{(1-\varepsilon)}{\varepsilon_l}(r_1) \tag{6.3}$$

$$\frac{dC_{ole,l}}{dt} = -\frac{u_l}{\varepsilon_l}\frac{dC_{ole,l}}{dz} - \frac{(1-\varepsilon)}{\varepsilon_l}(-r_1 + r_2) \tag{6.4}$$

$$\frac{dC_{para,l}}{dt} = -\frac{u_l}{\varepsilon_l}\frac{dC_{para,l}}{dz} + \frac{(1-\varepsilon)}{\varepsilon_l}(r_2) \tag{6.5}$$

$$\frac{dT}{dt} = \frac{-(u_g C_{p,g}\rho_g + u_l C_{p,l}\rho_l)\frac{dT}{dz} - (\Delta H)(1-\varepsilon)(r_1 + r_2)}{(\varepsilon_g \rho_g C_{p,g} + \varepsilon_l \rho_l C_{p,l})} \tag{6.6}$$

$$r_1 = k_{0,1}\exp\left(\frac{-Ea_1}{RT}\right)C_D C_{H_2} \tag{6.7}$$

$$r_2 = \frac{k_{0,2}\exp\left(\frac{-Ea_2}{RT}\right)C_O C_{H_2}}{1 + k_{0,ad}\exp\left(\frac{-Ea_{ad}}{RT}\right)C_D} \tag{6.8}$$

At quench section:

$$(Q_f + Q_q)C_{H_2,l}^{B2} = Q_f C_{H_2,l}^{F} + Q_q C_{H_2,l}^{Q} \tag{6.9}$$

$$(Q_f + Q_q)C_{di,l}^{B2} = Q_f C_{di,l}^{F} + Q_q C_{di,l}^{Q} \tag{6.10}$$

$$(Q_f + Q_q)C_{ole,l}^{B2} = Q_f C_{ole,l}^{F} + Q_q C_{ole,l}^{Q} \tag{6.11}$$

$$(Q_f + Q_q)C_{para,l}^{B2} = Q_f C_{para,l}^{F} + Q_q C_{para,l}^{Q} \tag{6.12}$$

$$T^{B2} \quad = \quad \frac{u_g A \rho_g C_{p,g} T^F + \rho_l C_p (Q_f T^F + Q_q T^Q)}{(u_g A \rho_g C_{p,g} + (Q_f + Q_q) \rho_l C_{p,l})} \qquad (6.13)$$

In this work, the control of the reactor temperature at outlet from the top catalyst bed is chosen as a case study. The temperature rise across the catalyst bed, which is caused by heat released from hydrogenation reactions, is one of the important operating variables that are necessary to monitor for smooth process operation and meeting product specification. To ensure the complete elimination of unstable compounds in pyrolysis gasoline, high reactor temperature is preferred. However, it should not be too high because higher temperature favors the production of polymers that are deposited on the catalyst particles resulting to catalyst deactivation. Furthermore, higher temperature reduces the flow of liquid through the catalyst bed, thus decreasing the washing effect.

In industrial practice, the inlet temperature of the reactor is used to maintain the temperature rise across the catalyst bed at a suitable condition. Therefore, the MPC is implemented to determine the inlet temperature (T_{in}: a manipulated variable) for controlling the temperature at the outlet of the top catalyst bed.

6.2 Formulation of Model Predictive Control

The formulation of the MPC controller based on solving an on-line optimal control problem is described as follows.

The optimal control problem can be given by an objective function (performance index):

$$\min_{T_{in}(t)} \int_{t_0}^{t_0+T_P} \left(T^{sp}(z_{B1}) - T(z_{B1}, t)\right)^2 dt \qquad (6.14)$$

subject to the process models:

$$Equations \, (6.1) - (6.13) \qquad (6.15)$$

bound on a manipulated variable:

$$343 \leq T_{in} \leq 403 \qquad (6.16)$$

and an end point constraint:

$$T(z_{B1}, T_P) = T^{sp}(z_{B1}) \tag{6.17}$$

where $T^{sp}(z_{B1})$ is the set point value of the reactor temperature at outlet of the top catalyst bed.

It is noted that Equation (6.17) is included in the MPC formulation to ensure the stability of the system; the optimal controls have to force the states of the system to a desired set point at the terminal time $(t_0 + T_P)$. In this work, the prediction horizon (T_P) is set to be 1 hr which is large enough to guarantee that $T(z_{B1}, T_P) \rightarrow T^{sp}(z_{B1})$. The frequency of updated control action is chosen to be 0.1 hr. Therefore, the number of future controls in the MPC problem is equal to 10.

The structure of the MPC employed in this study is shown in Figure 6.2. It is assumed that all state variables of the system are measured. It can be seen that feedback information consists of *i)* a measurement of both the reactant concentrations (C) and the reactor temperature (T), and *ii)* an error signal (e) of the controlled variable (T at the outlet of the top catalyst bed) which is the difference observed between the measured value and the predicted value from the model. This error signal will go to zero if there are no unmeasured process disturbances to the system and the system model accurately represents the real plant. Otherwise, there is a disturbance feedback signal to the MPC controller.

In this work, the effect of modeling error is treated as an additive step disturbance in the output and is determined at the kth sampling time as shown in Equation (6.18). The disturbance term (d_k) is added to the output prediction over the entire prediction horizon (T_P) in the MPC objective function (Equation (6.14)).

$$d_k = T(z_{B1}, k)_{measured} - T(z_{B1}, k)_{predicted} \tag{6.18}$$

After updating the feedback information from the system, the MPC computes a sequence of control inputs, T_{in}, by solving the optimal control problem (Equations (6.14) to (6.17)). However, only the initial value of this control profile is applied to the system and this procedure is repeated for the next sampling time.
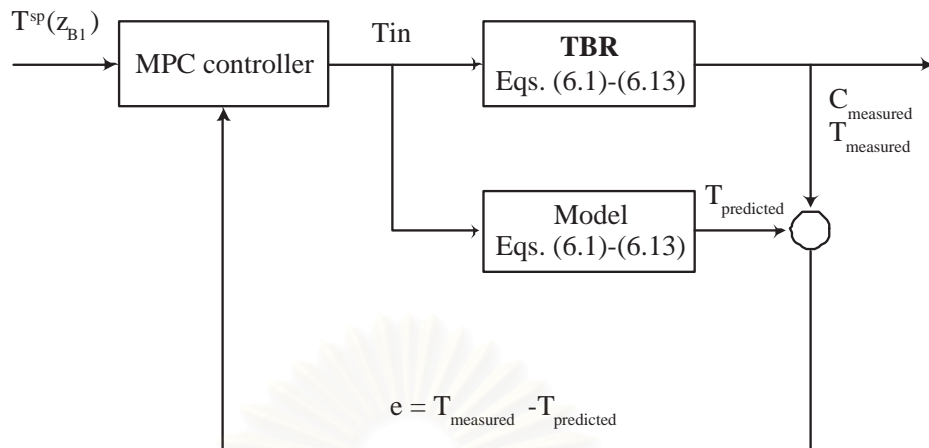
Figure 6.2: Structure of model predictive control

To find the solution of the optimal control of processes described by a system of partial differential equations (PDEs), we utilize the orthogonal collocation method on finite elements to discretize the spatial derivative term. This converts the PDEs into an ordinary differential equations. Then, the sequential solution approach by the PREOP package (Morrison, 1984) is used to solve the discretized optimal control problem.

6.3   Model Predictive Control Algorithm

The algorithm of the MPC controller can be summarized as follows

Step 1 Specify the future desired output (objective function) and initial states of the system.

Step 2 Calculate a sequence of future controls minimizing the objective function over a finite prediction horizon.

Step 3 Implement the initial value of the controls.

Step 4 Measure outputs and go back to Step 2 in order to calculate a new control sequence for the next sampling time based on new feedback information.

6.4   Simulation Results and Discussions

This section demonstrates the implementation of the MPC to control the reactor temperature at the outlet of top catalyst bed within the trickle bed reactor by adjusting the inlet feed temperature (a manipulated variable). The performance of the MPC controller is compared with that of a PID control algorithm in velocity form (Seborg et al., 1989). The trial and error procedure (Seborg et al., 1989) is utilized to obtain the PID tuning parameters ($K_c = 0.3$, $\tau_i = 1$, and $\tau_d = 0.001$).

The control performance of both controllers is evaluated in set point tracking and disturbance rejection cases under nominal condition in which all model parameters are specified correctly. The set point change and disturbance are introduced to the system at time, $t = 10$ min in all cases. Since the MPC controller is based on the model of the system to be controlled, we investigate its robustness property under model mismatch conditions i.e. changes in $k_{0,1}$ and ΔH.

In the simulation studies, we assumed that the trickle bed reactor is started at a steady state condition. The values of nominal process parameters and initial inlet stream conditions are given in Table 6.1.

The first set of simulations illustrates the nominal case; all process parameters of the reactor models used in the MPC algorithm are known exactly. In case of set point tracking of the top catalyst bed outlet temperature from its nominal value (449.6 K) to 455 K, it can be seen from Figure 6.3 that the MPC controller can control the temperature at the desired set point with small overshoot. On the other hand, the PID controller shows more overshoot and some oscillation in the response as can be seen in Figure 6.4. Similar results can be observed for the case where the temperature set point is decreased to 445 K. The MPC controller still gives a good control response as shown in Figure 6.5. It is able to drive the temperature to its desired set point smoothly with fast setting time while the PID shows slower and oscillated response (Figure 6.6).

The MPC and PID controllers are then tested in cases of the disturbance rejection that consists of 20% change in feed flow rate of pyrolysis gasoline from its nominal

Table 6.1: Process parameters and initial conditions

Pressure	$P = 29.73\ atm$
Diffusivity	$D_{l,H_2} = 10^{-5}\ cm^2/s$
Heat of reaction	$\Delta H = \text{-30}\ kcal/mol$
Hydrogen gas feed	
Flow rate	$Q = 8350\ kg/hr$
Temperature	$T = 391.63\ K$
Concentration	
Hydrogen	$C_{H_2} = 0.926\ kmol/hr$
Pyrolysis gasoline feed	
Flow rate	$Q = 68.69\ m^3/hr$
Temperature	$T = 391.63\ K$
Density	$\rho = 820\ kg/m^3$
Concentration	
Diolefins	$C_{di} = 1.48\ kmol/hr$
Olefins	$C_{ole} = 1.23\ kmol/hr$
Paraffins	$C_{para} = 2.97\ kmol/hr$
Quench	
Flow rate	$Q = 15.43\ m^3/hr$
Temperature	$T = 309.67\ K$
Concentration	
Olefins	$C_{ole} = 2.20\ kmol/hr$
Paraffins	$C_{para} = 3.11\ kmol/hr$
Hydrogen	$C_{H_2} = 0.25\ kmol/hr$

Table 6.2: Comparison of the MPC and PID control performance in the nominal case

Case studies	IAE	
	MPC	PID
Set point tracking		
(1) change T^{sp} to 455	2.4511	9.3862
(2) change T^{sp} to 445	1.9982	8.4008
Disturbance rejection		
(3) 20% increase in feed flow rate	1.2849	4.5246
(4) 20% decrease in feed flow rate	1.9172	1.9430

Note that: IAE $= \int |T^{sp} - T(t)|\, dt$

value.

With a 20% increase in the flow rate of gasoline feed, the result shows that the MPC controller (Figure 6.7) is able to elimate this disturbance and give faster control response, compared with the PID controller (Figure 6.8).

For the case of a 20% decrease in the feed rate, it can be seen that both controllers provide a good control performance as illustrated in Figures 6.9 and 6.10 and can also seen from the IAE value in Table 6.2. However, some oscillation can be observed in the PID control response.

Table 6.2 summarizes the control results of the MPC and PID controller in term of the IAE value for all simulation studies in the nominal condition. They clearly indicate that the control performance of the MPC controller is better than that of the PID controller in all case studies.

Next, The robustness property of the MPC controller has been examined with respect to uncertainties in model parameters employed in the MPC algorithm.

Figures 6.11 and 6.12 show the results of a mismatch in heat of reaction, ΔH (20% decrease), in case of set point tracking of the reactor temperature (approximately ± 5 K from its nominal set point). The MPC controller is able to drive the reactor temperature to a new desired set point; although, some error are observed in the first sampling time interval. This is because the MPC controller computes the control

Table 6.3: The MPC performance under model mismatch conditions

Case studies	IAE	
	20% decrease in ΔH	20% decrease in $k_{0,1}$
Set point tracking		
(1) change T^{sp} to 455	14.0797	9.8088
(2) change T^{sp} to 445	10.2721	10.6590
Disturbance rejection		
(3) 20% increase in feed flow rate	9.3185	9.6889
(4) 20% decrease in feed flow rate	9.6515	9.0933

input based on the model with the incorrect parameter value. However, the effect of modeling error is compensated through feedback information at the next sampling time and therefore, the MPC controller can bring the reactor temperature to the desired value.

Similarly, in case of disturbance rejection with the same model mismatch (20% decrease in ΔH), the MPC controller still provides resonably good control response; it can bring the system back to its original set point value as seen in Figures 6.13 and 6.14. This shows the ability of the MPC controller to reject the disturbance in the presence of the model mismatch.

With a 20% decrease in the reaction rate constant, $k_{0,1}$, Figures 6.15 and 6.16 illustrate the capability of the MPC controller to control the system at the desired temperature set point value; although, there are some error in the first sampling time due to the model mismatch. With the proposed strategy, the modeling error is reduced after the MPC receives new feedback information from the system.

For disturbance rejection case with the change in the feed flow rate under model mismatch in $k_{0,1}$ (20% decrease), it can be seen from Figures 6.17 and 6.18 that the MPC controller can control the reactor temperature at its set point and then maintain it at the set point throughout an entire simulation. Table 6.3 provides the control performance of the MPC controller in term of the IAE value for all case studies under model mismatch conditions.

6.5 Conclusions

This chapter has investigated the performance of a MPC strategy to control the temperature of a trickle bed reactor where hydrogenations of pyrolysis gasoline take place. The reactor models developed in Chapter 4 was utilized to the formulation of the MPC problem. The results showed that in the nominal condition where all model parameters are specified correctly, the MPC controller can provide satisfactory control response and control the reactor temperature at the desired set point value in both set point tracking and disturbance rejection cases. The control performance of the MPC controller is better than that of a PID controller in all cases. In the presence of model mismatch, the MPC controller still provides reliable control performance and is robust with respect to errors in model parameters.
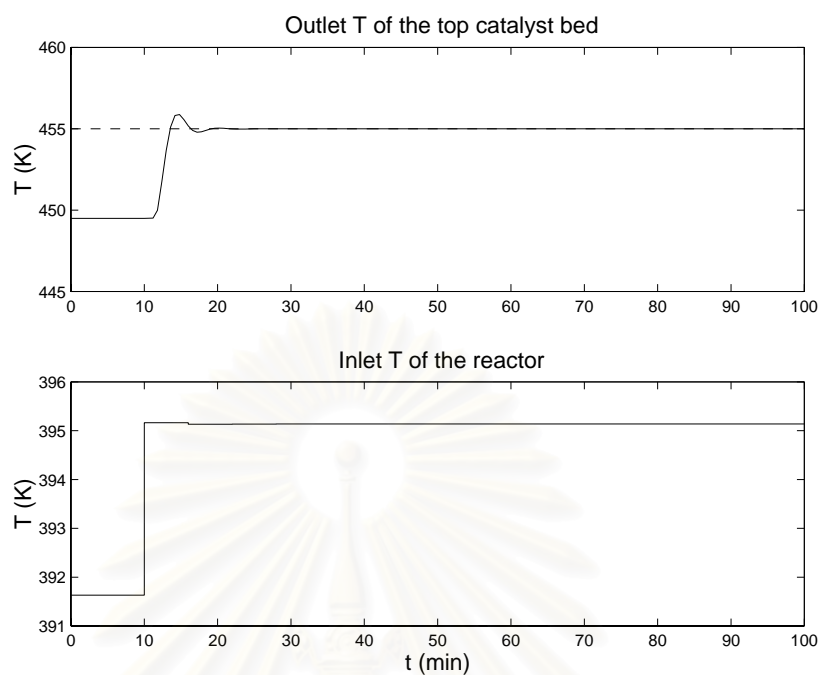
Figure 6.3: Control response of the MPC controller for set point tracking ($T^{sp} = 455$ K)
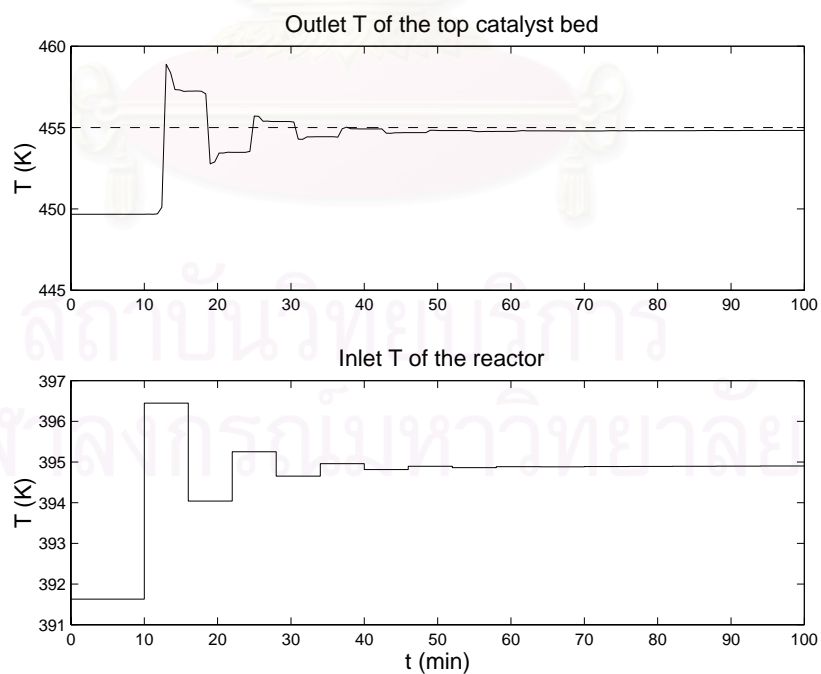
Figure 6.4: Control response of the PID controller for set point tracking ($T^{sp} = 455$ K)
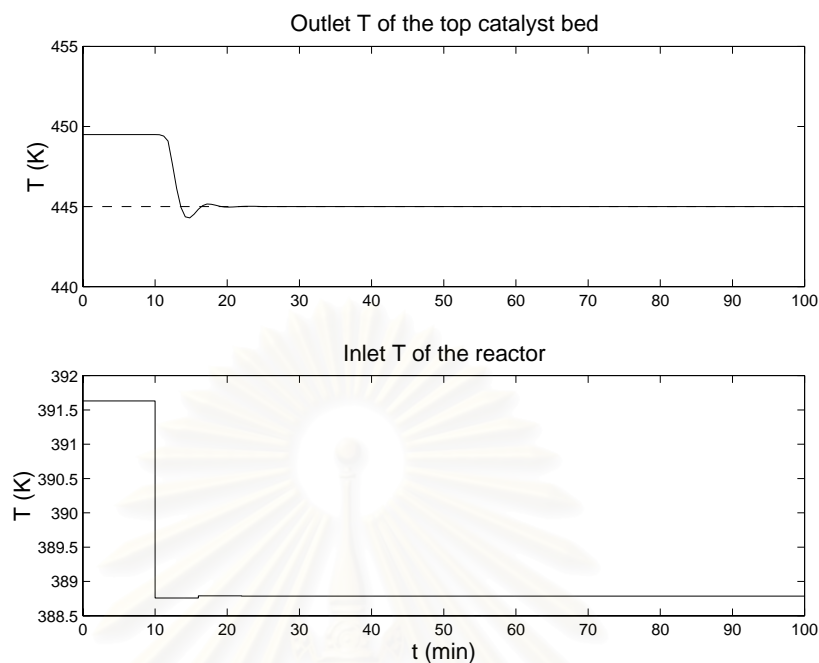
Figure 6.5: Control response of the MPC controller for set point tracking ($T^{sp} = 445$ K)
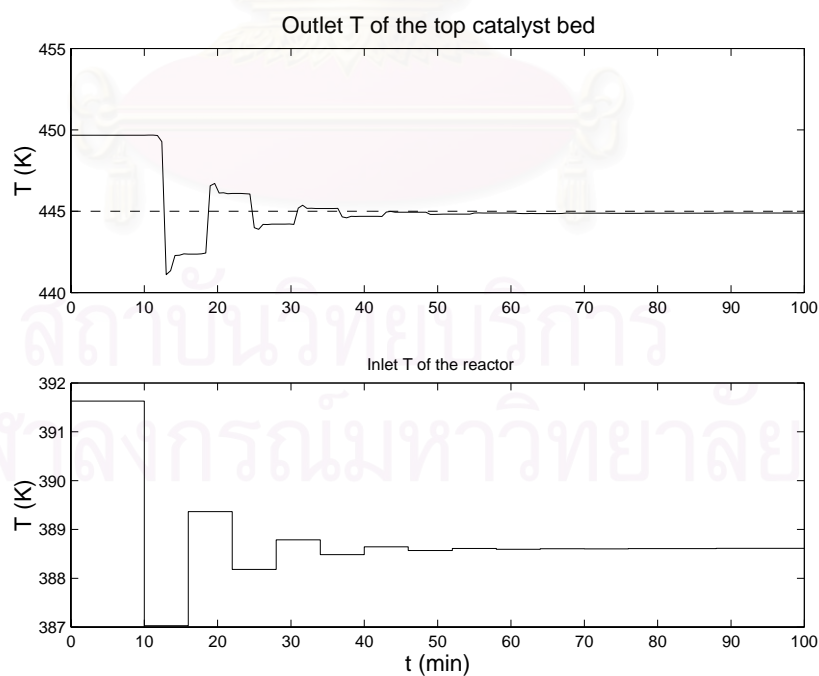
Figure 6.6: Control response of the PID controller for set point tracking ($T^{sp} = 445$ K)
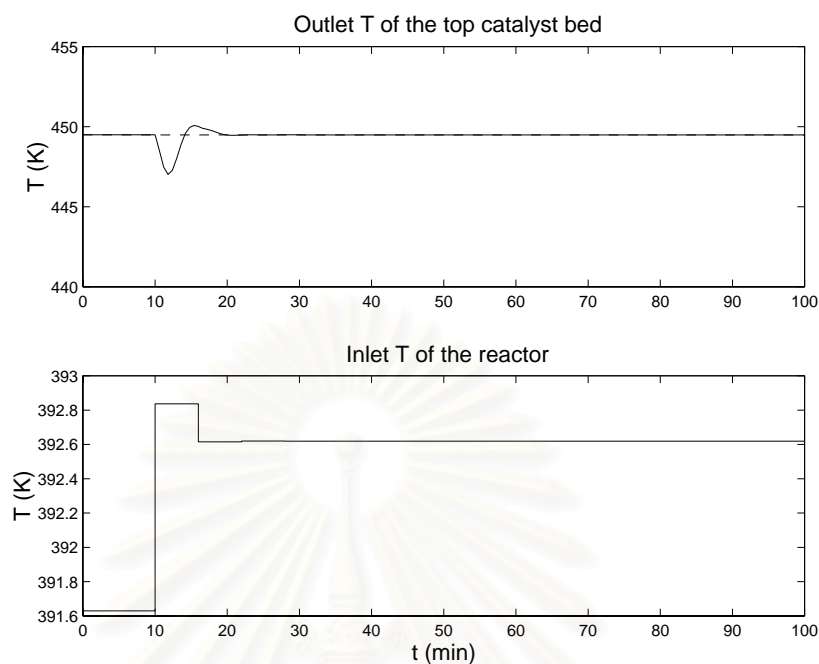
Figure 6.7: Control response of the MPC controller for disturbance rejection with 20% increase in feed flow rate
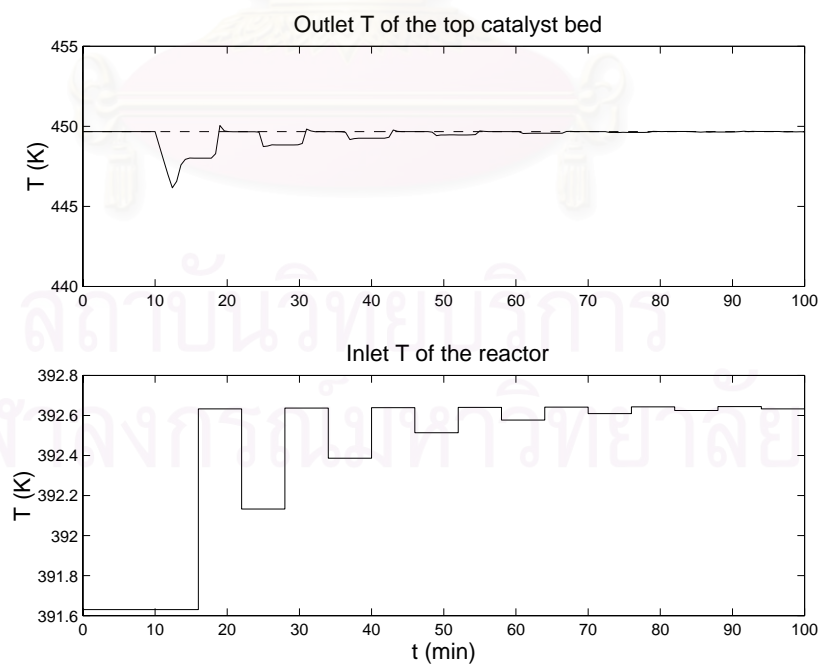
Figure 6.8: Control response of the PID controller for disturbance rejection with 20% increase in feed flow rate
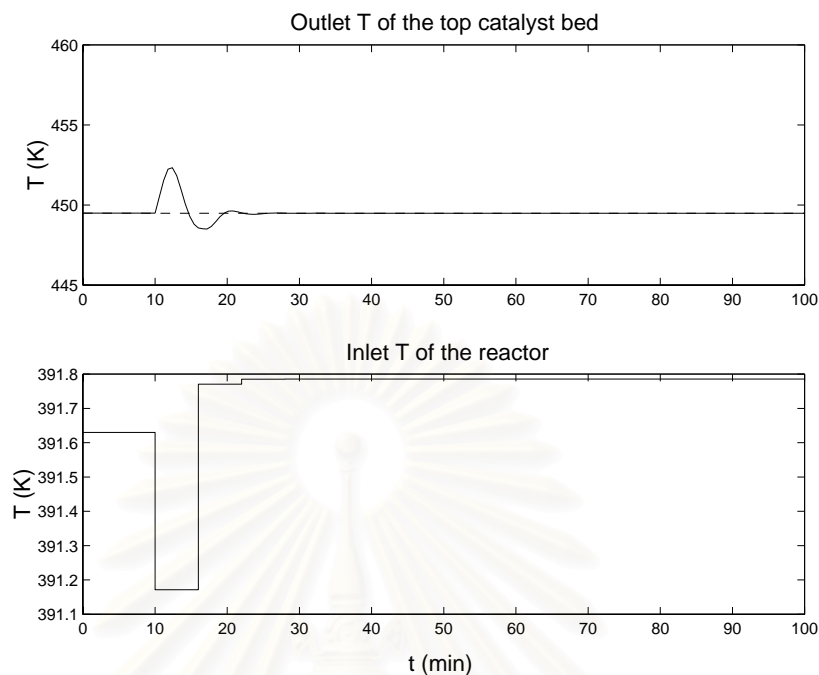
Figure 6.9: Control response of the MPC controller for disturbance rejection with 20% decrease in feed flow rate
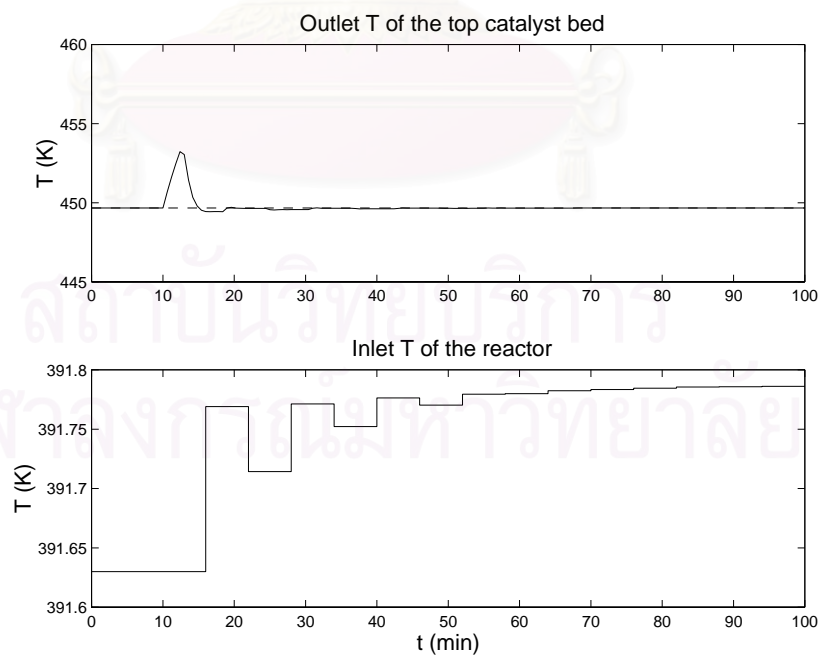
Figure 6.10: Control response of the PID controller for disturbance rejection with 20% decrease in feed flow rate
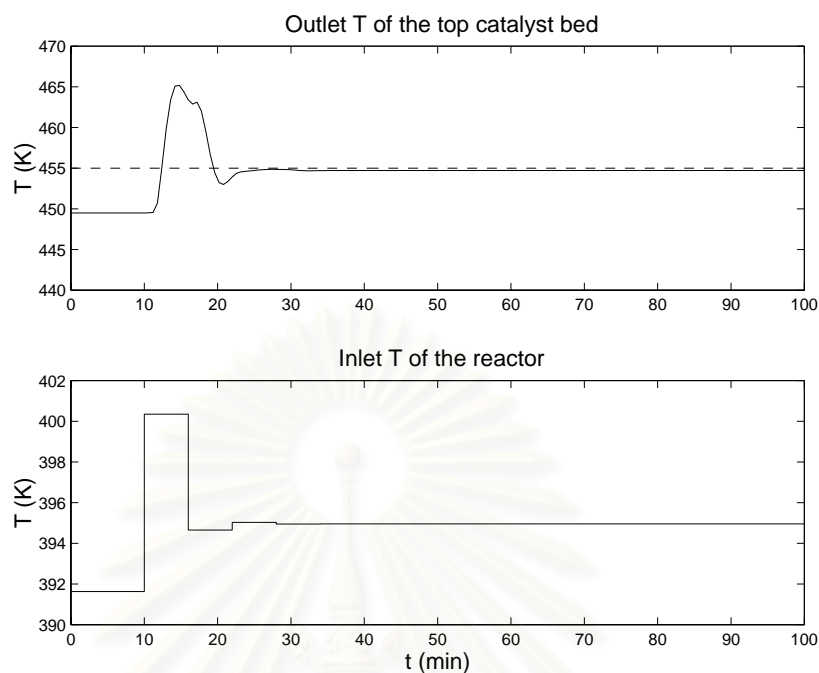
Figure 6.11: Control response of the MPC controller for set point tracking ($T^{sp} = 455$ K) with a mismatch in ΔH (20 % decrease)
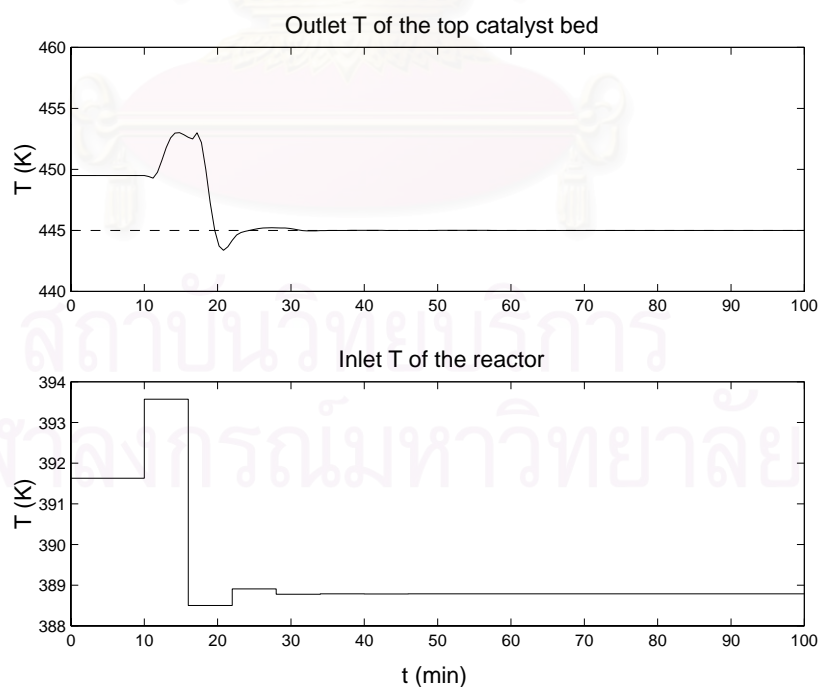
Figure 6.12: Control response of the MPC controller for set point tracking ($T^{sp} = 445$ K) with a mismatch in ΔH (20 % decrease)
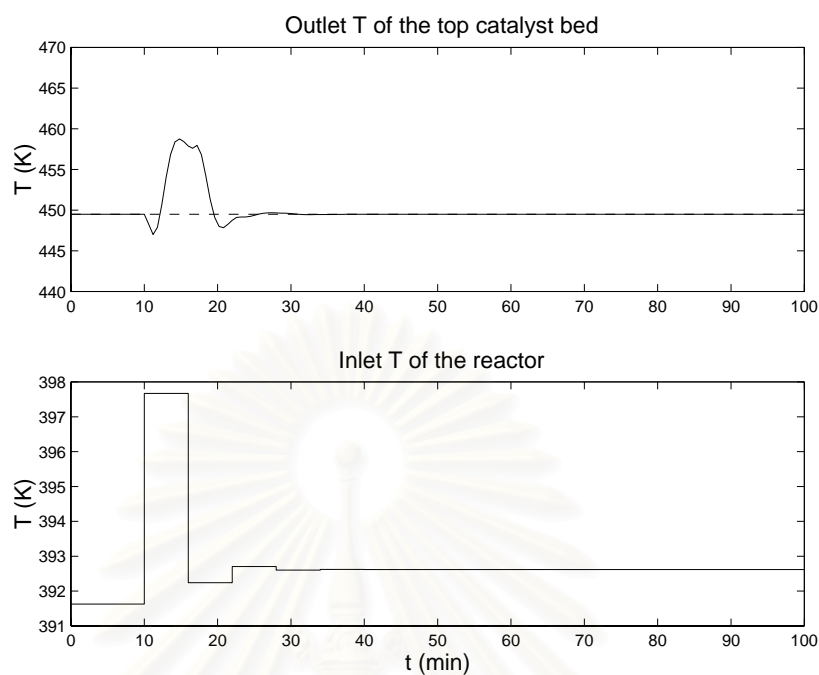
Figure 6.13: Control response of the MPC controller for disturbance rejection (20 % increase in feed rate) with a mismatch in ΔH (20 % decrease)
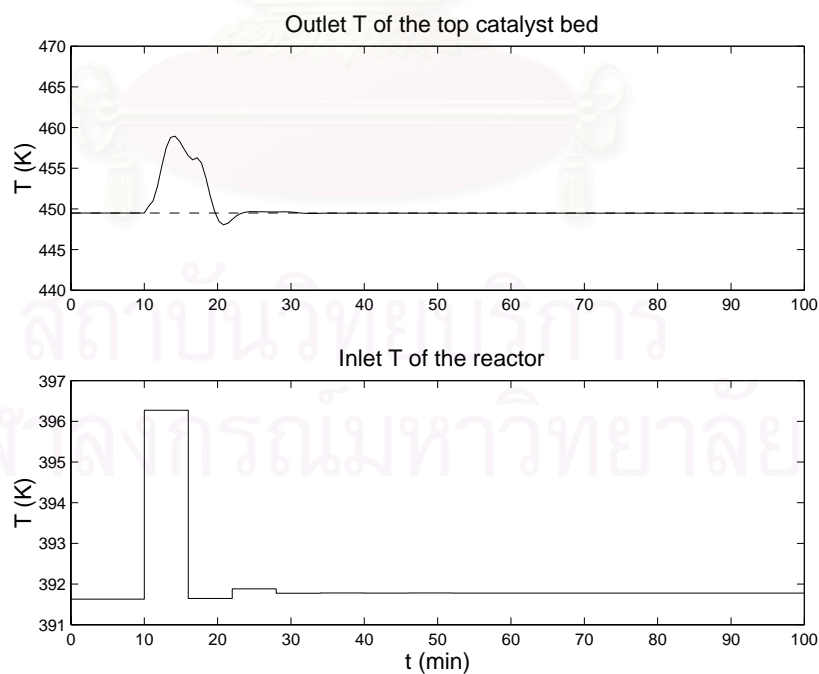
Figure 6.14: Control response of the MPC controller for disturbance rejection (20 % decrease in feed rate) with a mismatch in ΔH (20 % decrease)
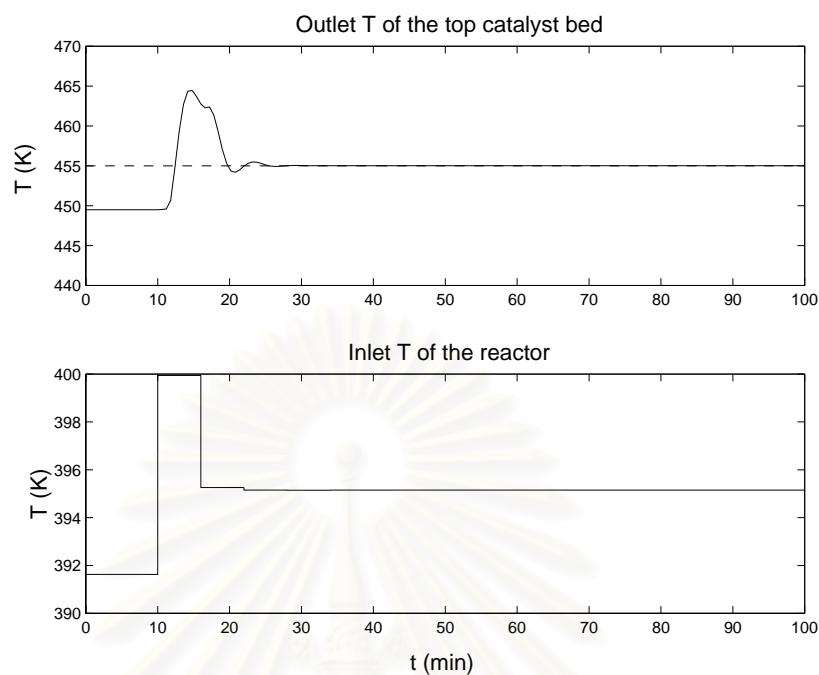
Figure 6.15: Control response of the MPC controller for set point tracking ($T^{sp} = 455$ K) with a mismatch in $k_{0,1}$ (20 % decrease)
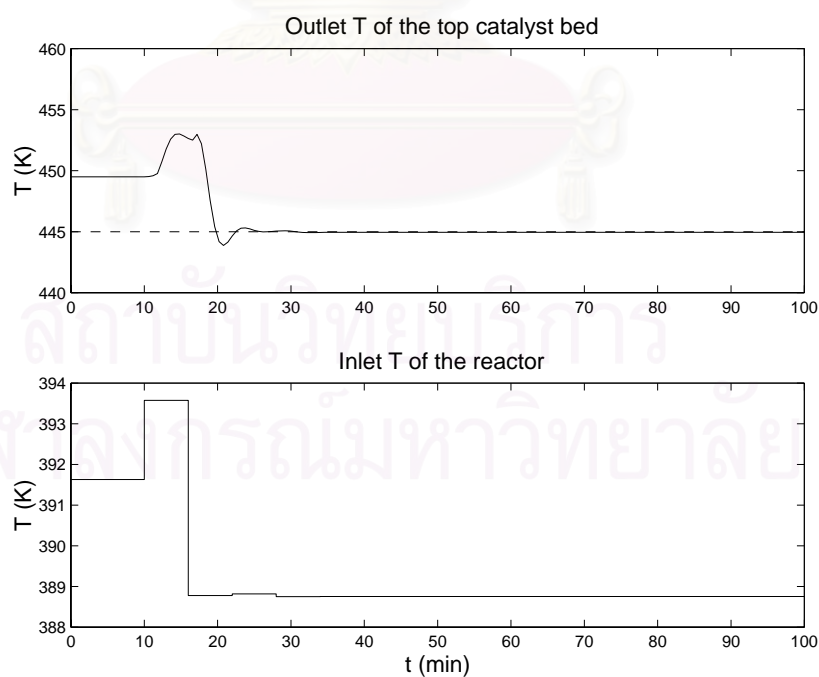
Figure 6.16: Control response of the MPC controller for set point tracking ($T^{sp} = 445$ K) with a mismatch in $k_{0,1}$ (20 % decrease)
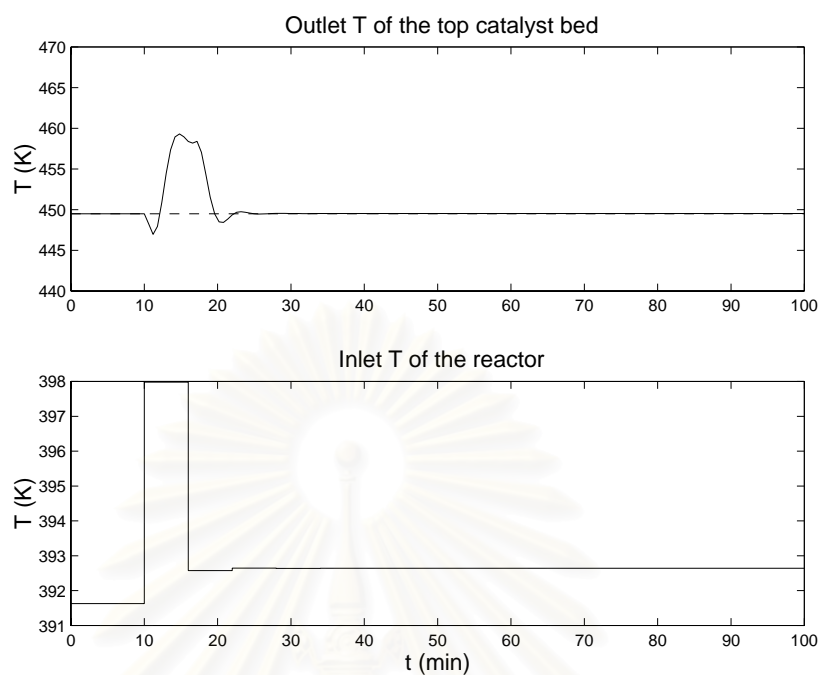
Figure 6.17: Control response of the MPC controller for disturbance rejection (20 % increase in feed rate) with a mismatch in $k_{0,1}$ (20 % decrease)
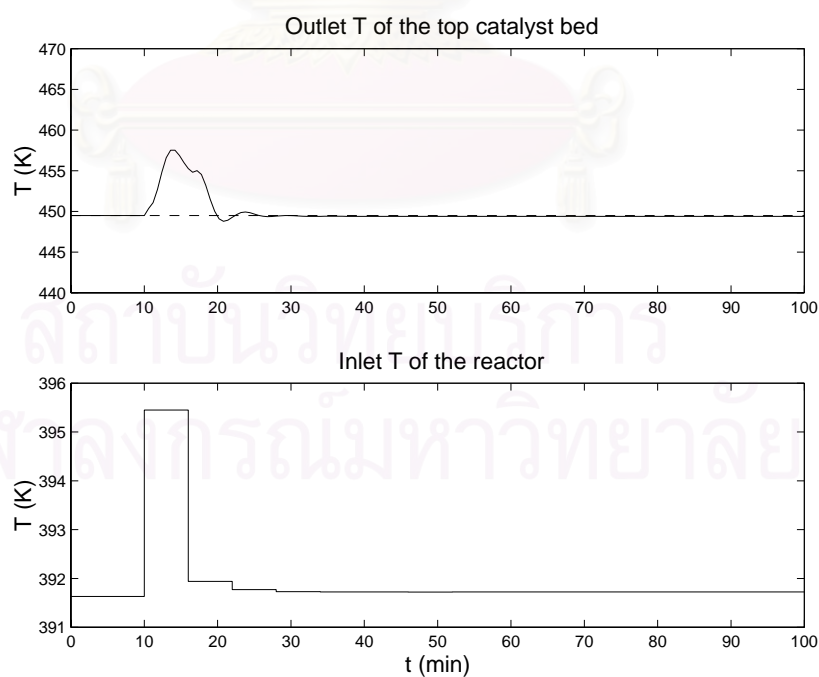
Figure 6.18: Control response of the MPC controller for disturbance rejection (20 % decrease in feed rate) with a mismatch in $k_{0,1}$ (20 % decrease)

Chapter 7

Conclusions

The objective of this research is to develop and implement an advanced control scheme for the control of a trickle bed reactor which is typically characterized by high nonlinearity and spatial variation, and naturally modeled by a system of nonlinear partial differential equations (PDEs). Controlling such a system is known to be difficult and provides a challenging problem. This motivates the need of an efficient control algorithm.

The work presented in this thesis studies on a model predictive control (MPC) to control the trickle bed reactor where hydrogenation of pyrolysis gasoline, a byproduct from an olefin plant, is chosen as an illustrative case study. Since the MPC controller uses a model of the process to be controlled in its algorithm to determine manipulated variables, the modeling of the process is of importance. Therefore, a mathematical model of the trickle bed reactor is developed. The model is identified with data obtained from a real industrial plant. This model representation is then used to design the MPC strategy.

In addition to applying the MPC method to the trickle bed reactor, the implementation of MPC to other reactor systems: a batch and a continuous chemical reactor, is investigated.

The main issues studied in this research are summarized below.

7.1 Trickle Bed Reactor Modeling

A dynamic model for an industrial adiabatic trickle bed reactor in which catalytic hydrogenation of a pyrolysis gasoline from an olefin production plant occurs, has been

developed in this work. To reduce the complexity of the multi-component system, the model developed assumes that all hydrocarbon components in the system are lumped into three pseudocomponents: diolefins, olefins and paraffins. The dynamic model results in a system of partial differential equations which is solved numerically by the method of lines. The orthogonal collocation method is used to discretize the spatial derivative term.

An optimization problem was formulated to find kinetic parameters based on the industrial plant data. The reactor model with the estimated kinetic parameters was validated with plant data. It was observed that although the model contained some simplifying assumptions, it was found to be in good agreement with plant data; the model gave a good prediction of temperature and lumped components in the reactor. This showed that the model can reliably represent the real system and can be used to formulate a model-based control technique to control the reactor.

7.2 MPC for Chemical Reactors

7.2.1 Batch Reactor

Since batch reactors are generally applied to produce a wide variety of specialty products, there is a great deal of interest to enhance batch operation to achieve high quality and purity product while minimizing the conversion of undesired by-product. The use of process optimization in the control of batch reactors presents a useful tool for operating batch reactors efficiently and optimally. In this research, an approach based on the idea of MPC, an on-line dynamic optimization strategy, was employed to modify optimal temperature set point profile for batch reactors.

Two different optimization problems concerning batch operation: maximization of product concentration and minimization of batch time, were considered. An extended Kalman filter (EKF) was incorporated into the proposed approach in order to update current states from their delayed measurements and to estimate unmeasurable state variables. A nonlinear model-based controller: a generic model control algorithm (GMC) was applied to drive the temperature of the batch reactor following the desired

profile. A batch reactor with complex exothermic reaction scheme was used to demonstrate the effectiveness of the proposed approach. The simulation results indicated that with the proposed strategy, large improvement in batch reactor performance, in term of the amount of a desired product and batch operation time, could be achieved compared to the method that optimal temperature set point is pre-determined.

7.2.2 Continuous Reactor

This research addresses the implementation of a MPC and a dual mode MPC strategy integrating the MPC with a local linear control method to control the product concentration in a continuous stirred tank reactor (CSTR), where a single exothermic reaction is carried out.

For safe reactor operation, a reactor temperature path constraint was also considered in the MPC formulation. Two well developed linear controllers: state feedback linearizing control (SFC) and proportional-integral-derivative control (PID) techniques were studied within the dual mode control framework. An extended Kalman filter (EKF) was also incorporated into the dual mode MPC to on-line estimate the unmeasured concentration of substances in the CSTR as well as uncertain key model parameters using an available temperature measurement. It has been found via simulation studies that the proposed dual mode MPC, using either the SFC or PID controller, connected with the EKF provides satisfactory control performance for set point tracking problem. The robustness of the controller in the presence of parametric uncertainties is also enhanced by the inclusion of EKF. Moreover, the on-line computational time required by the dual mode MPC is substantially decreased compared to that of an original MPC.

7.2.3 Trickle Bed Reactor

The performance of a MPC strategy for the control of a trickle bed reactor has been investigated. The reactor models developed has been employed in the MPC algorithm and also utilized to represent the real plant for control studies. In this work, the MPC

controller was applied to regulate the temperature at the outlet of top catalyst bed in the trickle bed reactor. Simulation studies were performed in set point tracking as well as disturbance rejection cases under the nominal condition in which all model parameters are specified correctly.

The results have demonstrated that the MPC controller is able to stabilize the reactor. It can control the reactor temperature at its desired set point in both set point tracking and disturbance rejection cases, and provide a better control performance when compared with a PID controller.

The robustness property of the MPC controller has also been examined with respect to model mismatchs i.e. changes in heat of reaction and reaction rate constant. It has been shown that the MPC controller can successfully control the reactor temperature at the desired set point for both set point tracking and disturbance rejection studies in the presence of model mismatch.

References

Afonso, P. A., Oliveira, M. C. and Castro, J. A. (1996) Model predictive control of a pilot plant reactor with a simulated exothermic reaction. **Computers and Chemical Engineering** 20(suppl.): s769-s774.

Ahn, S. M., Park, M. J. and Rhee, H. K. (1999) Extended Kalman filter-based nonlinear model predictive control for a continuous MMA polymerization reactor. **Industrial and Engineering Chemistry Research** 38: 3942-3949.

Ali, E. E. and Elnashaie, S. E. (1997) Nonlinear model predictive control of industrial type IV fluid catalystic cracking (FCC) units for maximum gasoline yield. **Industrial and Engineering Chemistry Research** 38: 389-398.

Allgower, F. and Ogunnaike, B. A. (1997) Dual-mode adaptive control of nonlinear processes. **Computers and Chemical Engineering** 21(suppl.): s155-s160.

Armaou, A. and Christofides, P. D. (2002) Dynamic optimization of dissipative PDE systems using nonlinear order reduction. **Chemical Engineering Science** 57: 5083-5114.

Arpornwichanop, A. and Kittisupakorn, P. (2002) Dual mode NMPC for regulating the concentration of exothermic reactor under parametric uncertainties. (submitted for publication in Journal of Chemical Engineering of Japan)

Arpornwichanop, A. and Kittisupakorn, P. (2003) Modeling and control of a trickle bed reactor. (in preparation)

Arpornwichanop, A., Kittisupakorn, P. and Hussain, M. A. (2002) Model-based control strategies for a chemical batch reactor with Exothermic Reactions. **Korean Journal of Chemical Engineering** 19: 221-226.

Arpornwichanop, A., Kittisupakorn, P. and Mujtaba, I. M. (2002a) Dynamic modeling of catalytic hydrogenation of pyrolysis gasoline in tickle bed reactor. In J.

Grievink and J. Schijndel (eds.), **Computer Aided Chemical Engineering**, Vol. 10, pp. 421-426. Elsevier.

Arpornwichanop, A., Kittisupakorn, P. and Mujtaba, I. M. (2002b) On-line dynamic optimization and control strategy for improving the performance of batch reactors. (submitted for publication in Chemical Engineering and Processing)

Asteasuain, M., Tonelli, S. M., Brandolin, A. and Bandoni, J. A. (2001) Dynamic simulation and optimization of tubular polymerization reactors in gPROMS. **Computers and Chemical Engineering** 25: 509-515.

Aziz, N., Hussain, M. A. and Mujtaba, I. M. (2000) Performance of different types of controllers in tracking optimal temperature profiles in batch reactors. **Computers and Chemical Engineering** 24: 1069-1075.

Aziz, N., Hussain, M. A. and Mujtaba, I. M. (2001) Optimal control of batch reactor: comparison of neural network based GMC and inverse model control approach. **Proceedings of 6th World Congress of Chemical Engineering**, Melbourne, Australia.

Aziz, N. and Mujtaba, I. M. (2002) Optimal operation policies in batch reactors. **Chemical Engineering Journal** 85: 313-325.

Bequette, B. W. (1991) Nonlinear control of chemical processes: a review. **Industrial and Engineering Chemistry Research** 30: 1391-1413.

Berber, R. (1996) Control of batch reactors: a review. **Trans IChemE.** 74(Part A): 3-20.

Biegler, L. T. (1984) Solution of dynamic optimization problems by successive quadratic programming and orthogonal collocation. **Computers and Chemical Engineering** 8: 243-248.

Bitmead, R. R., Gevers, M. and Wertz, V. (1990) **Adaptive optimal control - the thinking man's GPC.** New York: Prentice Hall.

Bojkov, B. and Luus, R. (1994) Time-optimal control by iterative dynamic programming. **Ind. Eng. Chem. Res.** 33: 1486-1492.

Bonvin D. (1998) Optimal operation of batch reactors - a personal view. **Journal of Process Control** 8: 355-368.

Boskovic, D. M. and Krstic, M. (2002) Backstepping control of chemical tubular reactors. **Computers and Chemical Engineering** 26: 1077-1085.

Bressa, S. P., Alves, J. A., Mariani, N. J., Martinez, O. M. and Barreto, G. F. (2003) Analysis of operating variables on the performance of a reactor for total hydrogenation of olefins in a C_3-C_4 stream. **Chemical Engineering Journal** 92: 41-54.

Carey, G. G. and Finlayson, B. A. (1975) Orthogonal collocation on finite elements. **Chemical Engineering Science** 30: 587-596.

Carvantes, A. and Biegler, L. T. (1999) Optimization strategies for dynamic systems. In C. Floudas and P. Pardalos (Eds), **Encyclopedia of Optimization**, Kluwer Acadamic Publishers.

Chaudhari, R. V., Jaganathan, R., Mathew, S. P., Julcour, C. and Delmas, H. (2002) Hydrogenation of 1,5,9-Cyclododecatriene in fixed-bed reactors: down- vs. up-flow modes. **AIChE Journal** 48: 110-124.

Chen, C. L. (1988) **A class of successive quadratic programming methods for flowsheet optimization.** Doctoral dissertation, Department of Chemical Engineering and Chemical Technology, Imperial College of Science and Technology, University of London.

Chen, H. and Allgower, F. (1998a) A computationally attractive nonlinear predictive control scheme with guaranteed stability for stable systems. **Journal of Process Control** 8: 475-485.

Chen, H. and Allgower, F. (1998b) A quasi-infinite horizon nonlinear model predictive control scheme with guaranteed stability. **Automatica** 34: 1205-1218.

Chen, H. and Allgower, F. (1998c) Nonlinear model predictive control schemes with guaranteed stability. In R. Berber and C. Kravaris (eds), **Nonlinear Model Based Process Control**, Kluwer Acadamic Publishers.

Chen, C. and Shaw, L. (1982) On receding horizon feedback control. **Automatica** 18: 349-352.

Cheng, Y. M., Chang, J. R. and Wu, J. C. (1986) Kinetic study of pyrolysis gasoline hydrogenation over supported palladium catalyst. **Applied Catalysis** 24: 273-285.

Christofides, P. and Daoutidis, P. (1996) Feedback control of hyperbolic PDE systems. **AIChE Journal** 42: 3063-3086.

Christofides, P. and Daoutidis, P. (1998) Robust control of hyperbolic PDE systems. **Chemical Engineering Science** 53: 85-105.

Christofides, P. (2001) **Nonlinear and robust control of partial differential equation systems: methods and applications to transport-reaction processes.** Boston: Birkhauser.

Cott, B. J. and Macchietto, S. (1989) Temperature control of exothermic batch reactors using generic model control. **Industrial and Engineering Chemistry Research** 28: 1177-1184.

Cuthrell, J. E. and Biegler, L. T. (1987) On the optimization of differential-algebraic process systems. **AIChE Journal** 33: 1257-1270.

Dadebo, S. A. and Mcauley, K. B. (1995) Dynamic optimization of constrained chemical engineering problems using dynamic programming. **Computers and Chemical Engineering** 19: 513-525.

Derrien, M. L. (1986) Selective hydrogenation applied to the refining of petrochemical raw material produced by steam cracking. In: Stud. Surf. Sci. Catal. 27, L. Carveny (Ed.), **Catalytic Hydrogenation**, pp. 613-655. Elsevier.

Derrien, M. L., Andrews, J. W., Bonnifay, P. and Leonard, J. (1974) Selective hydrogenation process. **Chemical Engineering Progress** 70: 74-80.

Devetta, L., Canu, P., Bertucco, A. and Steiner, K. (1997) Modelling of a trickle-bed reactor for a catalytic hydrogenation in supercritical CO_2. **Chemical Engineering Science** 52: 4163-4169.

Dochain, D., Maamar, N. T. and Babary, J. P. (1997) On modeling, monitoring and control of fixed bed bioreactors. **Computers and Chemical Engineering** 21: 1255-1266.

Dudukovic, M. P., Larachi, F. and Mills, P. L. (1999) Multiphase reactors - revisited. **Chemical Engineering Science** 54: 1975-1995.

Eaton, J. W. and Rawlings, J. B. (1990) Feedback control of chemical processes using on-line optimization techniques. **Computers and Chemical Engineering** 14: 469-479.

Edgar, T. F. and Himmelblau, D. M. (1989) **Optimization of chemical processes.** McGraw-Hill.

Feehery, W. F. (1998) **Dynamic optimization with path constraints.** Doctoral dissertation, Department of Chemical Engineering, Massachusetts Institute of Technology.

Fikar, M., Latifi, M. A., Fournier, F. and Creff, Y. (1998) Control vector parameterisation versus iterative dynamic programming in dynamic optimisation of a distillation column. **Computers and Chemical Engineering** 22(suppl.): s625-s628.

Garcia, C. E., Pret, D. M. and Morari, M. (1989) Model predictive control: theory and practice - a survey. **Automatica** 25: 335-348.

Genceli, H. and Nikolaou, M. (1993) Robust stability analysis of constrained l1-norm model predictive control. **AIChE Journal** 39: 1954-1965.

Gentric, C., Pla, F., Latifi, M. A. and Corriou, J. P. (1999) Optimization and nonlinear control of a batch emulsion polymerization reactor. **Chemical Engineering Journal** 75: 31-46.

Gianetto, A. and Specchia, V. (1992) Trickle-bed reactors: state of art and perspectives. **Chemical Engineering Science** 47: 3197-3213.

Gill, P. E., Murray, W. and Saunders, M. A. (1998) User's guide for SNOPT 5.3: a fortran package for large-scale nonlinear programming.

Hanczyc, E. M. and Palazoglu, A. (1995) Sliding mode control of nonlinear distributed parameter chemical processes. **Industrial and Engineering Chemistry Research** 34: 557-566.

Hanika, J. and Lange, R. (1996) Dynamic aspects of adiabatic trickle bed reactor control near the boiling point of reaction mixture. **Chemical Engineering Science** 51: 3145-3150.

Hanika, J., Sporka, K, Ruzicka, V. and Pistek, R. (1977) Dynamic behavior of an adiabatic trickle bed reactor. **Chemical Engineering Science** 32: 525-528.

Henson, M. A. (1998) Nonlinear model predictive control: current status and future directions. **Computers and Chemical Engineering** 23: 187-202.

Herskowitz, M and Smith, J. M. (1983) Trickle-bed reactors: a review. **AIChE Journal** 29: 1-18.

Hofmann, H. (1977) Hydrodynamics, transport phenomena, and mathematical models in trickle-bed reactors. **International Chemcial Engineering** 17: 19-28.

Hua, X. and Jutan, A. (2000) Nonlinear inferential cascade control of exothermic fixed-bed reactors. **AIChE Journal** 46: 980-996.

Ju, J. Chiu, M. S. and Tien, C. (2000) Multiple-objective based model predictive control of pulse jet fabric filters. **Trans IChemE.** 78 (Part A): 581-589.

Keerthi, S. and Gilbert, E. (1988) Optimal, infinite-horizon feedback laws for a general class of constrained discrete-time systems. **J. Optimiz. Th. Appl.** 57: 265-293.

Kravaris, C., Wright, R. A. and Carrier, J. F. (1989) Nonlinear controller for trajectory tracking in batch processes. **Computers and Chemical Engineering** 13: 73-82.

Kershenbaum, L. S. and Kittisupakorn, P (1994) The use of a partially simulated exothermic (PARSEX) reactor for experimental testing of control algorithms. **Trans IChemE.** 72(Part A): 55-63.

Kittisupakorn, P. (1995) **The use of nonlinear model predictive control techniques for the control of a reactor with exothermic reactions.** Doctoral dissertaion, Department of Chemical Engineering and Chemical Technology, Imperial College of Science and Technology, University of London.

Kittisupakorn, P. and Arpornwichanop, A. (1999) Modeling of a trickle bed reactor for gasoline hydrogenation process. **AIChE Annual Meeting.** Dallas, USA.

Korsten, H. and Hoffmann, U. (1996) Three-phase reactor model for hydrotreating in pilot trickle-bed reactors. **AIChE Journal** 42: 1350-1360.

Lee, P. L. and Sullivan, G. R. (1988) Generic model control (GMC). **Computers and Chemical Engineering** 12: 573-580.

Lee, T. T., Wang, F. Y., Islam, A. and Newell, R. B. (1999) Generic distributed parameter model control of a biological nutrient removal (BNR) activated sludge process. **Journal of Process Control** 9: 505-525.

Limqueco, L. C. and Kantor, J. C. (1990) Nonlinear output feedback control of an exothermic reactor. **Computers and Chemical Engineerign** 14: 427-437.

Liptak, B. G. (1986) Controlling and optimization chemical reactors. **Chemical Engineering** 5: 69-81.

Liu, Z. H. and Macchietto (1995) Model based control of a multipurpose batch reactor - an experimental study. **Computers and Chemical Engineering** 19(suppl.): s477-s482.

Loeblein, C., Perkins, J. D., Srinivasan, B. and Bonvin, D. (1997) Performance analysis of on-line batch optimization systems. **Computers and Chemical Engineering** 21(suppl.): s867-s872.

Luus, R. (1990) Optimal control by dynamic programming using systematic reduction in grid size. **Int. J. Control** 51: 995-1013.

Luus, R. (1996) Numerical convergence properties of iterative dynamic programming when applied to high dimensional systems. **Trans IChemE.** 74(Part A): 55-62.

Maner, B. R., Doyle, F. J., Ogunnaike, B. A. and Person, R. K. (1996) Nonlinear model predictive control of a simulated multivariable polymerization reactor using second-order Volterra models. Automatica 32: 1285-1301.

Mayne, D. Q., Rawlings, J. B., Rao, C. V. and Scokaert, P. O. M. (2000) Constrainted model predictive control: stability and optimality. **Automatica** 36: 789-814.

Mayne, D. Q. and Michalska, H. (1990) Receding horizon control of nonlinear systems. **IEEE Transaction on Automatic Control** 35: 814-824.

Mcauley, K. B. and Macgregor, J. F. (1992) Optimal grade transitions in a gas phase polyethylene reactor. **AIChE Journal** 38: 1564-1576.

Meadows, E. S. and Rawlings, J. B. (1997) Model predictive control. In M. A. Henson and D. E. Sebord (Eds), **Nonlinear Process Control**, pp. 223-310, Prentice Hall.

Michalska, H. and Mayne, D. Q. (1993) Robust receding horizon control of constrained nonlinear systems. **IEEE Transaction on Automatic Control** 38: 1623-1633.

Morari, M. and Lee, J. H. (1999) Model predictive control: past, present and future. **computers and Chemical Engineering** 23: 667-682.

Morison, K. R. (1984) **Optimal control of process described by systems of differential and algebraic equation.** Doctoral dissertaion, Department of Chemical Engineering and Chemical Technology, Imperial College of Science and Technology, University of London.

Muske, K. R. and Edgar, T. F. (1997) Nonlinear state estimation. In M. A. Henson and D. E. Seborg (Eds), **Nonlinear process control**, pp. 311-370. Prentice-Hall.

Nevistic,V. (1997) **Constrained control of nonlinear systems.** Doctoral dissertation, Swiss Federal Institute of Technology.

Ng, K. M. and Chu, C. F. (1987) Trickle-bed reactors. **Chemical Engineering Progress** pp. 55-63.

Nicolao, G., Magni, L. and Scattolini, R. (1996) Robust predictive control of systems with uncertain impulse constraints. **Automatica** 32: 1475-1479.

Nicolao, G., Magni, L. and Scattolini, R. (2000) Stability and robustness of nonlinear receding horizon control. In F. Allgower and A. Zheng (Eds), **Nonlinear model predictive control**, pp. 3-22. Birkhauser Verlag.

Norquay, S. J., Palazoglu, A. and Romagnoli, J. A. (1999) Application of Wiener model predictive control (WMPC) to an industrial C2-splitter. **Journal of Process Control** 9: 461-473.

Patwardhan, A. A., Wright, G. T. and Edgar, T. F. (1992) Nonlinear model predictive control of distributed parameter systems. **Chemical Engineering Science** 47: 721-735.

Petzold, L. R. (1982) A description of DASSL: a differential/algebraic system solver. SAND82-8637, Sandia national laboratories.

Primbs, J. A. and Nevistic, V. (1998) A framework for robustness analysis of constrained finite receding horizon control. In: **Proceedings of the American Control Conference**, pp.2718-2722.

Qin, S. J. and Badgwell, T. A. (1997) An overview of industrial model predictive control technology. In J. C. Kantor, C. E. Garcia, and B. Carnahan (Eds), **Chemical Process Control V**, pp. 232-256. AIChE.

Qin, S. J. and Badgwell, T. A. (2000) An overview of nonlinear model predictive control applications. In F. Allgower and A. Zheng (Eds), **Nonlinear Model Predictive Control**, pp. 369-392. Birkhauser.

Qin, S. J., Martinez, V. M. and Foss, B. A. (1997) An interpolating model predictive control strategy with application to a waste treatment plant. **Computers and Chemical Engineering** 21(suppl.): s881-886.

Ramachandran, P. A. and Chaudhari, R. V. (1983) **Three-phase catalytic reactors** Gordon and Breach Science Publishers.

Ramirez, W. F. (1994) **Process control and identification.** Academic Press.

Rawlings, J. B. (2000) Totorial overview of model predictive control. **IEEE Control Systems Magazine** June: 38-52.

Rawlings, J. B. and Muske, K. R. (1993) The stability of constrained receding horizon control. **IEEE Transaction on Automatic Control** 38: 1512-1516.

Ray, W. H. (1981) **Advanced process control.** New York: McGraw Hill.

Renfro, J. G., Morshedi, A. M. and Asbjornsen, O. A. (1987) Simultaneous optimization and solution of systems described by differential/algebraic equations. **Computers and Chemical Engineering** 11: 503-517.

Renou, S., Perrier, M. and Dochain, D. (2001) Concentration control in a tubular reactor by a late lumping approach. **Proceedings of 6th World Congress of Chemical Engineering**, Melbourne, Australia.

Richalet, J. (1993) Industrial applications of model based predictive control. **Automatica** 29: 1251-1274.

Rotstein G. E. and Lewin D. R. (1992) Control of an unstable batch chemical reactor. **Computers and Chemical Engineering** 16: 27-49.

Ruppen, D., Bonvin, D. and Rippin, D. W. T. (1998) Implementation of adaptive optimal control operation for a semi-batch reaction system. **Computers and Chemical Engineering** 22: 185-189.

Satterfield, C. N. (1975) Trickle-bed reactors. **AIChE Journal** 21: 209-228.

Scokaert, P. and Rawlings, J. B. (1996) Infinite horizon linear quadratic control with constraints. In **IFAC 13th Triennal World Congress** vol.M, pp. 109-114.

Seborg, D. E., Edgar, T. F. and Mellichamp, D. A. (1989) **Process dynamics and control.** John Wiley & Sons.

Seki, H., Ogawa, M., Ooyama, S., Akamatsu, K., Ohshima, M. and Yang, W. (2002) Industrial application of a nonlinear model predictive control to polymerization reactors. **Control Engineering Practice** 9: 819-828.

Semino, D., Morretta, M. and Scali, C. (1996) Parameter estimation in extended kalman filters for quality control in polymerization reactors. **Computers and Chemical Engineering** 20(suppl.): s913-s918.

Shah, Y. T. (1979) **Gas-liquid-solid reactor design.** McGraw Hill.

Shen, J. X., Chiu, M. S. and Wang, Q. G. (1999) A comparative study of model-based control techniques for batch crystallization process. **Journal of Chemical Engineering of Japan** 32: 456-464.

Sistu, P. B. and Bequette, B. W. (1991) Nonlinear predictive control of uncertain processes: application to a CSTR. **AIChE Journal** 37: 1711-1723.

Somer, A., Shah, Y. T. and Paraskos, J. (1976) Kinetics of diolefin hydrogenation in a trikle bed reactor. **Chemical Engineering Science** 31: 759-765.

Soroush, M. (1998) State and parameter estimation and their applications in process control. **Computers and Chemical Engineering** 23: 229-245.

Tarhan, O (1983) **Catalytic reactor design.** McGraw Hill.

Tsang, T. H., Himmelblau, D. M. and Edgar, T. F. (1975) Optimal control via collocation and non-linear programming. **Int. J. Control** 21: 763-768.

Villadsen, J. and Michelsen, M. L. (1978) **Solution of differential equation models by polynomial approximation.** Prentice-Hall.

Yuce, S., Hasaltun, A., Erdogan, S. and Alpbaz, M. (1999) Temperature control of a batch polymerization reactor. **Trans IChemE.** 77(Part A): 413-420.

Warna, J. and Salmi, T. (1996) Dynamic modelling of catalytic three phase reactors. **Computers and Chemical Engineering** 20: 39-47.

Wu, W. and Liou, C. T. (2001) Output regulation of nonisothermal plug-flow reactors with inlet perturbations. **Computers and Chemical Engineering** 25: 433-443.

Zhan, J. and Ishida, M. (1997) The multi-step predictive control of nonlinear SISO process with a neural modle predictive control (NMPC) method. **Computers and Chemical Engineering** 21: 201-210.

Zheng, A. and Morari, M. (1993) Robust stability of constrained model predictive control. **Proceedings of the American Control Conference**, pp. 379-383.

Zhukova, T. B., Pisarenko, V. N. and Kafarov, V. V. (1990) Modeling and design of industrial reactors with a stationary bed of catalyst and two-phase gas-liquid flow - a review. **Internation Chemical Engineering** 30: 57-122.
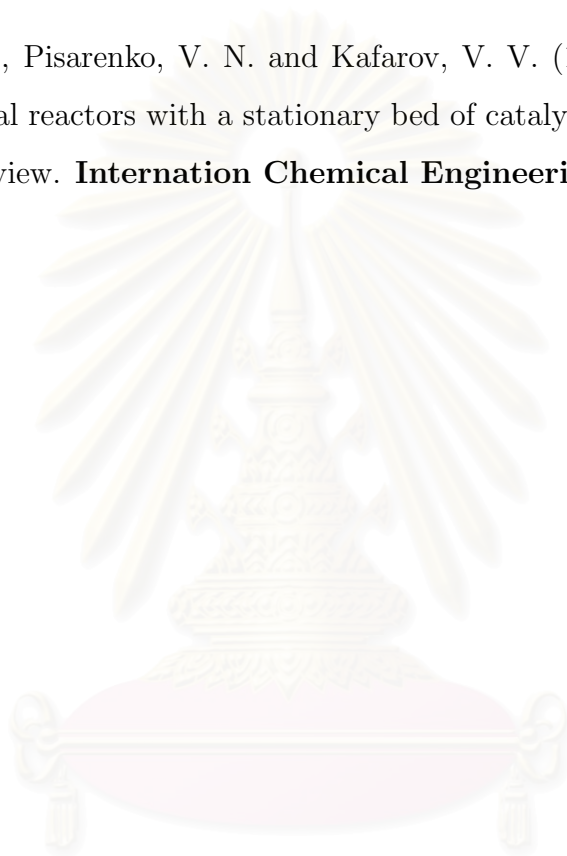
Appendices

Appendix A

Open-Loop Optimal Control: Basic Solutions

An optimal control can be defined as a class of modern control technique that determines a set of control variable profiles (optimal control policy) for systems, such that a given performance criteria is optimized. This appendix gives a brief overview in a basic solution of the optimal control problem. Two basic solution methods: the calculus of variation and dynamic programming approach, are introduced.

Let us consider the optimal control problem in which the initial time and initial state variables are given; the final time is fixed; the states at the final time is free. This problem can be stated mathematically as: find the control $u(t)$ minimizing the objective function:

$$\min_{u(t)} J = \int_t^{t_f} F(x, u, t) dt \tag{A.1}$$

subject to dynamic process models:

$$\dot{x} = f(x, u, t) \tag{A.2}$$

$$x(t_0) = x_0 \tag{A.3}$$

$$t \in [t_0, t_f] \tag{A.4}$$

A.1 Variation Approach

The first approach to a solution of the optimal control is described here. The variation approach is known as an indirect method because it focuses on obtaining the solution of necessary conditions, which lead to a two-point boundary value problem, for optimality

rather than solving the optimization directly. These conditions can be developed for the optimal control problem through the use of the classic calculus of variation.

A.1.1 Necessary Conditions for Optimality

Since the basic concept of the variation approach is based on the solution of the optimality necessary conditions that determine the optimal control, u(t), we first need to develop these conditions.

To solve the optimal control problem (Equations (A.1) to (A.4)), a lagrange multiplier is defined and used to augment the dynamic model constraint (Equation (A.2)) to the objective. Thus, the augmented objective performance is:

$$J_A = \int_{t_0}^{t_f} \left[F(x, u, t) + \lambda^T(t) \left(f(x, u, t) - \dot{x} \right) \right] dt \tag{A.5}$$

where $\lambda(t)$ is the lagrange multiplier which is a function of time. This variable is also known as an adjoint or costate variable.

At this stage, the original control problem consisting of the performance index (Equation (A.1)) and process model constraint (Equation (A.2)) has been converged to the problem without constraint (Equation (A.5)); however, the solution of the augmented objective still has the same as in the original problem.

For convenience, the Hamiltonian is defined as:

$$H(\dot{x}, x, u, \lambda, t) = F(x, u, t) + \lambda^T(t) \left[f(, x, u, t) - \dot{x} \right] \tag{A.6}$$

Deriving the necessary conditions, the first variation of the objective function is essential to be defined. To compute the first variation, we first consider the increment of the function by introducing the variation, $\delta \dot{x}$, δx, δu, $\delta \lambda$, and δt_f into the objective:

$$J_A = \int_{t_0}^{t_f} H(\dot{x}, x, u, \lambda, t) dt \tag{A.7}$$

Therefore, the increment of the function is:

$$\Delta J = \int_{t_0}^{t_f} H(x + \delta \dot{x}, x + \delta x, u + \delta u, \lambda + \delta \lambda, t) dt - \int_{t_0}^{t_f} H(\dot{x}, x, u, \lambda, t) dt \tag{A.8}$$

Expanding the increment in a Taylor series about $H(\dot{x}, x, u, \lambda)$, the first variation, which is the linear part of the increment in $\delta\dot{x}$, δx, δu, $\delta\lambda$, and δt_f becomes

$$
\delta J_A = \int_{t_0}^{t_f} \left(\frac{\partial H}{\partial x} - \frac{d}{dt}\frac{\partial H}{\partial \dot{x}}\right)^T \delta x dt + \left(\frac{\partial H}{\partial \dot{x}}(t_f)\right)^T \delta x(t_f) - \left(\frac{\partial H}{\partial \dot{x}}(t_0)\right)^T \delta x(t_0)
$$
$$
+ \int_{t_0}^{t_f} \left(\frac{\partial H}{\partial \lambda}\right)^T \delta\lambda dt + \int_{t_0}^{t_f} \left(\frac{\partial H}{\partial u}\right)^T \delta u dt \tag{A.9}
$$

The fundamental theorem of the calculus of variations states that the first-order necessary conditions for an optimum u of the function J_A can be found by setting the variation of J_A equal to zero. Therefore, from Equation (A.9), we have:

$$
0 = \int_{t_0}^{t_f} \left[\frac{\partial H}{\partial x} - \frac{d}{dt}\left(\frac{\partial H}{\partial \dot{x}}\right)\right] \delta x dt + \left(\frac{\partial H}{\partial \dot{x}}(t_f)\right) \delta x(t_f) - \left(\frac{\partial H}{\partial \dot{x}}(t_0)\right) \delta x(t_0)
$$
$$
+ \int_{t_0}^{t_f} \left(\frac{\partial H}{\partial \lambda}\right) \delta\lambda dt + \int_{t_0}^{t_f} \left(\frac{\partial H}{\partial u}\right) \delta u dt \tag{A.10}
$$

Equation (A.10) is satisfied if the following equations are hold.

$$
\frac{\partial H}{\partial x} - \frac{d}{dt}\left(\frac{\partial H}{\partial \dot{x}}\right) = 0 \tag{A.11}
$$

$$
\frac{\partial H}{\partial \lambda} = 0 \tag{A.12}
$$

$$
\left(\frac{\partial H}{\partial \dot{x}}(t_f)\right) \delta x(t_f) - \left(\frac{\partial H}{\partial \dot{x}}(t_0)\right) \delta x(t_0) = 0 \tag{A.13}
$$

$$
\frac{\partial H}{\partial u} = 0 \tag{A.14}
$$

The above equations are the necessary conditions to determine the optimal control u that minimizes the performance index (Equation (A.1)) subject to system models (Equation (A.2)). The condition of Equation (A.11) is known as *Euler-lagrange equation* whereas Equation (A.13) is often called *the transversality boundary condition* which vary with the specification of $x(t)$ at the initial and final time conditions.

The necessary conditions, Equations (A.11) to (A.14), can be simplified by substituting the Hamiltonian function as follows:

$$
\dot{\lambda} = -\frac{\partial F}{\partial x} - \lambda^T \frac{\partial f}{\partial x} \tag{A.15}
$$

$$
\dot{x} = f(x, u, t) \tag{A.16}
$$

$$x(t_0) \;=\; x_0 \tag{A.17}$$

$$\lambda(t_f) \;=\; 0 \tag{A.18}$$

$$\frac{\partial F}{\partial u} + \lambda^T \frac{\partial f}{\partial u} \;=\; 0 \tag{A.19}$$

It is noted that the necessary conditions for optimality developed here are for the specific case of the optimal control problem in which the objective function is given in the form of Equation (A.1) and the process model equations are represented by a set of ordinary differential equations. Moreover, we assume that the control (manipulated) variables are unconstraint.

It can be seen that the necessary conditions (Equations (A.15) to (A.19)) are expressed in a two-point boundary value problem (TPBVP); that is, the state equations are given at the initial conditions whereas the costate equations are specified at the final conditions. As a result, the solution of the optimal control problem is determined by solving the TPBVP instead. This type of problem can be solved with different numerical strategies e.g. control vector iteration (CVI), single/multi shooting, and invariant embedding method. Most of these methods are generally based on an iterative method that uses an initial guess to find a solution and then updates the initial guess for the next iteration to make the solution satisfy the desired criteria.

A.1.2   Control Vector Iteration (CVI) Method

The control vector iteration (CVI) is one of several methods that have been proposed to solve numerically the optimal control problem through the solution of the optimality necessary conditions. This method requires an iterative integration of the state and costate differential equations. The computational procedure is based on adjusting the estimate of a control function in order to improve the value of the objective function. One advantage of this method is that since the state equations are solved exactly at each step, each iteration produces a feasible solution (Ray, 1981).

A general algorithm of the control vector iteration method can be summarized as follows:

Step 0 Guess the control profile, $u(t)$.

Step 1 Integrate the state equation (Equation (A.16)) forward in time with the initial conditions to produce the value of state, $x(t)$, and the performance index, J_i.

Step 2 Integrate the costate equation (Equation (A.15)) backward in time with the final boundary conditions using the state value from step 1.

Step 3 Update the control $u(t)$ by

$$u_{i+1} = u_i + \delta u$$

Step 4 Check the termination criteria as shown below. If it is satisfied, the computation is stopped. Otherwise, return Step 1.

$$|J_{i+1} - J_i| < e \qquad \text{where } e \text{ is a small positive number.}$$

There are several algorithms that have been used for updating the control u (δu) with this approach. The basic algorithm is known as the steepest descent method. In this method, the gradient of the control u with respect to the objective (Equation (A.14)) is used to find the direction (g_i) for the new control profile while the step length (α_i) can be either kept constant for every iteration or varied form one iteration to the next one. The main disadvantage of this method is that the convergence is quite slow as the minimization is approached. To improve the convergence property, the conjugated gradient method have been developed and chosen as a search direction (Edgar and Himmelblau, 1989). It combines the gradient information from the previous step with that from the current step to obtain a new search direction for the next step.

However, although the convergence property to the solution is improved, the application of the control vector iteration still has an additional difficulty which arises from the requirement of the backward integration of the costate equations, which can be inefficient and unstable.

A.1.3 Single/Multiple Shooting Method

Another method to deal with the solution of the TPBVP derived from the necessary conditions for optimality is the single shooting method. This approach can be divided

into two steps. The first one is to substitute the control u, which may be assumed to be solved explicitly from Equation (A.19), into the costate and state equations (Equations (A.15) and (A.16)). Note that obtaining the explicit solution of u is found in limited simple cases (Ray, 1981).

The next step is to assume the missing initial condition value of the costate equations $[\lambda(t_0)]$ and then integrate the Equations (A.15) and (A.16) in the same direction by differential equation solvers. Consequently, the difficulty from the backward integration is avoided. An updated iteration, e.g. by Newtons method, is applied to adjust the guessed initial value so that the final conditions are equal to the given value. From a procedure in updating the boundary conditions, this method is sometimes referred to *the boundary-condition iteration method*. However, the main limitation of this method is due to a difficulty in choosing reasonable initial guess of the missing conditions and a small region of convergence.

Similarly, the multiple shooting method follows the same idea as the single shooting method, but the integration horizon is divided into small subintervals. In another word, the problem is transformed into a multipoint boundary value problem for both state and costate variables. Therefore, the missing initial conditions are guessed at each subinterval. Newtons type method is also used to updated the new guesses based on the deviation between the guessed and the obtained value at each point. The subintervals in the multiple shooting method cause less nonlinearity and less sensitivity to the guessed values than in the single shooting method.

A.1.4 Invariant Embedding Method

An alternative technique that assumes the structure of the control solution using the Riccati transformation is termed as the invariant embedding method. This special technique is often used in a classical optimal control problem: Linear quadratic regulator (LQR) problem which involve determining the optimal control for a linear system with a quadratic performance function. Solution result from this class of the problem leads to the optimal state feedback control law (Ramirez, 1994).

A.2   Dynamic Programming (DP) Approach

The second class of the optimal control solution, referred as dynamic programming, is presented in this section. This approach is based on the optimality principle which characterizes global optimality in a local sense, using the concept of an optimal value function. This indicates the difference of this approach from the variation approach that views the optimality by utilizing an optimal control trajectory concept.

The optimality principle proposed by Bellman states that if $u^*(t)$ is optimal over the interval $[t, t_f]$, starting at states $x(t)$, then $u^*(t)$ is necessarily optimal over the subinterval $[t + \Delta t, t_f]$ for any Δt such that $0 < \Delta t \leq t_f - t$. The basic assumption under the optimality principle is that the system states $x(t)$ at time t are resulted from the effect of all inputs $u(t)$ prior to time t. This allows for a local characterization of optimality in the formal statement of the optimality principle (Nevistic, 1997).

By using the principle of optimality in the dynamic programming approach, it can derive the Hamilton-Jacobi-Bellman equation which determines the solution of the optimal control problem.

A.2.1   Hamilton-Jacobi-Bellman Equation

Let us now consider the problem determining the optimal control, $u(t)$, that minimizes the objective function of the form:

$$\min_{u(t)} J = \varphi(x(t_f), t_f) + \int_{t_0}^{t_f} F(x, u, t) dt \tag{A.20}$$

subject to a process model:

$$\dot{x} = f(x, u, t) \qquad x_0 = x(t_0) \tag{A.21}$$

The solution of the optimal control problem by dynamic programming approach based on the optimality principle is given as follows. The optimality principle can be used to derive the Hamilton-Jacobi-Bellman equation (HJB) which leads to the solution of the optimal control problem. To develop the HJB equation, the value

function, also called as Bellman's function, is first defined as:

$$V(x,t) = \min_{u(t)} J \tag{A.22}$$

Using the additive properties of integrals and the optimality principle gives:

$$V(x,t) = \min_{u[t,t+\Delta t]} \left(\int_t^{t+\Delta t} F(x,u,t)dt + V\left(x(t+\Delta t), t+\Delta t\right) \right) \tag{A.23}$$

It can be seen from Equation (A.23) that by using the optimality principle, the problem of determining an optimal control over the interval $[t, t_f]$ has been reduced to finding the optimal control over the interval $[t, t+\Delta t]$.

From Equation (A.23), approximating the integral term by $F(x,u,t)\Delta t$ and applying the Taylor series expansion of $V[x(t+\Delta t), t+\Delta t]$ give:

$$-\frac{\partial V}{\partial t} = \min_{u(t)} \left\{ F(x(t), u(t), t) + \left(\frac{\partial V}{\partial x} \right) f(x(t), u(t), t) \right\} \tag{A.24}$$

with the boundary condition: $V(x, t_f) = \varphi(x)$. Equation (A.24) is known as the Hamilton-Jacobi-Bellman equation (HJB) which must hold at the optimum. Nevistic (1997) presented two steps for solving this HJB partial differential equation. First, the minimization problem in Equation (A.24) is performed, leading to a control law:

$$u^* = \phi\left(\frac{\partial V}{\partial x}, x, t \right) \tag{A.25}$$

Then, substituting u^* into Equation (A.24) gives:

$$-\frac{\partial V}{\partial t} = F(x, \phi, t) + \left(\frac{\partial V}{\partial x} \right) f(x, \phi, t) \tag{A.26}$$

The solution of this nonlinear partial differential equation gives a value of $V(x,t)$ as the function of x and t. So we can produce the control law u^* by computing the gradient of $V(x,t)$ and replacing it in Equation (A.25).

As shown above, the optimal control solution through the dynamic programming approach is obtained by the solution of the HJB equation expressed by partial differential equations (PDEs). It is well known that to solve such PDEs is a very difficult task especially when the system dimension is high; the computational load increases rapidly

with the number of state variables. The solution of the HJB equation is possible only for a simple control problem e.g. the linear quadratic regulator problem (LQR) in which the process is represented by a linear model system and the performance index is in a quadratic form.

However, in the last decade, a reliable numerical method, an iterative dynamic programming, has been proposed as another choice to solve the optimal control problem. This method applies the optimality principle to approximate the solution of the original control problem with a finite dimension optimization instead of obtaining the optimal control solution by solving the HJB equation as in the dynamic programming approach.

A.2.2 Iterative Dynamic Programming (IDP)

Another class of the method that has been developed to solve the optimal control problem is known as an iterative dynamic programming (IDP). The basic concept of the IDP method introduced by Luus (1990) is still based on the optimality principle.

In the iterative dynamic programming, it is assumed that the given final time (t_f) is divided into P subintervals with equal length. In each subinterval, the control variables can be generally represented either as a piecewise constant or a piecewise linear function. Applying the principle of optimality as stated earlier, the last subinterval is optimized first. After the optimal control is determined, the preceding interval is optimized based on the control obtaining from the last stage. This process is repeated in a backward direction until t = 0. As described, this technique concentrates on obtaining the optimal control u_i for each subinterval starting from the last one instead of finding the optimal control for all stages simultaneously.

The simplified algorithm of the iterative dynamic programming with the piecewise constant control is concluded as:

Step 1 Divide the time interval $[0, t_f]$ into P time stages with equal length L.

Step 2 Choose the number of allowable values R for control variables.

Step 3 Choose the initial value for each u_i, the initial region size r_i, the contraction factor γ, and the number of iterations to be used.

Step 4 Integrate the system from $t = 0$ to $t = t_f$ to generate the state profile using the initial trajectory as specified in Step 3 and store the value of the states at the beginning of each time stage.

Step 5 Starting from the stage P, integrate the system for $t = t_f - L$ to $t = t_f$ using the initial state value at the stage $P - 1$ from Step 4 with each of the allowable value for the control. Choose the control $u_P - 1$ that gives the minimum value of the objective and store this value.

Step 6 Step back to the stage $P - 1$, corresponding to $t = t_f - 2L$. For each allowable value of $u_P - 2$, integrate the system by using the initial value of the state at $P - 2$ obtaining from Step 4. Continue integration until $t = t_f$. During $t = t_f - L$ to $t = t_f$ use the control value $u_P - 1$ from Step 5. Choose the $u_P - 2$ minimizing the performance index.

Step 7 Continue the procedure until the stage 1, corresponding to the initial time $t = 0$

Step 8 Reduce the region for the allowable control, $r^{k+1} = \gamma r^k$, where k is an interation index. Use the optimal control policy from step 7 as the initial values for u at each stage.

Step 9 Increase the iteration index and go to Step 5. Continue the procedure for a specified number of iterations and examine the result.

Based on this basic algorithm, the iterative dynamic programming can be applied to solve a broad class of control problems. The IDP is an attractive alternative and well suited because of its simplicity and high reliability of obtaining the optimal control solution. However, this algorithm cannot directly cope with the effect of constraints on state variables. To include them in the IDP, a penalty function approach, one of effective ways, is used to penalize the constraint violation on the objective function; however, it may result in poor convergence property and lead to unsatisfactory solution

especially when a penalty term and a weighting factor are chosen inappropriately. The penalty term can be represented in several forms e.g. quadratic functions, absolution values and others. Nevertheless, it has been seen that the choice of this penalty function for optimal control problems in which state constraints are included has not been addressed (Dadebo and Mcauley, 1995).

The convergence property of the IDP is another important issue which should have to be considered. Since the lack of the sensitivity of objective function with respect to control variables may cause difficulties to find the optimal control solution. Luus (1996), therefore, studied the IDP convergence property by considering on high dimensional systems. In addition, they also investigated an effect of the parameters such as a number of allowable control value (R) and the contraction region (γ) to the optimal solution, in the IDP algorithm. The simulation results showed that the convergence of the IDP is found to be systematic. They also stressed on the importance of such parameters in the IDP to improve the computational time. Further works investigating on the convergence property of IDP for other systems can be found in e.g. Bojkov and Luus (1994) and Fikar et al. (1998).

Appendix B

Orthogonal Collocation Method

The orthogonal collocation method is one of several methods of weighted residuals which are used to obtain the solution of differential equations. The basic idea of the method of weighted residuals is to approximate the exact solution of differential equations over a domain by a trial function that is chosen to satisfy boundary conditions, with unknown coefficients that are chosen to give the best solution:

$$y(x) = \varphi_0(x) + \sum_{i=0}^{N} c_i \varphi_i(x) \tag{B.1}$$

The trial function, Equation (B.1), is substituted into the original differential equations and the result is a residual (R). If the trial function were exact, then the weighted residuals are minimized over the domain of the independent variable (x). In particular, the integral of the weighted residuals would be zero.

$$\int w_j R \, dx = 0 \tag{B.2}$$

The weighting factors (w_i) can be chosen in many ways i.e. the subdomain method, the least squares method, the Galerkin method, the collocation method, and the method of moment (Villadsen and Michelsen, 1978). Among the various methods, the collocation method has been proven to be effective in the solution of complex and nonlinear problems (Carey and Filayson, 1975)

For the collocation method, the weighting factors are chosen to be the Dirac delta function

$$w_j = \begin{cases} 1 & \text{for} \quad x = x_j \\ 0 & \text{for} \quad x \neq x_j \end{cases} \quad \text{or} \quad w_j = \delta(x - x_j) \tag{B.3}$$

Therefore,

$$\int w_j R \, dx = R|_{x_j} = 0 \tag{B.4}$$

This method forces the residual to be zero at N specified collocation points (x_j). As N increases, the residual becomes zero at more points.

B.1 The Method of Orthogonal Collocation

As mentioned above, in the collocation method, it is necessary to evaluate the residual at the collocation points. If such collocation points are chosen as roots of an orthogonal polynomial, this is known as the method of orthogonal collocation.

The basic property of the orthogonal polynomial is

$$\int_0^1 w(x)P_n(x)P_m(x)dx = 0 \qquad \text{n} = 0, 1, 2, \ldots \text{m} - 1 \tag{B.5}$$

where $P_m(x)$ is a polynomial function degree m of x. If the property in Equation (B.5) is satisfied, the polynomial $P_m(x)$ is orthogonal over the spatial domain $[0, 1]$.

In this work, the lagrange polynomial $(l_i(x))$ is chosen as the trial polynomial function since the solution can be derived in terms of its value at the collocation points, instead of in terms of the coefficients in the trial functions. Thus, the value of y at any desired point x can be computed from:

$$y(x) = \sum_{i=1}^{N+2} l_i(x)y(x_i) \tag{B.6}$$

$$l_i(x) = \frac{p_{N+2}(x)}{(x - x_i)p_{N+2}^{(1)}(x_i)} \tag{B.7}$$

$$p_{N+2} = (x - x_1)(x - x_2)\ldots(x - x_{N+2}) \tag{B.8}$$

where p_{N+2} is Legendre polynomial of order $N + 2$ satisfying the orthogonality relationship. The first and second derivatives of the trial function y at each collocation point are calculated from:

$$\left(\frac{dy}{dx}\right)_{x=x_j} = \sum_{i=1}^{N+2} l_i^{(1)}(x_j)y_i \tag{B.9}$$

$$\left(\frac{d^2y}{dx^2}\right)_{x=x_j} = \sum_{i=1}^{N+2} l_i^{(2)}(x_j)y_i \tag{B.10}$$

where N is the order of polynomial. All the coefficients $l_i^{(1)}(x_j)$ and $l_i^{(2)}(x_j)$, $i = 1, 2, \ldots, N + 2$ and $j = 1, 2, \ldots, N + 2$ are calculated from $p_{N+2}^{(1)}(x_j)$, $p_{N+2}^{(2)}(x_j)$, and

Table B.1: Roots and the first and second derivative matrix for Legendre polynomials

	$N = 1$	$N = 2$
x_j	0.5000	0.2113
		0.7887
A	$\begin{pmatrix} -3 & 4 & -1 \\ -1 & 0 & 1 \\ 1 & -4 & 3 \end{pmatrix}$	$\begin{pmatrix} -7 & 8.196 & -2.196 & 1 \\ -2.732 & 1.732 & 1.732 & -0.7321 \\ 0.732 & -1.732 & -1.732 & 2.732 \\ -1 & 2.196 & -8.196 & 7 \end{pmatrix}$
B	$\begin{pmatrix} 4 & -8 & 4 \\ 4 & -8 & 4 \\ 4 & -8 & 4 \end{pmatrix}$	$\begin{pmatrix} 24 & -37.18 & 25.18 & -12 \\ 16.39 & -24 & 12 & -4.392 \\ -4.392 & 12 & -24 & 16.39 \\ -12 & 25.18 & -37.18 & 24 \end{pmatrix}$

$p_{N+2}^{(3)}(x_j)$, $j = 1, 2, \ldots, N+2$. The derivation of these polynomials and their properties are discussed fully in Villadsen and Michaelsen (1978).

Equations (B.9) and (B.10) can be shown in simple expressions as follows:

$$\left(\frac{dy}{dx}\right)_{x=x_j} = \sum_{i=1}^{N+2} A_{ji} y_i \tag{B.11}$$

$$\left(\frac{d^2y}{dx^2}\right)_{x=x_j} = \sum_{i=1}^{N+2} B_{ji} y_i \tag{B.12}$$

where $A_{ji} = l_i^{(1)}(x_j)$ and $B_{ji} = l_i^{(2)}(x_j)$. Table B.1 shows the value of roots and of the first and second derivative matrix using Legendre polynomial. These values are calculated from the algorithm provided by Villadsen and Michaelsen (1978).

It should be noted that a system of partial differential equations (PDEs) can be reduced to a system of ordinary differential equations by applying Equations (B.11) and (B.12) to approximate the spatial derivative terms of the PDEs. The resulting differential equations can be solved using standard integration solvers. This approach is often known as the *method of lines.*

B.2   Orthogonal Collocation on Finite Elements

As known that in the orthogonal collocation procedure, a series of polynomials, each of which is defined over the entire range $0 \leq x \leq 1$, is used as a trial function. Nevertheless, complications with this global procedure arise in the presence of steep gradients or sharply changes in the solution profile. In such situations, it may be advantageous to use the method of orthogonal collocation that is defined over only part of the region and piece together adjacent functions to provide an approximation over the whole domain. Using such a procedure, smaller regions can be used near the location of the steep gradient and the approximation of the solution is improved. This leads to the method of *orthogonal collocation on finite elements*

In the orthogonal collocation on finite elements, the domain is divided into sub-domains (finite elements) as shown in Figure B.1. Within each element, we apply orthogonal collocation using Lagrange polynomials and then the residual is evaluated at each collocation point.

For the kth element, the approximation of the first and second derivative terms at collocation point i is defined by:

$$\frac{dy^i}{dx} = \frac{1}{h_k} \sum_{j=1}^{NCOL+2} A_{ij} y^j \tag{B.13}$$

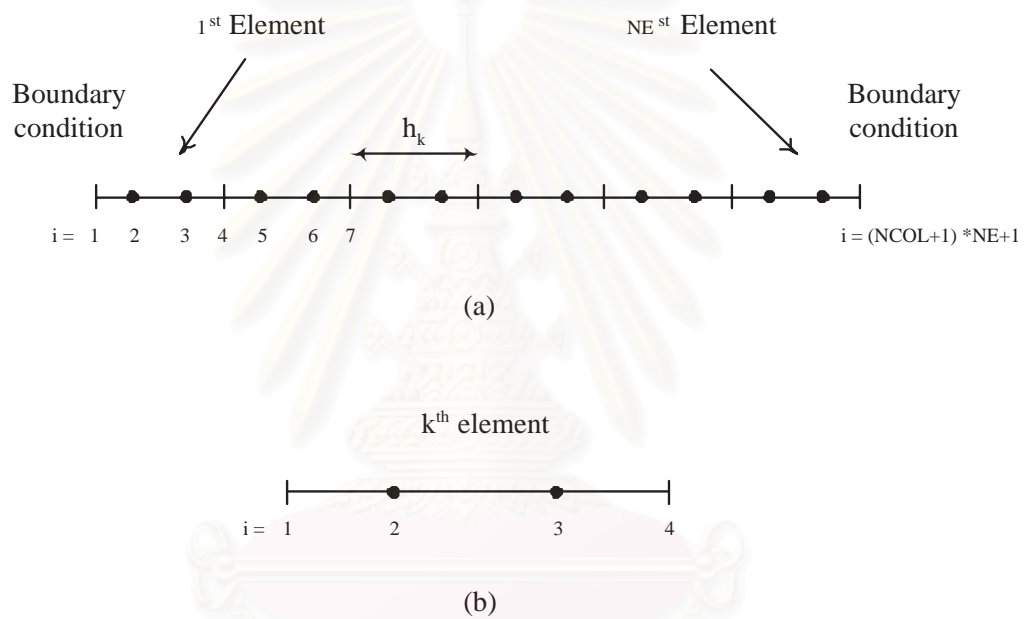$$\frac{d^2 y^i}{dx^2} = \frac{1}{h_k^2} \sum_{j=1}^{NCOL+2} B_{ij} y^j \tag{B.14}$$

Figure B.1: Orthogonal collocation points on finite elements with NE elements and 2 internal collocation points ($NCOL$) (a) Global numbering system (b) Local numbering system

Appendix C

Extended Kalman Filter

The implementation of a model predictive control technique requires the knowledge of current states and/or parameters in order to compute the solution of an on-line open loop optimal control problem. However, it is known that in many processes, only some of states can be directly measured. To overcome this difficulty, state and parameter estimation is employed and incorporated into the model predictive control algorithm.

C.1   The EKF Algorithm

The extended Kalman filter (EKF) is a recursive procedure for computing an optimal estimate, minimizing the mean square error of the deviation between the actual and estimated states of system. It computes a state estimate with two step approach. Firstly, using a Taylor's series expansion of the dynamic and measurement nonlinearities, the nonlinear functions are linearized so that the nonlinear estimation problem is reduced to a linear one. Secondly, using a known solution to this linear estimation problem, the states are estimated (Kittisupakorn, 1995). The basic algorithm of the EKF can be summarized as follows:

For nonlinear systems, the process model can be described by differential equations:

$$\dot{x} = F(x(t), u(t), t) + \zeta(t) \qquad \text{(C.1)}$$

$$y = G(x(t)) + \eta(t) \qquad \text{(C.2)}$$

where F is a vector of system function, G is a vector of measurement function, ζ is a non-zero mean Gaussian process noise with the covariance Q, and η is a non-zero mean Gaussian measurement noise with the covariance R.

The equations for the EKF are given by a set of correction and prediction equations as shown in below:

Correction phase: Correct the prior estimates of state at $k-1$ and update the weighting matrix

$$K_{k-1} = P_{k-1/k-2}C^T[CP_{k-1/k-2}C^T + R]^{-1} \tag{C.3}$$

$$\hat{x}_{k-1/k-1} = \hat{x}_{k-1/k-2} + K_{k-1}[y_{k-1} - C\hat{x}_{k-1/k-2}] \tag{C.4}$$

$$\hat{P}_{k-1/k-1} = [I - K_{k-1}C]\hat{P}_{k-1/k-2}[I - K_{k-1}C]^T + K_{k-1}RK_{k-1}^T \tag{C.5}$$

Prediction phase: Integrate the nonlinear state and covariance equations from time $k-1$ to k in order to acquire the estimate $\hat{x}_{k/k-1}$ and $\hat{P}_{k/k-1}$

$$\dot{\hat{x}} = F(x,u) \tag{C.6}$$

$$\dot{\hat{P}} = A_{k-1}\hat{P} + \hat{P}A_{k-1}^T + Q \tag{C.7}$$

where $\hat{x}_{k/k-1}$ denotes the estimate of state x at $t = k$ from information at $t = k-1$, K is Kalman gain matrix, P is covariance matrix of the estimated error, and A and C are the Jacobian matrix of the function F and G with respect to the state vector, respectively.

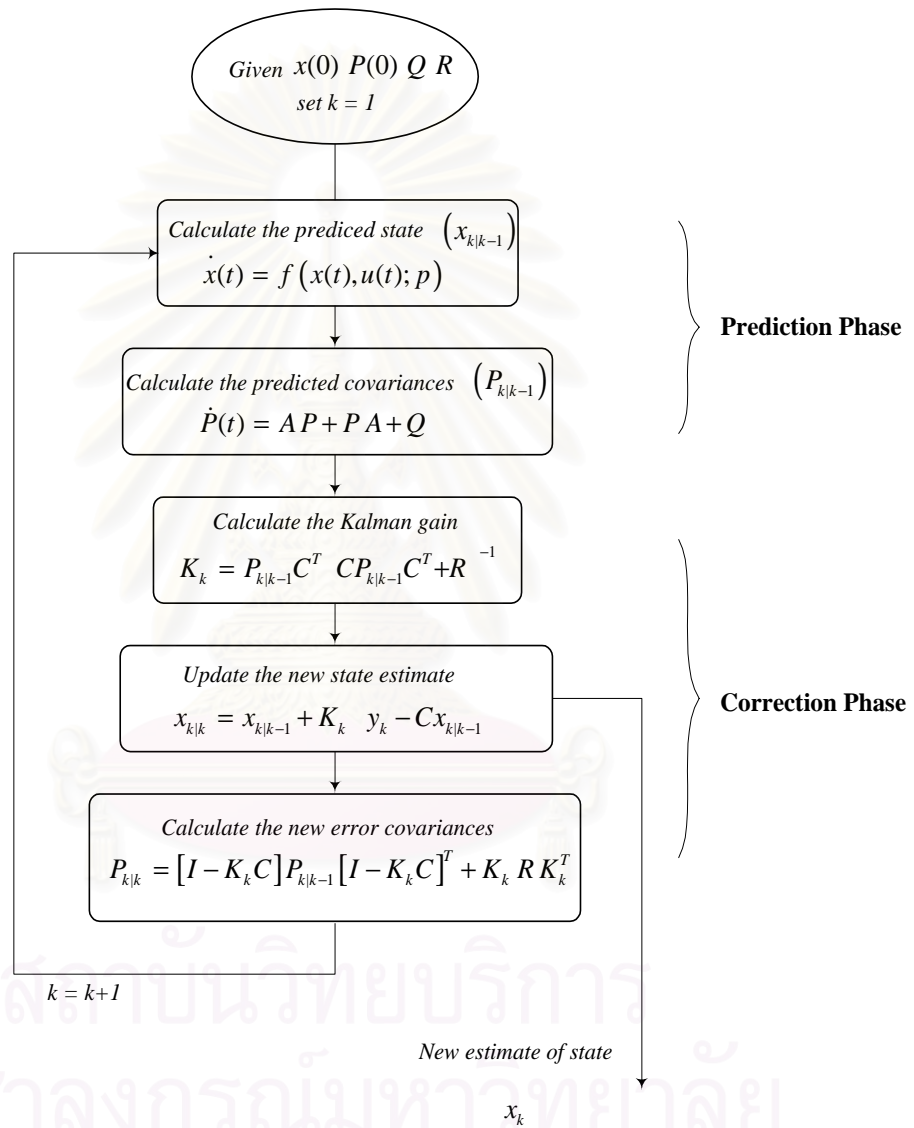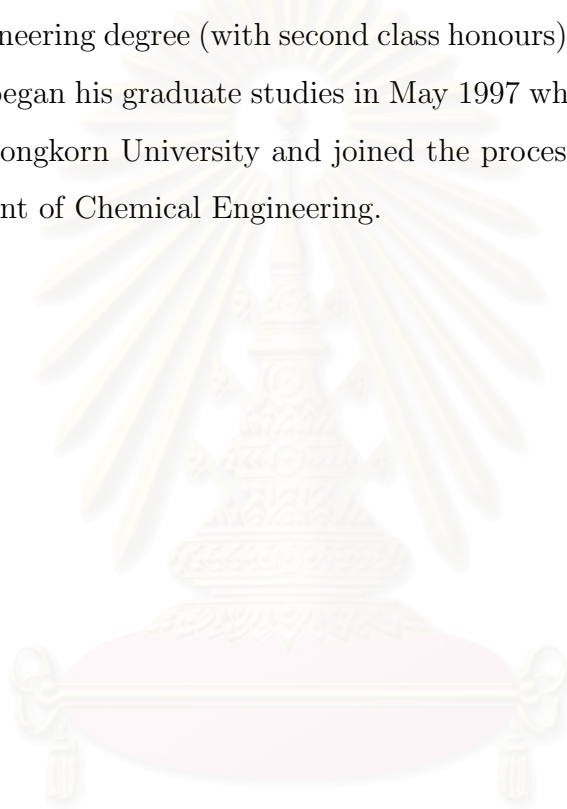Figure C.1 shows the flow diagram of the EKF algorithm in continuous/discrete form.

Figure C.1: Flow diagram of an extended Kalman filter

Vita

Amornchai Arpornwichanop, the second son of Somkiat and Jiraporn Arpornwichanop, was born in Ubonratchathani on August 21, 1974. After graduating high school from Suankularb College, he entered Chulalongkorn University in May 1993 and received his Bachelor of Engineering degree (with second class honours) in Chemical Engineering in April 1997. He began his graduate studies in May 1997 when he entered the Graduate School of Chulalongkorn University and joined the process control engineering group in the Department of Chemical Engineering.